UNIVERSIDAD CARLOS III DE MADRID

ENERGY ENGINEERING

DYNAMIC MODEL OF A WIND ENERGY CONVERTION SYSTEM BASED ON A DOUBLY FED INDUCTION GENERATOR

BACHELOR THESIS

JOAQUÍN GARCÍA CARRETERO

DIRECTOR

D. David Santos Martín

June 2017

Acknowledgments

I would like to thank all that people who has contributed directly or indirectly to this thesis, without them this would have never been achieved. During the last four years I have found a different way of looking at the world and it is due to passion, hard work and also some setbacks that led me to improve little by little and learn day by day.

Thank you, David, for your support and patience, giving me a scarce resource such as time. Thank you for getting me to know wind energy world and helping me through this thesis. I really appreciate your dedication and enthusiasm.

Special thanks to my parents, for their love, dedication, help, interest and such a long list of things that I have the honor to receive from you. You guided me in my first steps and you were my first professors, instilling me interest on learning. Of course, I also appreciate all the support and joy that my brother brings every time I need.

To my friends, thank you for being there, even at a distance of 3 478 Km you are one the reasons why this thesis exists.

Thank you to the university for being the knowledge center that everybody needs to develop their mind and providing me all kind of resources.

I would like to finish mentioning a sentence from a physicist that started in a patent office and ended up changing some of the fundamental basis of physics, Albert Einstein:

"There is a driving force more powerful than steam,

electricity and nuclear power: the will"

INDEX

page

FIGURES INDEX

page

TABLES INDEX

page

1. INTRODUCTION

Nowadays, modern wind energy convertion systems are composed by complex mechanisms and very specialized technologies. Many subjects from several fields are included in this type of energy, such as the aerodynamics, power electronics, electric engineering, mechanics or even economics for economical assessments, among others. Due to all that delicate disciplines, an accurate analysis of the wind power turbine stabilization and behavior along its lifetime becomes a not so easy task. Nevertheless, last years and thanks to the development of powerful computing tools, it is getting simpler to implement models to represent real life projects in an accurate way. This helps in saving large amounts of time and money, as that designs accept modifications without starting from scratch, are precise enough and have the ability of being built much faster due to the quick solving of complicated equations, giving ease to the construction of the final model. Therefore, because of the characteristics of the new software, computer modelling and model simulations are currently a common activity in all the different engineering branches. The final results obtained during the final simulation will depend mostly in three aspects:

- Previous knowledge on the functioning of the system. The more someone knows about the topic, the better the result of the simulation will be, avoiding minimal errors and implementing more accurate strategies when programming.

- Complexity degree achieved in the model. Once more, the implementation of more complex designs will be translated at the end in simulations that get really close to reality. However, this can have some disadvantages, since the more complex a simulation is, the longer it usually takes to run the calculations.

- Accuracy in the input parameters of the simulation, since introducing variables closer to reality, we would get closer outputs to what we want to accomplish.

The aim of this thesis is showing how a wind energy convertion system works, through a simulation of a Doubly Fed Induction Generator model, implemented with MATLAB and Simulink software, as well as achieving a better knowledge of the different systems that form a wind turbine, as further comprehension of dynamic behavior to reach improved stabilization methods.

In the simulation, several models have been described, identifying the necessary parameters and applying the steady state and dynamic equations that must be used in order to achieve an accurate approximation to the complexity of these systems.

During the development of this thesis, the obtained results and models have been validated and compared with examples from Ackerman [1] and G. Abad [2].

2. WIND ENERGY: FACTS AND STATISTICS

Energy is a natural resource that surrounds every process in the universe. Photosynthesis in the case of plants, our nutrition or even a rock falling down from the top of a mountain are examples of processes that involve a transformation of energy. That transformation became really important since the XVIII century with the industrial revolution, when enormous amounts of coal were used and the development of new machines that changed the ways we used to transport, produce and live. This new exploitation of the energy at big scale allowed the society to evolve creating new social classes and boosted the economy of the industrialized countries to levels never seen before [3].

Nowadays, energy is still one the basic pillars that supports the development of every country in the world and has become an international issue. Nevertheless, we are not living in the Industrial Revolution anymore and the challenges that energy involves are different too. Global warming and environmental concerns, security of supply or the unceasing increase in energy demand are some of the facts that obliges the institutions to implement new and better policies, pushing for the use of renewable technologies. Green, clean and infinite sources from a human point of view that come from the sun, such as biomass, tidal, hydroelectric, solar or wind power.

Among these new comers, wind energy systems have the advantages of being one of the cheapest technologies in terms of USD/kWe [4], it does not use water, a scarce resource used in other kinds of power installations for cooling as nuclear or thermal plants; and of course, is a renewable and easily accessible resource obtained from the sun. Sun radiates around 174 423 000 000 000 KWh to the Earth each hour [5]. This radiation heats the surface in a non-uniform manner, making the Equator and land areas to be warmer than polar regions, seas or oceans. Wind is the flow produced during the exchange of air at distinct temperatures among that regions. Approximately 1 or 2% of the energy that reaches our planet is finally converted naturally into wind energy and would be enough to cover the global energy demand [6].

2.1. Wind Energy History

Greeks believed that together with Water, Fire and Earth, Wind was one of the main elements in nature, employed to create the world and many of the first civilizations had a God dedicated to wind, as Aeolus in Ancient Greece or the Roman Empire.

Mankind has used wind for centuries, being one of the first purposes to utilize it for propelling ships in transport and improving the horizons of trading. However, we would have to wait until the X century in order to find the first windmills in Persia. These constructions had vertical axes and were used for grinding grain and pumping water utilizing the drag force of the wind. Similar windmills appeared in Europe in the Middle Ages around 1 100 as consequence of the cultural exchange between Eastern and Western countries during the Crusades, with Greece, Italy and Spain as the countries which were more influenced. Although these new ones had a horizontal axis and tilted sails instead of the wooden blades found in the East, both kinds of structures were used for the same purpose. Some centuries later, around 1 300, an innovative technology extended its scope

to countries such as the Netherlands or England. Built in wood, were also used for draining the water from the lower areas in Holland or grinding the grain in a more efficiently [7].

In the XIX century, most of the windmills were displaced by other kinds of power generation such as the thermal, steam or combustion engines. This fact was mainly due to the industrial revolution, making the rural and poorer regions to be the ones which preserved the harnessing of that structures [8]. During mid XIX century Daniel Halladay and John Burnham designed a new windmill which became very popular in the USA and was widespread all along the country, becoming an icon of the American West. This machine, the first commercially viable windmill in the history, had around 20 blades made in wood, was able to turn to meet the direction of the wind and could keep the velocity within a determinate range by changing the pitch of the blades without human action. Its aim was still the irrigation of fields through pumping of water [9].

But it is finally in the winter between 1887 and 1888, when Charles F. Brush builds the first wind energy turbine used for electricity generation. Despite being a model which accounted for only 12 kW, it was the biggest wind turbine of its time, with 17 meters of diameter and 144 wooden blades. Almost at the same time, in 1892, a meteorologist pioneer interested in the storage of energy and aerodynamics called Poul la Cour designed in Denmark another wind energy turbine focused in the generation of electricity [10]. In this way, the modern wind technology development starts, leaving behind the previous purposes in agriculture. In 1918 Denmark already had 3 MW of wind power installed in turbines between 20 and 35 kW, covering a 3% of the local electricity demand in that year.

However, at the beginning of the XX century, wind energy stagnates again its development reducing most of the activity to providing electricity to some homes which were too far from the main cities and communications. Moreover, this problem was also solved later by connecting the dwellings to the grid once the network was expanded and improved. One of the most remarkable events during that period was the construction of a 1250 kW wind turbine in 1941. Designed by Palmer Cosslett Putnam and manufactured by the Morgan Smith Company, it was the first wind energy turbine that surpassed a power generation of one megawatt and kept the record of being the largest wind energy turbine for almost 40 years, until 1979. Built in Vermont, USA, the machine was made in steel and had a rotor diameter of 53 meters. Nevertheless, the machine stopped working in 1945 when one of the blades failed [11]. Some other turbines were the 24 meters diameter Gedser machine, built in Denmark in 1956 with 200 kW, the light weight turbines designed by Ulrich Hütter between 1950 and 1960 or a 1.1 MW turbine tested by Electricite´ de France in 1963, which had a rotor diameter of 35 meters.

Despite these advances, wind energy convertion systems created little interest for its development and integration in the grid until 1973, with the 1973 oil crisis, when the prices for petroleum rose and the global energetic policy started changing. This crisis favored the creation of multiple incentives and programmes funded by different governments. Launched in countries such as Germany, Sweden, USA or UK, these events caused an extensive research of better efficiencies, more innovative concepts and cost-effective designs. Some of the new alternatives which were born in that period were a 4

MW Darrieus machine in Canada and an “H” rotor type wind energy convertion system in the UK able to produce 500 kW with its straight blades, both with vertical axis. One of the biggest prototypes built in that time was a horizontal axis machine of 3 MW tested in USA in 1981. Contrary to other turbines, this one used hydraulic transmission systems and an alternative to the yaw drive. Instead of rotating only the nacelle towards the wind direction, it was the whole structure the one which was able to rotate and re-orientate the wind turbine in order to take full advantage from the incident flow. The number of blades used in these machines was still variable and therefore most of the large turbines were designed with one, two or three blades.

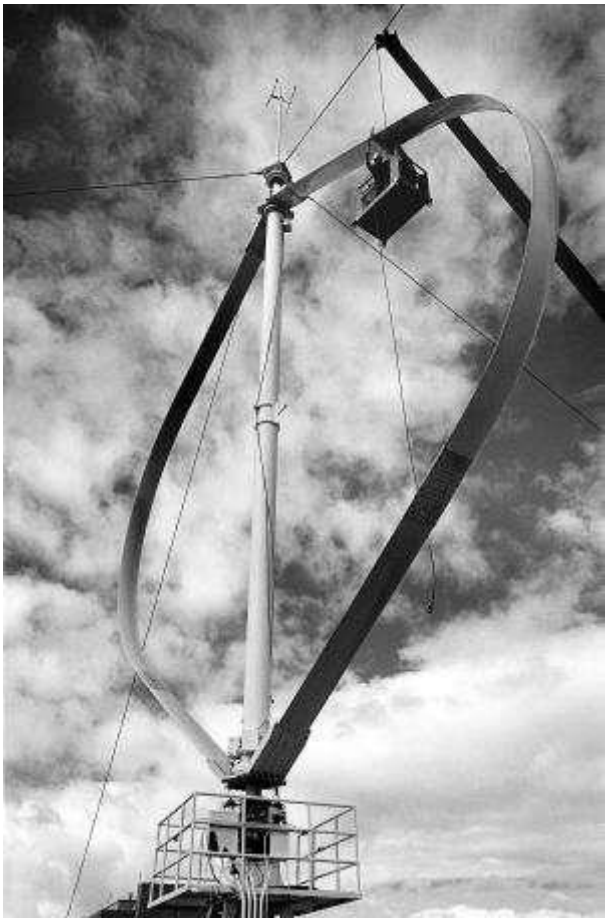

Figure 1. Vertical axis wind turbine installation in a platform in Bushland, Texas [12].

Thanks to all the developments that took place during the programmes, scientifics and engineers gathered a lot of valuable information and due to the advances, most of the designs worked as it was expected. On the other hand, problems such as reliability on some prototypes or the difficulties at managing the ungovernable wind climates, made really hard to operate the largest wind turbines of several megawatts. Because of that, private companies chose to manufacture, usually with some subsidies from the governments, much simpler and smaller turbines for commercial purposes. One of the consequences of this implementation could be observed in California during the 1980s, where a huge amount of wind energy convertion systems started working, accounting for less than 100 kW each. As these designs were not as big as the multiple megawatts machines, they also had a great advantage over this last type: modifications and reparations were easier and cheaper to apply.

In that period, it appeared the "Danish" concept of a wind energy convertion system, which was really successful. It consisted on a design with three blades and stall control working at a fixed speed. Due to its simple construction, the same model was applied later in other larger machines.

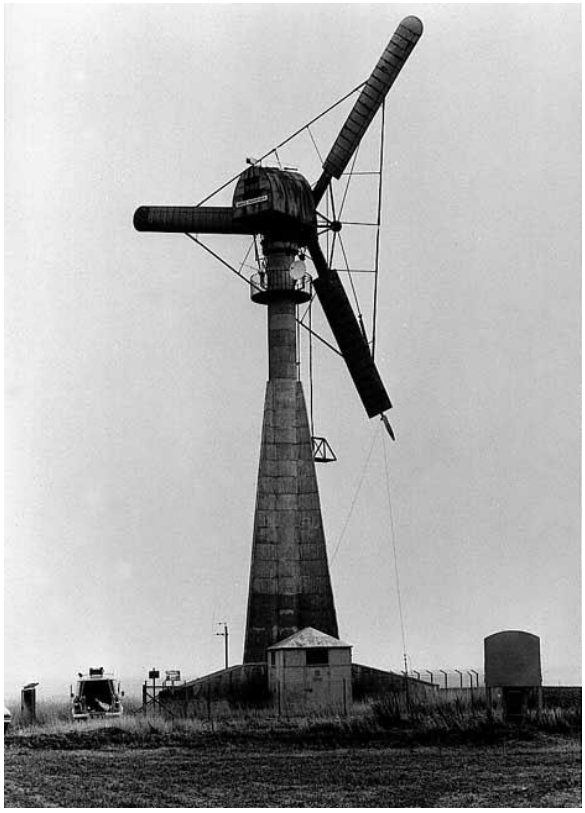

Figure 2. Gedser wind turbine designed by Johannes Juul in 1957, precursor of the Danish concept [10].

As the time goes by, the commercial turbines became larger, reaching similar ratings than the designs of the 1980s and introduced innovations such as full span rotor control, better materials as polyester, epoxy resin, fiberglass or carbon fiber instead of wood or steel and variable speed machines. Nowadays most of the wind energy convertion systems that are being installed are located in developing countries like China or India, as well as in already existing wind farms which are becoming obsolete and need to substitute the old machines from the 1970s and the 1980s [11].

The principal stimulus for developing wind energy and green technologies in general after 1973 was the oil prices and the concerns that started to convince the population about the limitations of fossil fuel resources over the time, while currently the motivations for installing clean energy sources are centered around generating power reducing the CO_2 emissions or releasing as little as possible during the complete cycle of the goods, taking into account its manufacture, installation, operation and dismantling, contributing to reduce the effect on global warming and climate change. With this purpose, the European Commission started a plan to reach a 12% of the total energy demand coming from renewable resources for 2010. Wind energy had an important role in that project, expecting to increase the installed capacity from 2.5 GW in 1995 to at least 40 GW for 2010.

Nonetheless, wind energy is complex and it is not easy to achieve a correct assessment of the available resources, being one of the reasons why some countries are fulfilling their targets while others are having more difficulties. More important aspects that can have some impact in the future development of wind energy are the financial mechanisms mainly coming from public institutions like governments or international cooperation programmes, the local planning of the projects or the local perspective and opinion of the impact in the environment. Another alternative is the manufacture of offshore win energy convertion systems, which avoid the use of private property in the mainland and disturb less the inhabitants [11].

2.2. Renewable Energy and Power Generation Situation

In 2016 renewable energy was affected by different facts. Some of them are the huge decrease in several renewable energy technologies, such as wind power and solar photovoltaic, the low prices in fossil fuel energies and a continuous investment in energy storage. Again, CO_2 emissions coming from fossil fuels and industry for energy use were almost flat regarding last years, increasing only a 0.2% instead of the 2.2% of growth rate observed in the last decade [13].

The main reason why this decrease can be noticed is the decline in use of coal in most of the countries, being 2015 the second year in a row in which this happens, as well as improvements in energy efficiencies and the rise of renewable energy production. Coal has also been an important topic for countries like the Netherlands, Finland, France or Brazil, as they signed different commitments to stop using this fossil fuel in the next years, or at least to stop financing it, as in the Brazilian case. However, even with coal clearly declining, renewable energies still have more competitors that has received subsidies along the year, reaching low prices all over the globe. These are the natural gas and the oil, facing the green technologies in markets as the heating energy or transport.

Similar to last year, global final energy consumption coming from renewables was around 19.3%, being divided in traditional biomass, used in rural areas of developing countries for cooking and heating, which accounted to 9.1% and a 10.2% for modern renewables, where 3.6% belongs to hydropower, renewable generation as wind, solar power, non-traditional biomass and geothermal power accounted to 1.6%, biofuels for transport reached a 0.8% and renewable heat coming from biomass, geothermal or solar being of 4.2% of the global final energy consumption. The fossil fuel sources accounted for a 78.4%, while nuclear power reached a 2.3%.

Although the renewable energy sector is growing a lot during the last decades and specially technologies such as wind or solar power, this is not translated in a that big change in the final consumption. The cause of this is associated to the unstoppable increase in energy demand, which only declined in 2009 due to the strong crisis followed by an economic recession all around the world. Due to this, even with the rise in use of the larger part of renewables, the traditional biomass, it is not enough to reach the growing rate of the total demand.

During 2016, most of the growth in green energies could be appreciated in the electricity generation, while other renewables like transport or heating and cooling remained almost

constants regarding last years. This increase in generation was stronger in technologies as solar PV and wind energy, while the predominant source was still hydropower, being the one with the most capacity already installed and the one which produces more electricity. Biomass was the leader in the heating and transport rankings.

The world leader in renewable energy capacity installation has been China during the last eight years, although there are a great number of developing countries that are also investing hard in this sector, expanding quickly their green energy capacities and becoming relevant markets in a few years. This is the case of countries like Argentina, India or Mexico, where the reliable forecasts joined to the efficient and low-cost technologies made them grow in a considerable way. Nevertheless, developing counties still have lots of problems at getting the necessary infrastructures for extracting all the power they are demanding.

Policies played also an important role, setting targets at national and international levels. Despite the change in the United States administration, entering Trump as president of the North American country and the modifications in some of the commitments that meant, in general there were more countries that made regulations in order to increase the share of renewable energies in their markets and rise the supports to that technologies, going from 173 to 176 the regions that were involved in any green energy commitment. Moreover, most of the countries made their regulations more ambitious. These new policies were mostly focused in the power generation side, despite being less relevant in the total final share of energy consumption that other sectors like transport or heating.

Some important events that affected the development of the regulations, were the Paris Agreement, which was held in 2015 under the United Nations Framework Convention on Climate Change and the Marrakesh Conference in 2016, submitted by many countries that had to adapt most of their policies to reach the goals agreed during the meetings. Although it is still early to see the impact of that new policies, it is expected that they will be noticed in the short term. In total 48 of the countries claimed a 100% renewable transition and did their commitments to reach it in their home nations. Other important policies as the carbon taxes or the emissions trading system were implemented in several places worldwide, incentivizing in that way the installation of more renewable energies and a declining use of fossil fuel resources, as these new regulations would increase the price of non-renewable energies compared to green technologies. The consequence of these policies was also translated in more employment for the renewable energy sector. The estimated number of current jobs is of 9.8 million worldwide, being most of them in Asia [13].

By applying new policies, it is expected to reach some targets. In the case of renewable energy, these policies, focused on creating commitments for the implementation of more and better green technologies, have been increasing in number and support quantity for the investors. As mentioned above, during 2016 there were 176 countries that set some kind of regulation involving renewable energy. Most of that policies had as target the use of green energy in the power sector, being 150 the countries that have some regulation to set a minimum share of renewables for the coming years and other 89 targeting more ambitious results as the impact in the economy of primary and final energy shares. Although there are several policies that regulate transport and heating and cooling, these

are introduced with much lower importance than the power generation ones and can be seen only in a range from 40 to 50 countries during 2016. This policies and targets can be set at regional, national and international levels. Some ambitious commitments have been the 100% renewable electricity target signed by 48 countries in the Climate Vulnerable Forum, claiming for applying measures to avoid climate change and the consequences it could cause in different nations. Pointing in the same direction, the European Union presented a plan that should be accomplished for 2030, having as main targets the implementation of at least a 27% of the energy consumption coming from renewable energies and a minimum efficiency improvement of 27%, in order to reduce the greenhouse gas emissions in more than a 40% for 2030, in comparison to 1990 levels. Besides that agreement, Canada, Mexico and the United States arranged a deal in order to generate at least a 50% of the electricity in their countries from non-carbon resources.

In the case of Asian countries, many targets have been set during the last years. An example of this is one of the latest plans released by China in order to install a minimum renewable energy capacity of 680 GW for 2020. If this target is fulfilled, it will mean the achievement of a 27% of total power generation coming from renewable energy. Another Chinese plan was also set in ocean energy, expecting at least a built total capacity of 50 MW in tidal, wave and temperature gradient technologies before 2020. Among other targets adopted by countries such as France, South Africa, Finland, Argentina, Norway, Mexico or Saudi Arabia, it is remarkable the commitment of Aruba to become 100% renewable in its electricity generation. Although most of the targets are set for generation technologies, most of the developed countries have implemented targets on transport too. For instance, Finland and Norway are both countries that are making progress in that direction. A 30% of the transport using biofuels and a 40% using renewable fuels by 2030 was fixed in the case of Finland, while Norway signed biofuel to be used in at least 20% of the transport by 2020.

Nevertheless, targets must be revised from time to time, as they can get outdated if the aim is reached much before the due date, as it is happening in Europe with the solar PV targets, fixed for 2020 and accomplished much before in many of the nations. On the other hand, targets can also be too ambitious and fail when the due date comes, as it could be seen in the same 2020 objectives, with European countries like the Netherlands or the United Kingdom not being able to reach their goals.

In 2016 there were also important innovations in green technologies. The most relevant ones included better installation and manufacturing of solar photovoltaic, together with increasing efficiencies and performance; introduction of new materials in wind turbines and improvements in operation and maintenance, which led to reduced costs and an increase in capacity factors; upgrades in thermal energy storage mainly for solar thermal power; better formulas for the production of biofuels; and new control techniques for the control of electric grids, making easier the introduction and integration of more renewable energy. Another technology that is gaining attention during the last years is the appearance of the electric vehicle, which is expected to contribute positively in different aspects such as air quality or the ability to manage the variable renewable energy injected to the grid, being connected as a battery.

One of the characteristics that is receiving most of the interest in being improved, getting a lot of incentives and being pushed to a key aspect is the efficiency. Important for achieving targets such as energy security, declining levels of contamination or industrial competitiveness among others, efficiency is considered to be a critical player for the biggest problems like climate change and global warming. Implemented in renewable energies, a better efficiency can help to reach higher demands producing more energy from the same amount of resources, save money and increase to a larger share the renewable energy generated in the energy mix. Receiving most of the investments, efficiency pushes the innovations in technology, giving a great advantage once in the market.

Due to the lack of accurate indicators for energy efficiency, some approximations are usually used, like the primary energy intensity, this is, primary energy supply divided by the gross domestic product of the country. Therefore, in order to reach a better efficiency, the primary energy intensity must be lower. For instance, when using the same primary energy than other year and generating a higher gross domestic product, the final division will result in a lower value. So, if utilizing the same, more output has been obtained, the efficiency of the process has improved. In 2015, this variable decreased by a 2.6% regarding the previous year and it is also the average rate that must be accomplished from 2010 to 2030 in order to reach one of the goals in energy efficiency. However, during the previous years that average was not accomplished, making not so clear a final satisfactory achievement.

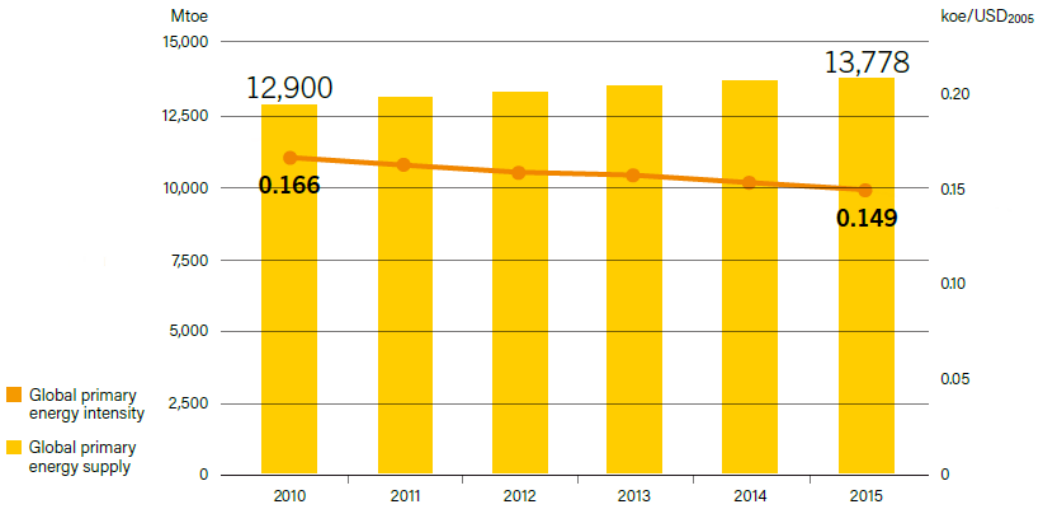

Figure 3. Global energy intensity and global energy supply evolution [13].

Furthermore, it is a fact that energy intensity varies a lot depending on the region that is being analyzed. In general, better results were obtained in developing countries rather than developed ones. This is due to the fact that developing countries are growing faster during the last years, making the primary energy intensity to be lower. In this way, developing countries have more efficiency potential remaining. For instance, China's total primary energy supply increased a 0.9%, obtaining the lowest rate since 1997, while the GDP was augmented in a 6.9%, making the primary energy intensity to be 5.8%. The

opposite example is Brazil, with an increasing energy intensity due to the fast growth in energy supply and the economic problems.

High primary energy intensity values can be obtained if some of the following facts are present: large energy intensive industry, as the growth in that sector would have as consequence the fast increase in energy consumption; the use of technologies that are less efficient than before, again due to the increase in energy consumption that the new technology would create in comparison to the previous machinery; underutilization of the available power capacity, which causes the same effect than the loss in efficiency of technologies, as it is not used in the optimum conditions, wasting energy that is not taken into account for generation; and having a large share of thermal power in the energy mix, with energies like coal. In 2014, the last data available, a 38% of the total primary energy supply came from power generation, which accounted to 13 699 Mtoe. In the case of buildings, industry and transport, the usage was of 32, 29% and 28% respectively of the total final consumption, which reached the 9 425 Mtoe.

During 2016, the renewable power capacity increased around 161 GW worldwide, being the largest increase ever in only one year with 9% more regarding 2015 and reaching a total amount of 2.02 TW. The greatest increase was seen in solar photovoltaic, which rose a 47%, while other technologies like wind power or hydropower accounted for a 34% and a 15.5% respectively of the new renewable power capacity installed. These installations mean a 62% of the new total power capacity this year, far over the 48% coming from fossil fuel and nuclear and this distance is even larger in several countries worldwide. In this year, it was also achieved a relevant penetration of renewable energy in the grid, being clear examples Denmark, Ireland or Portugal, with 37.6%, 27% and 24% respectively in wind power penetration; and Costa Rica or Honduras accounting a 9.8% and a 7.3% respectively in solar photovoltaic. But taking into account short periods of time, these values rise to the astonishing figures of 140% in Denmark and 106% in Scotland.

The renewable energy expansion, motivated thanks to the decreasing prices in many of the technologies, the always growing global energy demand and the incentives and mechanisms that governments are implementing, is producing that more and more technologies are able to enter in the competition against fossil fuels. This is the case of solar PV and wind energy, which are now cheaper than fossil resources in many countries. Offshore wind power is also decreasing prices significantly in the last years. The low prices and introduction of better technologies is at the same time favoring the global expansion to happen in less developed regions, which had isolated grids in most of the cases, and where the previous high electricity prices and power generation shortages created the perfect environment for renewable energy to be competitive.

Asia was the world leader in installed capacity thanks to China’s investments in hydropower, wind and solar photovoltaic energies. The biggest increase was seen in solar PV, as it rose its capacity a 45% respect to the previous year. However, one of the most important problems in China, as it is the curtailment, increased too, showing the challenges that this country still has to solve. In the rest of the continent, hydropower is the predominant renewable resource, although it is reducing its share in comparison with other technologies, mainly due to the cheap prices in solar PV and wind energy coming

from the competitive markets of China. India made also a remarkable investment in its wind and solar capacities, while Turkey outstands because of its geothermal installations during 2016.

In Europe, the renewable energy capacity accounted to 86% of the total new power in 2016, continuing with the last years course. However, some restlessness started to appear in the agents involved in the sector, when the European Commission stated that renewables dispatch and priority access should be removed from the European targets for 2030 [13].

In America, the United States experienced an increase in the renewable energy used in electricity generation, turning the 13.7% of last year into a 15% in 2016. This statistic increased due to the large increment in wind and solar, which covered the decline in bio-power. The most installed technology in that country was the solar photovoltaic and the first offshore wind farm was built, indicating the future way for a new market. Canada was dominated in generation by hydropower, although wind, following the development of many of the countries in the world, was the most installed power source, as it has been during the last 11 years. In Central and South America, high shares of renewable energy were reached. Clear examples of this are the 9.8% of electricity generation in Honduras coming from solar photovoltaic, or the 22.8% of electricity consumption coming from wind power in Uruguay in 2016. Moreover, some of the Caribbean islands such as Aruba or Curaçao, with problems to integrate renewable energies due to their isolated systems, surpassed the threshold of 10% of renewable power in their energy mix. On the other hand, was Brazil, which got a remarkable result in hydropower capacity, but cancelled some of the renewable power auctions as consequence of the economic recession and the declining electricity demand, causing insecurity and uncertainty in manufacturers and energy markets.

In Oceania, the only remarkable country was Australia, as the continent is formed by islands in which is really difficult to reach a stable grid if too much renewable energy is generated. Most of the Australian green energy comes from hydropower, accounting a 59% and wind power, which reached a 32% during 2016. Solar PV is also growing fast in this country.

Africa is another continent in which renewable energies had an important development. The countries leading the region were Egypt and Morocco, both with distinguished hydropower capacities. Having a look at the Sub-Saharan countries, South Africa reached a 5% of renewable energy from its total electricity generation capacity during 2016. This continent is also generating some interest in the energy market because of the new industries of wind energy and solar photovoltaic components, as well as the concentrated solar power plants in the north, with participants as Egypt, Algeria and Morocco. Africa is also implementing some hydropower projects that will be built in next years.

In Middle East, fossil fuels are still predominant and renewable resources like solar photovoltaic, wind power or concentrated solar do not have as much relevance as in other regions. However, there are some projects under construction and even countries such as Oman, the United Arab Emirates, Jordan or the State of Palestine are installing more than 200 MW in green energies.

2.3. Global Wind Energy Situation

Wind energy turbine installation's data gives the chance to get a general overview of the actual situation of this sector and its evolution last years and also allows to show the importance of wind energy worldwide. A total amount of 54 315 MW was installed globally during 2016, resulting in a decrease of 14% regarding the wind power installations of 2015, when the figure was 63.1 GW. This fact was mainly due to China's reduction of investment in this technology due to the changing rates that could be appreciated in the markets, installing 6 965 MW less in 2016 than the year before. Taking into account the installed capacity during 2016, the global wind energy capacity sums up to 486 831 MW, that is a 12.1% increase from 2015 [14].

Unlike the large decrease in China's market, stability was predominant in the rest of the countries, from the well-stablished markets in Europe and North America to the new incoming Latin-American and Asian Pacific markets.

Europe installed around 14 GW in 2016, accounting for a 25.7% of the global wind energy market that year. Although the installed capacity was lower than in 2015, the difference was inappreciable, a bare change of 19 MW, adding up to a total new capacity of 13,915 GW during 2016. Germany was ahead of this statistic in the Old Continent with 5 443 MW and it is currently immersed in creating a competitive process of auctions. In this country, the market is really stable due to last years' policies, guarantying a feed-in tariff premium payment. France and Turkey were two of the countries which installed the most in Europe during 2016, only behind Germany, with 1 561 and 1 387 MW respectively. On the other hand, the United Kingdom continues its downwards trajectory decreasing its installed wind energy capacity. If the figures were of 1 467 MW during 2014 and 975 MW in 2015, in 2016 the total new capacity diminished to 736 MW. This fact is a consequence of the conservative government that changed during 2015 and 2016 the way incentives were given to investors in onshore wind power. With the absence of this type of wind energy, the United Kingdom has deflected the tendency of the almost steady European market.

In America as a whole, this figure amounted to 12.4 GW, very close but still under the threshold of 14.5 GW that were set during 2015, representing a 22.9% of the new global wind energy capacity in 2016. The main reason why this decline happened was the reduction in added capacity in countries like Brazil or Canada. In the American market the leader was the United States, which installed 8.2 GW in 2016 and certified its strength and commitment with wind energy, being the second largest country in installed capacity, only after China. This fact comes also as result of the long-term incentives that give a continued stability and profits to the investments in the sector. Something similar happened with Mexico, a country where the total installed capacity went down from 714 MW to 454 MW, but have important policies to develop and deploy a better exploitation of the wind resource, so it is expected an increase in their statistics in the following years. In this continent Chile and Uruguay showed strong installation rates, promoting the investment in Latin America.

South and East Asia managed almost a half of the global installations with their 49.7% of new capacity during 2016, also very close to their previous register of 52.6% in 2015. The total installed capacity of these areas adds up to 26 994 MW, being the regions with

highest figures. The most important contributors were China and India. China did not feel the strain of the decrease in its power capacity installations and was again the world leader in this field with 23.3 GW, while India experienced a great increase in its share going from the 2.62 GW in 2015 to 3.16 GW through the following year, maintaining its steady growth in new capacity over the years and implementing new policies in wind energy.

Region	Units	Installed 2015	Cumulative 2015	Installed 2016	Cumulative 2016	% Installed 2016
Total Americas	(MW)	14,503	102,667	12,438	113,754	22.9%
Total Europe	(MW)	13,934	146,396	13,915	160,874	25.6%
Total South & East Asia	(MW)	33,201	171,897	26,994	198,839	49.7%
Total OECD Pacific	(MW)	677	8,717	538	9,154	1.0%
Total Africa	(MW)	603	3,480	418	3,718	0.8%
Total Other Continents and Areas	(MW)	218	950	12	490	0.0%
Annual Installed Capacity	**(MW)**	**63,135**	**-**	**54,315**	**-**	**N/A**
Cumulative Installed Capacity	**(MW)**	**-**	**434,109**	**-**	**486,831**	**N/A**

Table 1. Wind power capacity installed by region in 2015 and 2016 [14].

About offshore wind energy capacity, a total amount of 2.2 GW was installed globally, reaching a total capacity of 13.5 GW worldwide. These new offshore statistics were led by Europe with countries such as Germany and the Netherlands. China also stimulated its offshore, suffering an increase in its market despite its relatively new entrance in this technology and installed more than 600 MW, being 592 MW finally online. The USA was also initiated in the offshore technology with its first project in Rhode Island. Some recent changes in several States also improves the expectations of the United States in offshore for the following years. However, these figures were much lower than the ones from 2015, when only Germany accounted for 2.4 GW. Moreover, it should be taken into account that 2015 was an uncommon year due to delays from 2014 that inflated the registers of the following year.

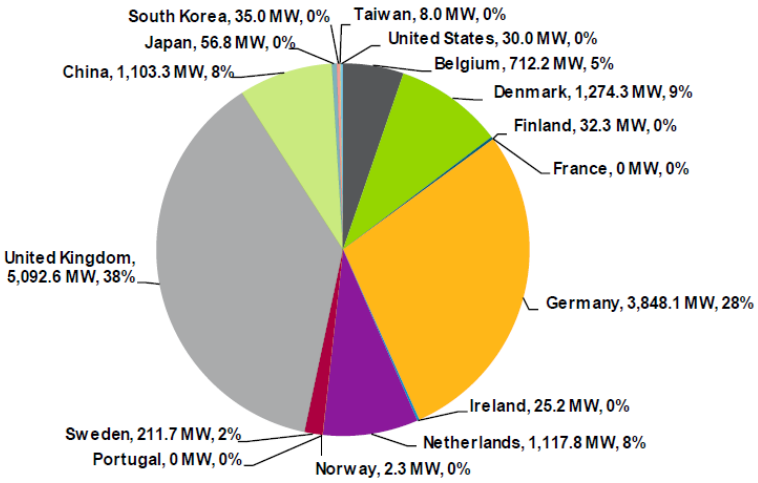

Figure 4. Total capacity and share of online offshore [14].

Without great differences, the list of the largest countries in wind energy installation has remained the same over the last three years. China, world leader in this sector with more than double of the amount installed by any of the other countries, installed again a remarkable quantity of wind energy in 2016, despite the fact that it was not able to surpass the limit set by itself in 2015. Due to its characteristics as strong industry, incentivized

investments and powerful economy, China is expected to maintain that top position for long time. The United States, second country in annual installed capacity since 2015, keeps its growing path in the wind market and although 2016 was not better than the previous year, it is consolidated with a great distance of almost 3 GW this last year. Germany appears in the top 3 installing more than 5 GW and a 10% of the world share. India is the fourth and Brazil the fifth, changing positions regarding previous years. This is due to the strong incentives and a high demand in the Indian market, as well as the saturation of projects that Brazil is experiencing, joined to the economic problems the South American country is going through. Other countries in the top 10 are France, Turkey, the Netherlands, United Kingdom and Canada. It should be remarked the upwards trajectory of Turkey and the Netherlands, as well as the decrease in installed capacity of the United Kingdom and Canada. While the first ones are enjoying strong incentives and supportive policies, the opposite reaction of the last ones withdrawing the supports and reducing that incentives led them to lower positions. The top 10 countries in annual installed capacity account for an 87% of the total capacity installed in the wind energy market during 2016.

Country	Units	2014	2015	2016	% Share	% Cumulative Share
P.R. China	(MW)	23,300	30,293	23,328	42.9%	43%
United States	(MW)	4,854	8,598	8,203	15.1%	58%
Germany	(MW)	5,119	6,013	5,443	10.0%	68%
India	(MW)	2,315	2,623	3,162	5.8%	74%
Brazil	(MW)	2,783	2,754	2,014	3.7%	78%
France	(MW)	1,042	1,073	1,561	2.9%	80%
Turkey	(MW)	804	956	1,387	2.6%	83%
Netherlands	(MW)	162	586	887	1.6%	85%
United Kingdom	(MW)	1,467	975	736	1.4%	86%
Canada	(MW)	1,871	1,506	702	1.3%	87%
Total	**(MW)**	**43,717**	**55,378**	**47,423**	**N/A**	**N/A**
Percent of World	**(%)**	**85.3%**	**87.7%**	**87.3%**	**N/A**	**N/A**

Table 2. Top 10 wind energy power markets regarding annual installed capacity [14].

Classifying the countries by cumulative capacity, we obtain a similar result, as it can be observed in Table 3. The first four countries, these are China, the United States, Germany and India, remain in the same positions and are in the top positions because of the reasons explained before, that are equally applied for this case, as the supports and incentives are continued in time, not being a policy implemented last year. Opposite is the case of the following countries. Spain and the United Kingdom are instances in which the correct investments of past years led them to that top positions, but due to the actual problems in their economies (the Spanish case) or lack of incentives in onshore (British example), they have seen how their cumulative capacities remained almost stagnated these last years. The top 10 is closed with France, Canada, Brazil and Italy. This ten countries have a cumulative share of 84% of the total wind power existing in the world, having each country more than 9 GW installed for 2016.

Country	Units	2014	2015	2016	% Share	% Cumulative Share
P.R. China	(MW)	114,760	145,053	168,381	34.6%	35%
United States	(MW)	66,146	74,571	82,184	16.9%	51%
Germany	(MW)	39,223	44,986	50,129	10.3%	62%
India	(MW)	22,904	25,352	28,664	5.9%	68%
Spain	(MW)	22,665	22,665	23,075	4.7%	72%
United Kingdom	(MW)	12,413	13,388	14,542	3.0%	75%
France	(MW)	9,170	10,243	12,065	2.5%	78%
Canada	(MW)	9,684	11,190	11,892	2.4%	80%
Brazil	(MW)	6,652	9,346	10,740	2.2%	83%
Italy	(MW)	8,556	8,851	9,257	1.9%	84%
Total	**(MW)**	**312,173**	**365,646**	**410,930**	**N/A**	**N/A**
Percent of World	**(%)**	**83.8%**	**84.2%**	**84.4%**	**N/A**	**N/A**

Table 3. Top 10 largest wind energy power markets in cumulative installed capacity [14].

2.4. Manufacturers and Technology Issues

As important as the wind energy each country has installed is the analysis of the manufacturers and their presence in the different countries. In general, the reported delivered megawatts from every company is correlated with a very similar amount of megawatts connected to the grid, but in some special cases, as China, this is not always the case due to the policies, stating that renewables do not have priority access to the grid, complicated separation of the country in seven different transmission regions independent between them, or subsidies to installation, not to generation, fact that implies the stagnancy in the use of new technologies and the impossibility of generating more electricity when needed if the wind farms are not grid connected. Until now, all problems can be delayed due to the great economic growth of the country, but this is expected to change in the future, as China cannot keep the growth rate for ever.

During 2016, 25 264 new wind energy turbines were installed, being unable to reach the 28 749 units installed the previous year. The top 10 manufacturers represented up to a 75.6% of the total capacity installed in 2016.

Supplier	Cumulative MW 2015	Supplied MW 2016	Share 2016 %	Cumulative MW 2016	Cumulative Share %
Vestas (DK)	75,357	9,693	17.2%	85,049	17.1%
GE Energy (US)	49,885	6,819	12.1%	60,566	11.4%
Goldwind (PRC)	32,087	6,429	11.4%	38,516	7.8%
Gamesa (ES)	35,606	4,161	7.4%	39,767	8.0%
Enercon (GE)	40,147	3,851	6.8%	43,999	8.9%
Siemens (GE)	32,784	3,178	5.6%	35,961	7.2%
Nordex (GE)	13,324	2,643	4.7%	22,088	3.2%
Envision (PRC)	6,546	2,003	3.6%	8,550	1.7%
Ming Yang (PRC)	10,073	1,959	3.5%	12,032	2.4%
United Power (PRC)	14,279	1,908	3.4%	16,187	3.3%
Others	129,761	13,756	24.4%	143,517	28.9%
Total	**439,848**	**56,400**	**100%**	**496,248**	**100%**

Table 4. Top 10 largest wind turbine suppliers in the world [14].

Vestas is the manufacturer that has supplied the most wind turbines in 2016, being consolidated as number one and the reference in the sector. With 9 693 MW, it overcame itself by increasing a 30.5% the power installed during 2015, 7 430 MW. In 2015, Vestas was relegated to the second place due to the boom that there was in China, with Goldwind at the top. However, due to the Chinese downturn installing less MW and the high dependency of Goldwind on that market, linked to the success that Vestas has in a great variety of markets all around the world, the Danish company has recovered the leading position.

General Electric Energy had also one of its best years during 2016, installing a total capacity of 6 819 MW, in comparison with the 5 694 MW that were installed the previous year, making an increase of 19.8%. This change meant the second position in detriment of Goldwind, relegated to the third place. G. E. Energy reached that status also thanks to the acquisition of Alstom's wind energy division.

In the case of Goldwind, it changed the brief leadership of 2015 for the third place in the manufacturers ranking, installing 6 429 MW during 2016, this is a 18.9% less than the power installed in 2015, which added up to 7 930 MW. As it has been explained previously, the reason why Goldwind installations decreased so dramatically is the lack of diversification the company has. China suffered a great decrease in wind power installations, from 30.1 GW in 2015 to 23.3 GW in 2015. As most of Goldwind's projects were developed in China, the company experienced that lack of capacity that was installed during the year before.

Gamesa climbed up from the fifth to the fourth position, increasing its total installed power a 22.7% from 3 392 MW in 2015 to 4 161 MW in 2016. Due to the collapse in incentives to renewables in Spain, its home market, Gamesa successfully diversified its activities to other countries such as India, Brazil or Mexico, with growing markets. Due to this diversification, it has been able to participate in the Chinese market, where the domestic companies are clearly favored, or the American market, also far from its home market. However, the numbers of this company could be even better in the next years after the merge with Siemens. Adding the statistics of both companies it is estimated that Gamesa would be able to reach the second place in the biggest manufacturers, just after Vestas [14].

Enercon is the fifth company in the list. Coming from its home market in Germany, where this company had more than half of its projects, it was able to install 3 851 MW in 2016 worldwide, improving its previous figures of 3 133 MW in 2015 and increasing in that way a 22.9%. Having projects in more than 20 countries, its main strength relies on the onshore wind turbines. Some of the markets in which Enercon performance improved the last years are France and Canada.

Siemens, with 3 178 MW in 2016, continued its tendency one more year decreasing its global installed capacity, that amounted to 5 068 MW in 2014 and 4 748 MW in 2015. This was enough for siemens to appear as the sixth biggest company in wind power installations. The main reason why this decrease is happening is the drop in installed capacity in key markets for the German company as the United States, as well as poor investment in the geared onshore technologies, probably not enough to remain competitive. Again, the merge with Gamesa will be very relevant for the future of both

companies, creating a new giant in the wind energy sector that is expected to occupy the second position in the manufacturers ranking.

The last companies in the top 10 are Nordex, Envision, Ming Yang and United Power in that order. In that group, only Nordex was able to increase its share a 55.7%, from 1 697 MW installed in 2015 to 2 643 MW in 2016, breaking into the top 10 manufacturers. This fact was mainly due to the acquisition of the Spanish company Acciona. The cases of Envision, Ming Yang and United Power are very similar to the one of Goldwind, as all of them are Chinese companies with most of their activities taking place in their home market. As China had less installed power than other years, these companies suffered the consequences of not diversifying the projects.

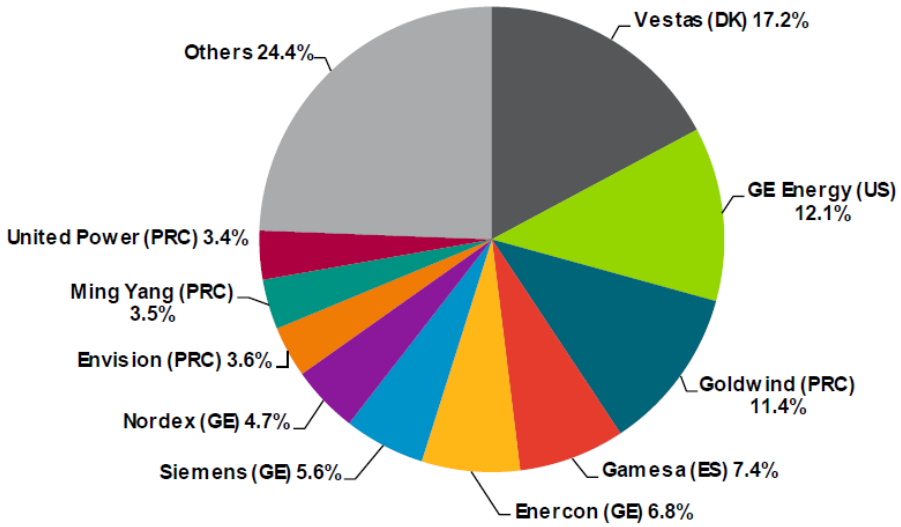

Figure 5. Top 10 largest wind turbine suppliers market share [14].

As it can be noticed, diversification and having some independency from a unique market gives a positive advantage at receiving projects to develop. In this direction, Vestas is the only company that can be really considered as a global company, due to its presence in almost all the existing markets around the world. The Danish company is followed by Enercon in number of markets where the German enterprise is present. Behind Enercon, in the third place appears G. E. Energy, which changed positions with Gamesa regarding last year. As explained before, the Chinese companies had little presence outside their home market and was Goldwind the only one which accounted more than 50 MW outside China's borders, with 77.5 MW installed in Thailand and another 7.5 MW in Panama.

Nevertheless, Goldwind is an exception in a world where domestic markets are not usually so demanding. Another problem that companies can suffer when all their activities take place in their home countries, is the inferior position that supplier enterprises have when negotiating with the investors. These strategies can work properly during years of good economic performance, but can also generate problems. One example of this was the case of G. E. Energy during 2013, when the US market collapsed and the American company had to diversify its activities outside the North American country, by acquiring Alstom and gaining in that way some international presence. More examples can be seen as the case of Enercon, with most of its activities in Germany but

with good performance in other countries these last years, or Nordex in Germany as well, helped thanks to the purchase of Acciona. Finally, a previously mentioned example of internationalized company through the merge of two big companies are Gamesa and Siemens, forming one wind energy giant expected to occupy the second place in the biggest companies ranking of wind energy.

2.5. Wind Power Market Forecast

As important as the evolution that wind energy has had in the last years, the forecasts of wind power can help to predict how the different countries or regions are going to evolve in energy terms and where it will be more profitable to invest.

In order to realize an accurate forecast, it is important to take into account the general aspects of the market for every country, as well as some dynamics and cycles that can be appreciated along the time. Some important premises have been taken into account [14]:

- There exist national plans and supports for renewable energies in general and wind energy in particular.
- Participation in national and international commitments to reduce carbon emissions and increase the renewables share.
- Similar evolution of the industry's behavior and growing market for the following years.
- Availability of wind resource assessments in the market in order to get the most from them.
- Technological development of the commercial designs, increasing efficiencies, decreasing costs and utilizing better one of the actual problems, the exploitation of energy at lower wind speeds.
- Previous cycles that are given from time to time in different markets and the likelihood to for that events to happen again.
- Information about long term projects.
- Increased interest from all type of investors, attracting people from the public and private sectors, commercial sectors or industrial customers.

Equally, forecasts can change a lot depending on the way wind energy is supported from the public institutions.

Some usual models to promote the development of activities in wind energy are having fixed prices for the power delivered to the grid, which favors the investments and predictions for return ratios, paybacks or first net profits, setting some standards in renewable energy such as a minimum percentage in the supply mix, that can be achieved through the creation of a markets for Renewable Energy Certificates, motivate the creation of competitive binding and power contract auctions, payment of purchase price premiums, investment incentives and the creation of markets for Renewable Energy Certificates [14].

Of the models mentioned above, it is the implementation of fixed prices for the power delivered to the grid the one that motivates the better a fast development of the projects and an increase in investment, having as examples the behavior in last years of countries

like Spain, Denmark, Germany, India or China. Due to the reduction in costs of the technology the last years, because of economies of scale and improvements in efficiency, the option of power contract auctions is also being appreciated, specially by governments, as this is an option that is less expensive for supporting institutions and other buyers of renewable energy. In the United States, it has been very successful the use of a tax credit system. Although it requires certain characteristics of the market in order to be implemented, it is the model applied actually for the North American country and has been taken into account for the forecasts. Another model tested in countries like Sweden with remarkable results is the Renewable Energy Certificates system, liked to the obligation to pay green energy of the consumer side. In many markets, there is no fixed model and several of them are used in order to incentivize the investment.

The following forecasts a growth in the market has been estimated, continued by a growth in the manufacturers statistics in order to meet the demand requirements. Wind energy is assumed to be around similar levels than the ones in 2016, this is, 55.3 GW are expected for 2017, taking into account the same factors that drove the change between 2015 and 2016.

Region	Units	Cumulative Installed Capacity by End of 2016	Installed Capacity in 2016	Forecast 2017-2021 (Including Offshore)					Installed Capacity between 2017 and 2021	Cumulative Installed Capacity by End of 2021
				2017	2018	2019	2020	2021		
Total Americas	(MW)	113,754	12,438	12,164	12,203	13,445	14,607	9,729	62,148	175,902
Total Europe	(MW)	160,874	13,915	13,769	13,285	11,025	9,700	10,050	57,829	218,703
Total South & East Asia	(MW)	198,839	26,994	27,678	26,675	26,275	25,325	25,375	131,328	330,167
Total OECD Pacific	(MW)	9,137	538	840	810	850	1,000	1,050	4,550	13,687
Total Other Areas	(MW)	4,226	431	809	555	675	750	875	3,664	7,890
Total New Capacity Every Year	**(MW)**	-	**54,316**	**55,260**	**53,528**	**52,270**	**51,382**	**47,079**	**259,519**	**746,350**
Cumulative Capacity	**(MW)**	**486,831**		**542,091**	**595,619**	**647,889**	**699,271**	**746,350**	-	-

Table 5. Total wind power capacity forecast by region in the 2017-2021 period [14].

Therefore, as can be seen in Table 5, in 2017 the annual capacity installations in wind power is expected to increase regarding 2016, reaching 55.3 GW and making a difference of 1.7%. However, from this year it is also expected to experience a downwards progression, installing less wind energy capacity each year. According to the forecast, the figures for the next five years will be around 53.5 GW in 2018, 52.3 GW in 2019, 51.4 GW in 2020 and an approximate value of 47.1 GW of wind power capacity installed during 2021. This decrease will be caused mainly to the drop in installations in important countries such as Germany or China. Another important factor taken into account is the change in American administration, which is implementing alterations in the direction that energy policies were pointing during the last years and will most likely mean a reduction in wind energy capacity installation in the United States these next years too. Despite the fact of expecting a decrease in every year installations, not everything is bad news, as the total capacity of wind energy will keep growing with acceptable rates, which will turn into a larger share of the renewable power in the electricity market and the achievement of one more step towards the accomplishment of national and international commitments about the reduction of carbon and gas emissions to the atmosphere. According to the forecast, between the years 2017 and 2021 it is expected to install another 259.5 GW of wind energy all around the world. At the end, this figure is divided among the different continents as follows: Europe will perform well, installing a 27.5% of its actual wind power capacity; America will behave in a similar way to Europe,

reaching an increase of 23.5%; Asia Pacific will experience the biggest increase in its wind energy installed capacity, achieving a total increment of 46.7%; and the rest of the world will see how its capacity is almost stagnated, as the increase is expected to be of only 2.3%. Nevertheless, there are some statistics that are quite sure to happen in the future. These are the leadership of China in annual wind energy turbines installations, with a great advantage over the rest of the countries in the world and the large investments of the United States in this sector, which will be consolidated in this very same ranking in the second position.

About the offshore wind forecasts, the last year it suffered a decrease from 3.7 GW in 2015 to 2.227 GW in 2016. However, the future expectations in this technology are quite hopeful, with approximately 19.2 GW of wind energy capacity to be installed in the following five years. As can be seen in Table 6, the forecasts for next years predict an increase of annual installed capacity regarding the current year and the decrease respect to 2015 is only due to the delay of many of the projects from 2014, making the figure of 2015 to be much bigger than it should be. Offshore market is permanently growing these last years and the same it is expected to happen in the short term [14].

The pushing regions in this sector are Europe and China, with installation capacities that will be close to 3.3 GW and 1 GW respectively. The most important European investments will be still seen in the United Kingdom and Germany, despite the decrease that both countries are experiencing during the last years. While the United Kingdom's forecasts show a figure of 1.56 GW during 2017, with a total new capacity of 5.3 GW in the next five years taking into account the decline when getting closer to 2021, Germany shows a total amount of 3.3 GW during the five years period. Other countries that also contributes to the offshore statistics in Europe are the Netherlands with more than 1.4 GW, Denmark with 400 MW or Belgium with a remarkable 1 GW. France is another of the countries that have important projects on the way, foreseeing a strong irruption in the European market with 800 MW before 2022.

In America, the United States will install around 30 MW of offshore wind power during 2016. Although it is an attractive market to invest in, USA has been a difficult decision to invest in regarding offshore, being relegated behind other markets. Due to that fact, it is expected that in the next years, with the tax incentives proven inefficient in offshore and only a few projects of 12 MW in 2020 and 21 MW in 2021 for the next five years, some uncertainty is surrounding the offshore market of the North American country. This does not improve if it is added to the equation the latest actions of the new administration, which could end up with the support and funding of some of the future projects.

In Asia, China is again the country which draws everyone's eyes. Having a development in offshore slower than expected due to the specialization that all technologies require at the beginning, the Asian country reached 592 MW of installed capacity in 2016 and it plans to install at least 1 GW more each year in following decade. This plan has real chances to be accomplished, just looking at the previous development of the Chinese market both in onshore and offshore. According to the forecasts, China will install around 6.1 GW in the 2017-2021 period. Other countries in the region that will make important investments are South Korea, Japan and Taiwan, which even being still a small market has an expected installation of 250 MW for the next five years.

Region	Units	Cumulative Installed Capacity by End of 2016	Installed Capacity in 2016	Offshore Forecast 2017-2021					Installed Capacity between 2017 and 2021	Cumulative Installed Capacity by End of 2021
				2017	2018	2019	2020	2021		
Belgium	(MW)	712	-	165	150	529	100	50	994	1,706
Denmark	(MW)	1,274	-	-	-	50	300	50	400	1,674
Finland	(MW)	32	-	-	-	-	-	-	-	32
France	(MW)	-	-	-	-	-	100	700	800	800
Germany	(MW)	3,848	813	1,476	600	500	250	500	3,326	7,174
Ireland (Rep.)	(MW)	25	-	-	-	-	-	-	-	25
Netherlands	(MW)	1,118	691	-	150	450	450	400	1,450	2,568
Norway	(MW)	2	-	-	-	-	-	-	-	2
Spain	(MW)	-	-	-	-	-	-	-	-	-
Portugal	(MW)	2	-	-	-	-	-	-	-	2
Sweden	(MW)	211	-	86	-	-	-	-	86	297
United Kingdom	(MW)	5,092	56	1,567	1,650	750	400	900	5,267	10,359
Europe	**(MW)**	**12,317**	**1,560**	**3,294**	**2,550**	**2,279**	**1,600**	**2,600**	**12,323**	**24,640**
Canada	(MW)	-	-	-	-	-	-	-	-	-
United States	(MW)	30	30	-	-	-	21	12	33	63
P.R. China	(MW)	1,103	592	1,000	1,200	1,300	1,300	1,350	6,150	7,253
South Korea	(MW)	35	30	-	99	-	-	100	199	234
Taiwan	(MW)	-	8	30	-	120	-	100	250	250
Japan	(MW)	57	7	-	-	100	-	150	250	307
Others	**(MW)**	**1,225**	**667**	**1,030**	**1,299**	**1,520**	**1,321**	**1,712**	**6,882**	**8,107**
Total World	**(MW)**	**13,542**	**2,227**	**4,324**	**3,849**	**3,799**	**2,921**	**4,312**	**19,205**	**32,747**
Offshore Global Share	***(%)***			***7.8%***	***7.2%***	***7.3%***	***5.7%***	***9.2%***	***7.4%***	***4.4%***
Cumulative Capacity	***(MW)***	***13,542***		***17,866***	***21,715***	***25,514***	***28,435***	***32,747***	***N/A***	***N/A***

Table 6. Offshore wind power capacity forecast in the 2017-2021 period [14].

3. STATE OF THE ART OF THE DOUBLY FED INDUCTION GENERATOR

In the second half of the XX century, wind energy turbines had a fast development, multiplying its nominal power by a factor of two or even three in some cases and implementing a great variety of new solutions. In the last decade of that century, most of the machines were fixed speed, operating with a rotor speed set by the frequency of the grid, the generator and the gearbox. The typical generators for fixed speed turbines were squirrel cage induction generator or the wound rotor induction generator, directly connected to the grid. Nonetheless, this configuration had important defects as the difficulties at controlling the power quality or the fact that it had only one point in which maximum efficiency was reached, given by a characteristic wind speed. Because of that, some ideas were suggested to improve the performance. Capacitor banks and soft starters were placed to regulate the reactive power consumption and the number of pair of poles was increased, attaining eight poles in most of the models. In that way, connecting four or six poles for medium wind speeds and eight for low speeds, two points of maximum efficiency were guaranteed. In addition, fixed speed turbines also had advantages as cheap electronic devices, simple and robust construction or high reliability. At the end, it was its own definition, fixed speed, the reason why the following technologies advanced in other direction. Due to the high restrictions in rotor speed, wind fluctuations were transmitted through the torque, delivering them to the grid. This could cause big problems, as that oscillations are usually translated into an increase of the current, which has as main consequence a rise in the power losses. This wind energy convertion systems were denominated as type I.

As the time went by, variable speed wind technologies became more popular than the fixed speed machines. Variable speed allowed to cover a wider range of wind speeds, being able to track the points of better efficiencies, extracting more power from the wind. The type II wind energy convertion systems were born and it used a wound rotor induction generator. Some other advantages of this technology were reduced stresses in the mechanical systems of the turbine and some control over the power output thanks to the slip. The slip was a consequence of adding resistances to the rotor of the generator, changing in that way variables as the current and reaching a narrow interval of values, between 10-16%, in which the power could vary. In type II machines there were still soft starters in order to guarantee a smooth integration of the power into the grid and capacitor banks, since some reactive power compensation had to be done, although it was much lower than in type I.

Type III wind energy convertion systems were more expensive that the previous two technologies, but it came also with an improvement of the slip, reaching values from 30% negative to 30% positive. This is a consequence of the higher number of generators types that can be applied in variable speed technologies, implementing the doubly fed induction generator configuration. This generator, using a partial-scale power converter, is able to inject currents and regulate the power much better than type II. Despite the increase in cost, former needs as the soft starter or the capacitor banks were no longer necessary and nominal power rose to the current commercial wind turbines of 2 and 3 MW.

In the case of type IV wind energy convertion systems, the implementation of a full-scale power converter is essential, implying extra losses and higher costs. On the other hand, this innovative technology is able to control both active and reactive power delivered to the grid, it allows the connection of a wound rotor induction generator and a permanent magnet synchronous generator and makes optional the election of having a gearbox. Type IV is having a big implementation for offshore wind energy during the last years and most of the biggest suppliers are focusing their efforts in this direction.

The following machines use the doubly fed induction generator configuration. They represent the current situation of the commercial type III wind energy convertion systems in the global market:

Turbine Model	Nominal Power [kW]	Rotor Diameter [m]	Turbine Model	Nominal Power [kW]	Rotor Diameter [m]
Acciona AW 70/1500 Class I'	1500	70	Nordex N90/2500 HS'	2500	90
Alstom ECO 100/3000 Class I'	3000	100	Nordex N90/2500 LS'	2500	90
Alstom ECO 110/3000 Class II'	3000	110	Nordex S70/1500 kW'	1500	70
Alstom ECO 122/2700 Class III'	2700	122	Nordex S77/1500 kW'	1500	77
Alstom ECO 122/3000 Class III'	3000	122	REpower 3.0M/122'	3000	122
Alstom ECO 74/1670 Class II'	1670	74	REpower 3.2M/114'	3200	114
Alstom ECO 80/1670 Class II'	1670	80	REpower 3.4M/104'	3400	104
Alstom ECO 80/1670 Class III'	1670	80	REpower MM100 50Hz'	2000	100
Alstom ECO 80/2000 Class II'	2000	80	REpower MM100 60Hz'	1800	100
Alstom ECO 86/1670 Class III'	1670	85.5	REpower MM82'	2050	82
DeWind D8.1'	2000	80	REpower MM92'	2050	92.5
DeWind D8.2'	2000	80	Samsung 2.5/90'	2500	90
DeWind D9.0'	2000	93	Siemens SWT-2.3-101'	2300	101
DeWind D9.1'	2000	93	Siemens SWT-2.3-108'	2300	108
DeWind D9.2'	2000	93	Siemens SWT-2.3-113'	2300	113
DeWind D6 62 m'	2000	62	Siemens SWT-2.3-82 VS'	2300	82.4
DeWind D6 64 m'	2000	64	Siemens SWT-2.3-93'	2300	93
Dongfang DF100-2500'	2500	100	Siemens SWT-3.6-107'	3600	107
Dongfang DF110-2500'	2500	110	Siemens SWT-3.6-120'	3600	120
Dongfang DF70-1500'	1500	70	Sinovel SL1500/60'	1500	60
Dongfang DF77-1500'	1500	77	Sinovel SL1500/70'	1500	70
Dongfang DF82-1500'	1500	82	Sinovel SL1500/77'	1500	77
Doosan WinDS3000'	3000	91.3	Sinovel SL1500/82'	1500	82
Fuhrländer FL 1500 77m'	1500	77	Sinovel SL3000/100'	3000	100
Gamesa G114-2.0 MW'	2000	114	Sinovel SL3000/105'	3000	105
Gamesa G114-2.5 MW'	2500	114	Sinovel SL3000/110'	3000	110
Gamesa G52- 0.85 MW'	850	52	Sinovel SL3000/115'	3000	115
Gamesa G58- 0.85 MW'	850	58	Sinovel SL3000/90'	3000	90

Gamesa G80-2.0 MW'	2000	80	Subaru 80/2.0 Prototype'	2000	80
Gamesa G87-2.0 MW'	2000	87	Vergnet GEV HP'	1000	62
Gamesa G90-2.0 MW'	2000	90	Vergnet MP C/R'	275	32
Gamesa G97-2.0 MW'	2000	97	Vestas V100 - 1.8 MW 50 Hz'	1800	100
Gamesa Made AE61'	1320	61	Vestas V100 - 1.8 MW 60 Hz'	1815	100
GE 1.5-77'	1500	77	Vestas V100 - 2.0 MW'	2000	100
GE 1.6-100'	1600	100	Vestas V100 - 2.6 MW'	2600	100
GE 1.6-82.5'	1600	82.5	Wind to Energy W2E-100/2.0'	2000	100
GE 1.7-100'	1790	100	Wind to Energy W2E-100/2.5'	2500	100
GE 2.5-100'	2500	100	Wind to Energy W2E-103/2.5'	2500	103
GE 2.5-120'	2530	120	Wind to Energy W2E-120/3fc'	3000	120
GE 2.75-100'	2750	100	Wind to Energy W2E-93/2.0'	2000	93
GE 2.75-103'	2750	103	Windtec DF 1650-AB37'	1650	77
GE 2.75-120'	2780	120	Windtec DF 1650-AB43'	1650	88
GE 3.2-103'	3230	103	Windtec DF 1650-WT 82'	1650	82
Hanjin HJWT1500-77'	1500	77	Windtec DF 2000-LZ53.4CCV'	2000	111
Hanjin HJWT2000-87'	2000	87	Windtec DF 2000-WB48.8'	2000	100
Hanjin HJWT2000-93'	2000	93	Windtec DF 2000-WT53'	2000	110
Hyosung HS50'	750	50	Windtec DF 2000-WT55'	2000	113
Hyosung HS90'	2000	90.6	Windtec DF 2000-WT86'	2000	86
Hyundai HQ1650 TC II'	1650	77	Windtec DF 2000-WT93'	2000	93
Inox WT 2000 DF'	2000	93	Windtec FC 2000-Sinoma 50.2'	2000	103
Lagerwey L93-2500'	2500	93	Windtec FC 2000-WB48.8'	2000	100
Mistubishi MWT62/1.0'	1000	61.4	Windtec FC 2000-WT53'	2000	110
Mitsubishi MWT100/2.4'	2400	100	Windtec FC 2000-WT55'	2000	113
Mitsubishi MWT102/2.4'	2400	102	Windtec FC 2000-WT86'	2000	86
Mitsubishi MWT92/2.3'	2300	92	Windtec FC 2000-WT93'	2000	93
Mitsubishi MWT92/2.4'	2400	92	Windtec FC 3000-100'	3000	100
Mitsubishi MWT95/2.4'	2400	95	Windtec FC 3000-130'	3000	130
MY 1.5 - 77'	1500	77	Windtec FC 3000-90'	3000	90
MY 1.5 - 82'	1500	82	Windtec FC 3000-Aeolon58'	3000	120
Nordex N60/1300 kW'	1300	60	Windtec FC 3000-EU100'	3000	100
Nordex N80/2500'	2500	80	Windtec FC 3000-LZ55'	3000	113
			Windtec FC 3000-WT115'	3000	115

Table 7. Current type III wind energy convertion systems available in the market.

From Table 7, we can observe that there are 123 different turbines being commercialized at the present time. There is a wide range of options to choose, from the lowest machine, as the Vergnet MP C/R', with 32 meters of diameter and 275 kW, to the largest ones, as we can observe in the Siemens SWT-3.6-107' and the Siemens SWT-3.6-120', both with

a nominal power of 3.6 MW, or the Windtec FC 3000-130', which although does not reach the 3.6 MW of nominal power, has the largest rotor diameter, achieving 130 meters.

Among the top 10 suppliers, the most common diameter is 100 meters, even though there is a great variety of nominal powers that can be obtained from that rotor dimensions, as it is the case of the leader in the wind turbine sector. Having five different products, the Danish company offers a range from 1800 to 2600 kW, all of them with the same size for rotor diameter. This makes easier the comparison between their turbines, as all of them have the very same catchment area. The main distinction is that while the lower power turbines are designed to extract as much as possible from lower wind speeds, while wind energy convertion systems with higher nominal power are usually located at regions where the wind speeds are high, tracking in a better way the maximum efficiency points.

For the wind division of General Electric, other of the big companies in the market, we find again that most of the products have 100 meters diameters. However, they also have some offers out of these dimensions, as two GE 120', with nominal power around 2.75 MW or other two products that provide around 1500 kW with 80 meters.

Gamesa is the entity that offers the most turbine designs, having a total of nine products in the market. The Spanish company provides turbines with lower nominal power than others like Vestas or General Electric, having models that move around 1 MW and specific turbines of 850 kW as the Gamesa G52- 0.85 MW', with rotor diameters from 50 to 60 meters or 2 MW machines with rotors that vary from 80 to 110 meters.

Siemens, another of the top 10 suppliers, offers wind energy convertion systems that move around two different nominal wind speeds, 2300 kW and 3.6 MW, while the rotor dimensions are again similar to other companies, being close to 100 meters.

It will be interesting to follow the development of Gamesa and Siemens in the next few years, after their merge became a fact and expecting to reach the second position as global wind energy turbine provider.

4. MODELS DESCRIPTION

This chapter describes the different models implemented for an adequate working of a wind energy convertion system.

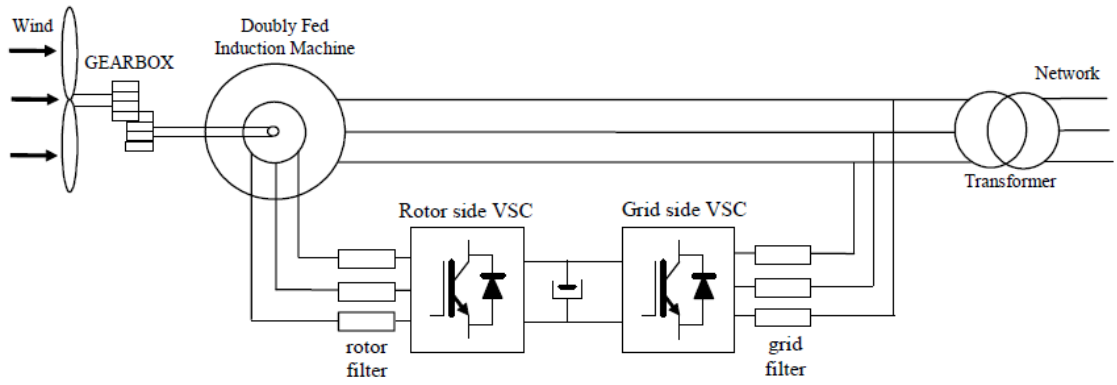

Figure 6. Complete scheme of the Wind Energy Convertion System [2].

The model is composed by the following parts, which will be explained with deeper details along this chapter:

Physical models

- Mechanical coupling model
- Aerodynamic model
- Wind speed model

Electrical models

- Rectifiers and inverters
- Frequency converter
- DC link capacitor model
- Inductance filter and transformer model

Control models

- Linear control techniques
- Non-linear control techniques
- Blades control system

4.1. Physical Models

4.1.1. Mechanical coupling model

The mechanical model of the wind energy convertion system consists on the blades attached with the hub, the rotor of the generator and the gearbox, all connected through two different axes, one for the low rotational speeds in the blades and another for the high rotational speeds needed in the rotor of the generator. The gearbox is the element in

charge of the correct correlation of velocities between the two axes, by multiplying the velocity in the blades side through several the stages located in the gearbox until an adequate velocity is reached for the generator side.

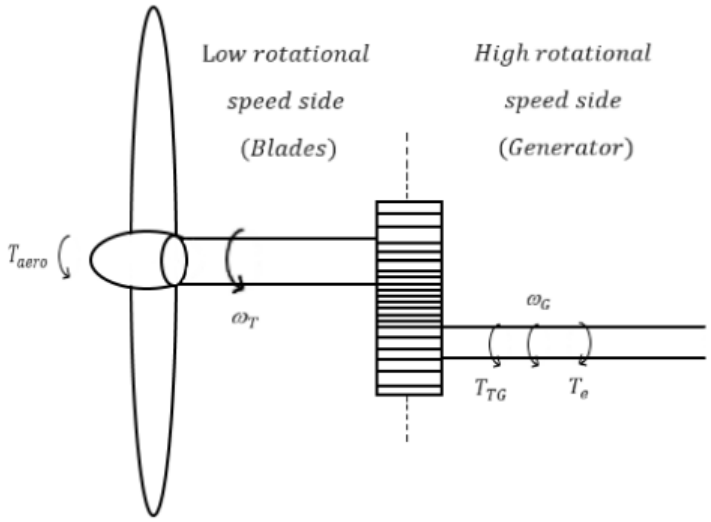

Figure 7. Mechanical coupling of the wind energy convertion system.

To describe the behavior of this components, some assumptions must be made. The blades, the hub, the low rotational speed shaft and the gearbox will be considered to be one mass, which means that all vibrations in the high-speed axis are neglected in comparison with the vibrations in the low rotational speed axis [15].

The two-mass model has been implemented with three equations, where T_{aero} is the aerodynamic torque, T_{TG} is the blades to generator torque, T_e is the torque coming from the generator, ω_T is the rotational speed in the blades side, ω_G is the rotational speed in the generator side, D is the damping coefficient for the high-speed shaft, K is the high-speed axis stiffness, J_T is the inertia of the mass in the blades side (blades, hub, low speed shaft and gearbox) and J_G is the inertia of the mass at the generator side:

$$J_T \frac{d\omega_T}{dt} = T_{aero} - T_{TG} - D \cdot (\omega_T - \omega_G) \tag{4. 1}$$

$$J_G \frac{d\omega_G}{dt} = T_{TG} - T_e + D \cdot (\omega_T - \omega_G) \tag{4. 2}$$

$$\frac{dT_{TG}}{dt} = K \cdot (\omega_T - \omega_G) \tag{4. 3}$$

As it is a linear model, we can directly express it in only one equation in matrixial form:

$$\frac{d}{dt}\begin{bmatrix}\omega_T \\ \omega_G \\ T_{TG}\end{bmatrix} = \begin{bmatrix}-\frac{D}{J_T} & \frac{D}{J_T} & -\frac{1}{J_T} \\ \frac{D}{J_G} & -\frac{D}{J_G} & \frac{1}{J_G} \\ K & -K & 0\end{bmatrix}\begin{bmatrix}\omega_T \\ \omega_G \\ T_{TG}\end{bmatrix} + \begin{bmatrix}\frac{1}{J_T} & 0 \\ 0 & -\frac{1}{J_G} \\ 0 & 0\end{bmatrix}\begin{bmatrix}T_{aero} \\ T_e\end{bmatrix} \tag{4. 4}$$

Therefore, a better and more accurate approach can be obtained than the one that could be reached with a one mass model. Because of the implementation of the two-mass modelling it can be observed that the velocity stabilization is much smoother than with a one mass model.

4.1.2. Aerodynamic model

Aerodynamics is the science and study of the physical laws of the behavior of objects in an air flow and the forces that are produced by air flows [16]. The way the variables are chosen and the parameters are measured is not arbitrary. Therefore, with the purpose of getting a simpler and easier approach to the model, the following figure must be studied:

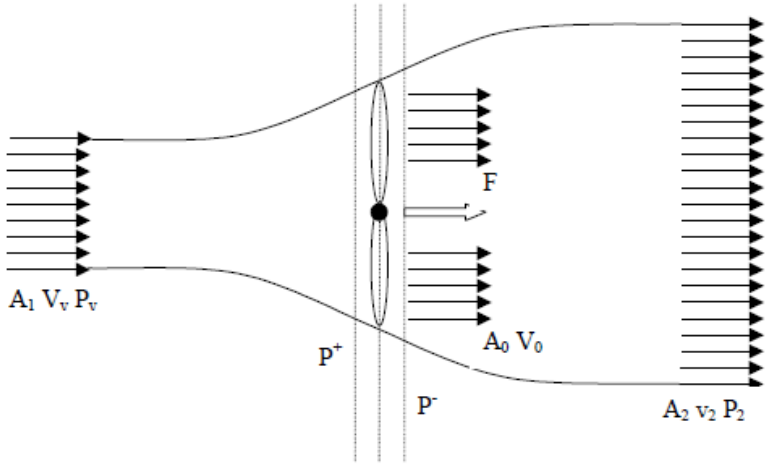

Figure 8. Layout of air flow through the blades of a wind turbine [2].

For the calculus of the aerodynamic power some assumptions can be done as incompressible air, steady motion of the fluid or same value for the parameters on a given section [2]. Furthermore, the power obtained from the wind will be proportional to the area covered by the blades (usually the area of a circle, as the blades describe a circumference around the hub) and proportional to the wind speed. This part can be tricky, as this velocity does not correspond to the one that strikes the blades, but to the upstream wind speed, represented by U_v in the previous figure. Then, the power available in the wind will be defined as:

$$A = \pi R^2 \tag{4. 5}$$

$$P_{wind} = \frac{1}{2}\rho A U_v^3 \tag{4. 6}$$

where ρ is the air density, with a value of 1.225 kg/m^3 around atmospheric pressure.

However, the wind turbine cannot utilize all the power contained in the wind, as extracting all the energy from the air means that there would be no stream of fluid at all after the blades. This utilization of energy leads to some pressure drop between the regions before and after the blades of the wind turbine, but can also be neglected, as in this case, by assuming steady flow.

Due to the impossibility of capturing all the energy, there is a power coefficient that measures the amount of power that can be utilized from the wind, completing the aerodynamic power equation:

$$P_{aero} = \frac{1}{2}\rho A U_v^3 \cdot Cp(\lambda, \beta) \tag{4. 7}$$

being β the pitch angle or angle of variation for the blades respect their original position and λ the tip speed ratio, this is, the maximum velocity in the wind turbine blades, which is observed at the tip. It is usually compared with the wind speed:

$$\lambda = \frac{\omega_T \cdot R}{U_v} \tag{4. 8}$$

From the previous expressions, the aerodynamic torque can also be calculated:

$$T_{aero} = \frac{P_{aero}}{\omega_T} \tag{4. 9}$$

In older wind energy convertion systems, blades were fixed and were not able to change their angular position in the hub. This means that the pitch angle β is constant in that turbines. This is called stall or passive stall control, as at high wind speeds, the blades will stall, reducing automatically the forces exerted on the blades and protecting the wind turbine from possible damages. Therefore, as the power coefficient (Cp) was previously defined as a function of the tip speed ratio λ and β, the evolution curve of the Cp in these turbines would depend only on the λ value:

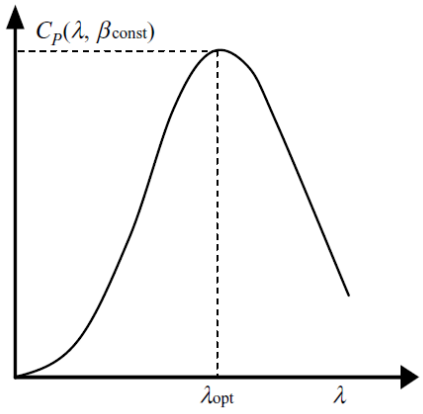

Figure 9. Cp for a fixed blade angle [1].

In modern wind energy convertion systems, it is possible to modify the pitch angle of the blades through a servo mechanism. This allows to change the angle of attack the relative wind velocity is impacting with, changing also in that way the forces exerted on the wind turbine and as consequence, the total power that is extracted from the wind. Due to this, it is important to find the optimum power coefficient, calculating the optimum tip speed

ratio and the optimum pitch angle. In order to do so, a MATLAB function has been implemented applying the following formulas [17]:

$$\Delta = \frac{1}{\lambda + k_6 \cdot \beta} - \frac{k_7}{1 + \beta^3} \tag{4. 10}$$

$$Cp = k_1 \cdot (\Delta - k_2 \cdot \beta - k_3 \cdot \beta^3 - k_4) \cdot e^{-\Delta \cdot k_5} \tag{4. 11}$$

where k_1, k_2, k_3, k_4, k_5 and k_6 are different constants that depend on the environment that surrounds the turbine.

Then, by finding the tip speed ratios and pitch angles, it is possible to calculate all the power coefficients. Arranging them, it results the same curve obtained in under stall control, having in this case a non-constant β:

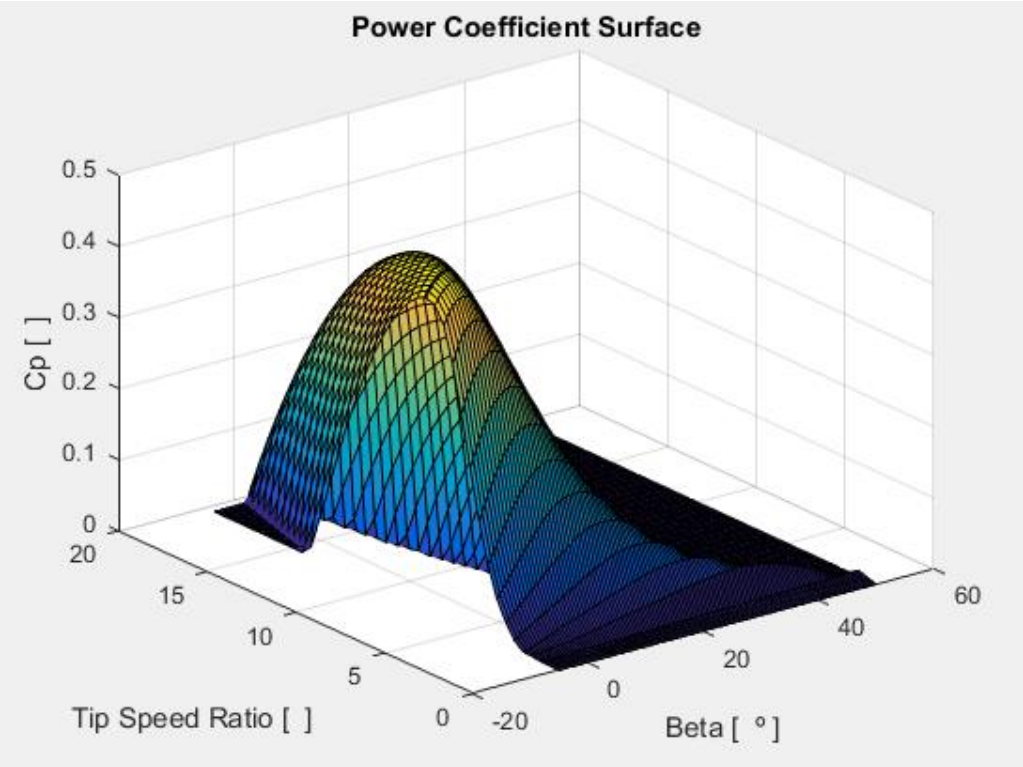

Figure 10. Cp for active control wind turbines.

After the corresponding theoretical demonstration, it can be shown that the maximum theoretical limit for the power coefficient is 16/27, this is 0.593. This demonstration was first done by the German physicist Albert Betz, who stated that only that 59.3% of the kinetic energy available in the wind can be extracted as maximum. However, current wind turbines have not been developed until that limit, reaching power coefficient values between 0.52 to 0.55.

4.1.3. Wind speed model

In order to simulate the behavior of the doubly fed induction generator, it is necessary to get the input values from wind. Wind speed sequences can be obtained directly by measuring the flow in a determined place, but this takes time, money and will not always cover the range of wind speeds or turbulence intensities that an existing wind energy convertion system experience and are needed for a correct and complete simulation. Another option, the one implemented here, is to create a synthetic wind speed sequence. The following wind model is divided in four different characteristics: average wind speed, ramp velocity, gust component and turbulences [18].

Average wind speed is an offset in order to introduce higher or lower wind speeds, regardless the other components that will make the model to go to higher or lower values.

The ramp velocity is just the introduction of increasing or decreasing variations in wind speed, favoring in that way a wider range for the analysis of the simulation, describing also the upward and downward movements that can be observed in real wind sequences. The following expression has been used in the wind model, as function of time:

$$U_{ramp}(t) = \begin{cases} 0, & t \leq T_{r1} \\ A_r\left(\dfrac{t - T_{r1}}{T_{r2} - T_{r1}}\right), & T_{r1} < t \leq T_{r2} \\ A_r, & t > T_{r2} \end{cases} \tag{4. 12}$$

where T_{r1} and T_{r2} indicate at which time the ramp component starts to be present and when does it finish. A_r is the maximum increase that can be reached by the ramp component.

The wind speed gust is a change in the wind speed that usually does not last for too long, causing sudden spikes in the sequence. In the model, gusts are described as:

$$U_{gust}(t) = \begin{cases} 0, & t \leq T_{g1} \\ \dfrac{A_g}{2}\left[1 - cos\left(2\pi\dfrac{t - T_{g1}}{T_{g2} - T_{g1}}\right)\right], & T_{g1} < t \leq T_{g2} \\ 0, & t > T_{g2} \end{cases} \tag{4. 13}$$

where T_{g1} indicate at which time the gust component starts and T_{g2} when does it finish. A_g represents the peak value of the gust.

Turbulences are the chaotic changes in wind speed that do not follow a predictable scheme. As approximation, wind speed turbulences can be written as sum of sinusoidal functions with random phase angle [19]:

$$U_{turb}(t) = \sum_{i=1}^{N} A_i \cdot (\omega_i \cdot t) + B_i \cdot \cos(\omega_i \cdot t) \tag{4. 14}$$

$$A_i = \sqrt{\frac{1}{2} \cdot S_f \cdot \Delta\omega} \cdot \sin(\Phi_i) \tag{4. 15}$$

$$B_i = \sqrt{\frac{1}{2} \cdot S_f \cdot \Delta\omega} \cdot \cos(\Phi_i) \tag{4. 16}$$

where Φ is a random variable uniformly distributed from 0 to 2π, ω_i a narrow range of frequencies and S_f is the power spectral density magnitude at frequency ω_i.

Therefore, after the calculation of all wind components, they should be added to get the final expression of a synthetic wind speed sequence:

$$U(t) = U_{avg} + U_{ramp}(t) + U_{gust}(t) + U_{turb}(t) \tag{4. 17}$$

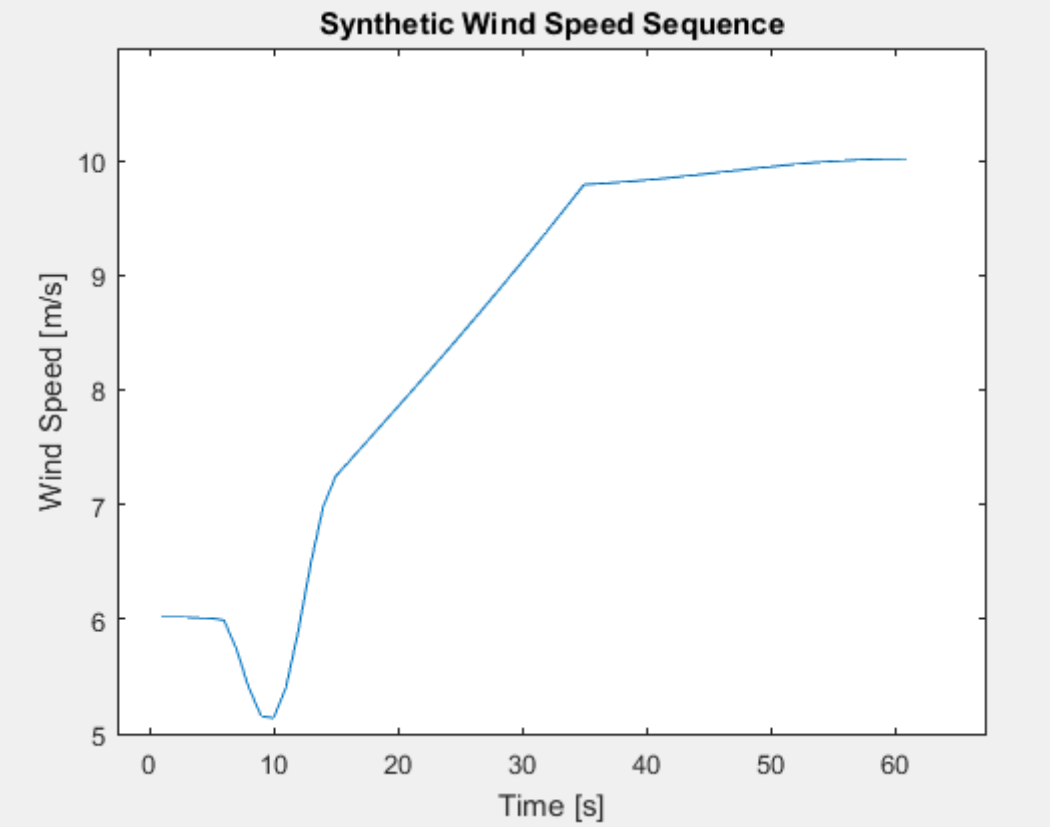

Figure 11. Synthetic Wind Speed Sequence.

4.2. Electrical Models

Power electronics are improving quite fast during the last years. Cheaper prices, better efficiencies and more reliable components are some of the reasons why wind energy markets are becoming more and more important in the energy sector. In the following

pages, some of the electrical devices that can be found in a wind energy convertion system will be described.

4.2.1. Rectifiers and inverters

Most of the frequency converters are formed by a rectifier in order to implement an AC to DC convertion with the power flowing in the DC direction, a DC link whose main component is a capacitor and an inverter that performs a DC to AC convertion with the power flowing in the AC direction.

Due to its simple design, low cost and low losses, the diode rectifier is one of the most used solutions. Nonetheless, it has important disadvantages such as the generation of harmonic currents or the allowance of power flow in a unique direction, this is, it is not able to regulate generator's voltages or currents and as consequence, its use is restricted to its implementation in a type III or type IV wind energy convertion systems with inverter, controlling in that way those variables.

Other cheap option with low losses is the thyristor-based inverter, although it has drawbacks as its necessary connection to the grid, the consumption of reactive power and the generation of wide harmonics. The latest requirements in better quality outputs are making this solution to be neglected in comparison to insulated-gate bipolar transistors (IGBT) or gate turn-off inverters (GTO). Specially IGBTs are showing a fast development in the power they can handle, despite their cost and high losses [1].

4.2.2. Frequency converter

In the last years, several types of frequency converters have been applied to wind energy convertion systems: back-to-back converters, matrix converters, multilevel converters, resonant converters and tandem converters. Although the multilevel and the matrix converters are becoming more popular, the most relevant one is the back-to-back, as it is the one that most of the wind turbines use currently. It is so relevant that even other converters are trying to improve theirselves by implementing the advantages that the back-to-back model presents.

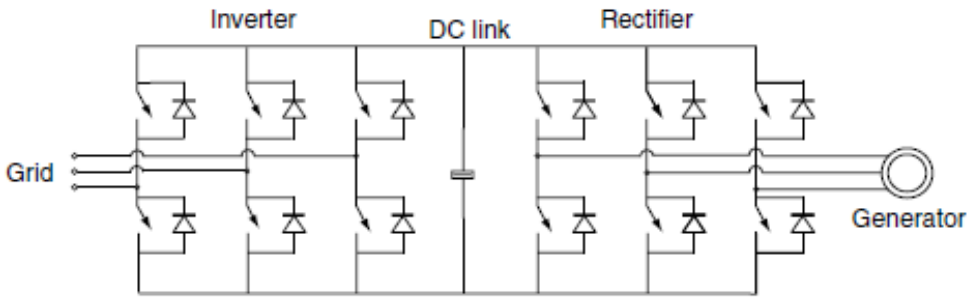

Figure 12. Back-to-back frequency converter [1].

The back-to-back converters consist on two pulse-width modulated voltage source converters. Both of them are formed by six IGBTs mounted in parallel with one diode each.

Depending on the operation mode of the doubly fed induction machine, this is, if it is running with motor or generator criteria, the voltage source converters can work as rectifiers or inverters. Moreover, this motor or generator criteria will define the direction of the power flow through the rotor, injecting or withdrawing it. Under subsynchronous operation, when the mechanical speed is rotating slower than the synchronous speed, the rotor side converter works as inverter and the grid side converter works as rectifier. In the opposite case, under supersynchronous operation, when the mechanical speed rotates faster than synchronous speed, the rotor side converter and grid side converter invert their roles, working the first as rectifier and the last one as inverter.

The main duties of the rotor side converter are controlling the electromagnetic torque and the reactive power of the stator, while the grid side converter is responsible of regulating the voltage level in the DC link. Besides that, grid side converter is also able to regulate the reactive power, but due to simplicity it is usually set to zero.

In comparison with other converters, the back-to-back has higher switching losses than a matrix converter, although this last type does not behave as well as the back-to-back during a fault situation. Matrix converter have more disadvantages, as its high conduction losses and its limitation in the output voltage converter. Other converter that should be taken into account is the multilevel, due to its harmonic results, being the converter with the best spectra on grid side and rotor side. This is due to its low demand on the input filters.

In the converter model, assuming similar frequencies in rotor and stator, all variables can be seen as being in a system in which terminal voltage terminal and q-axis are aligned. According to that, it can be derived:

$$u_{ds} = 0, \qquad u_{qs} = u_s$$

being u_s the stator voltage magnitude. Then, neglecting the resistance in the stator, the expression for the electromagnetic torque and the reactive power exchanged with the grid would be as follows:

$$T_e = -\frac{L_m u_s i_{qr}}{\omega_s \cdot (l_s + L_m)} \tag{4. 18}$$

$$Q_s = -\frac{L_m u_s i_{dr}}{(l_s + L_m)} - \frac{{u_s}^2}{\omega_s \cdot (l_s + L_m)} \tag{4. 19}$$

Nevertheless, not all the reactive power is exchanged between the converter and the grid. Therefore, the resultant active and reactive powers in the converter could be calculated as:

$$P_c = u_{rc} \cdot i_{rc} + u_{ic} \cdot i_{ic} \tag{4. 20}$$

$$Q_c = u_{ic} \cdot i_{rc} - u_{rc} \cdot i_{ic} \tag{4. 21}$$

where r and i are subscripts that stand for real or imaginary parts respectively and c is the letter used when the variable comes from the converter. It is important to note that for a doubly fed induction generator, the value of the active power in the converter corresponds to the active power delivered or withdrawn from the rotor to the grid. In the case of the reactive power, the amount exchanged with the grid would correspond to the sum of Q_c and Q_s, the reactive power in the stator. However, grid-side converter is set to zero in most of the cases [1].

4.2.3. DC link capacitor model

The DC link is a connection between the rectifier and the inverter that allows the storage of energy, stabilizing in that way the voltage. This link, formed by capacitors, has a high voltage regarding the grid, being able to regulate the grid current.

The capacitor, located between rectifier and inverter, allows to make a separate control on both rotor and grid sides, without causing any problem in the other side of the converter. A usual strategy for the DC link control is to maintain a constant DC voltage, while controlling the rotor side to reach the required values for the variables [1].

In addition, there have been some doubts about the use of a DC link in a back-to-back converter due to a possible reduction of the efficiency and lifetime of the converter, once compared with a converter without the DC link capacitor [20].

The DC link capacitor model can be described by the following equation:

$$i_{rs} - i_{gs} = C \cdot \frac{d}{dt} V_{DC}(t) \tag{4. 22}$$

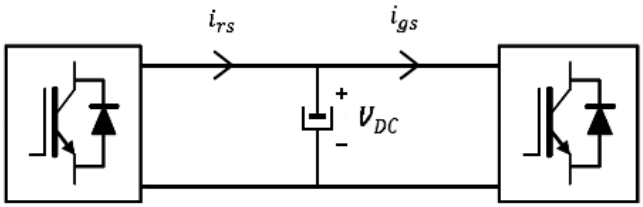

Figure 13. DC link.

4.2.4. Inductance filter and transformer models

Inductance filters are located at the entrance of the frequency converter, being in charge of reducing harmonics to a lower level and attenuating the peaks from the switching activity. In the case of the static transformer, its model can be derived from any of the books of classic bibliography.

The inductance filter model can be presented as:

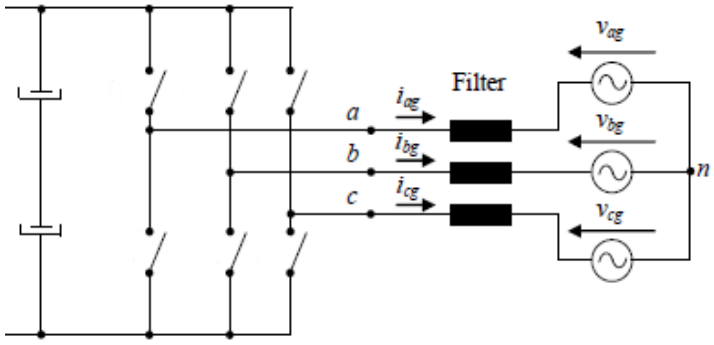

Figure 14. Inductance filter model [2].

where i_{ag}, i_{bg} and i_{cg} are the grid side converter currents for the three phases and v_{ag}, v_{bg} and v_{cg} are the grid voltages.

4.3. Control Models

At the beginning of the fast development that wind energy convertion systems are experiencing, most of the efforts were put on electronic, electric or mechanic disciplines and therefore, techniques as flux oriented control were enough at that moment for a correct control of the turbines. Nonetheless, this control techniques have also been evolving las years, as the requirements are also changing from the transmission system operators in order to inject power to the grid.

For any wind turbine, it is necessary to implement an optimal operating point tracking, following the points at which the maximum efficiency can be reached, obtaining the as much energy as possible from the wind.

In order to get a better idea of the model, the following characteristic curves will be presented:

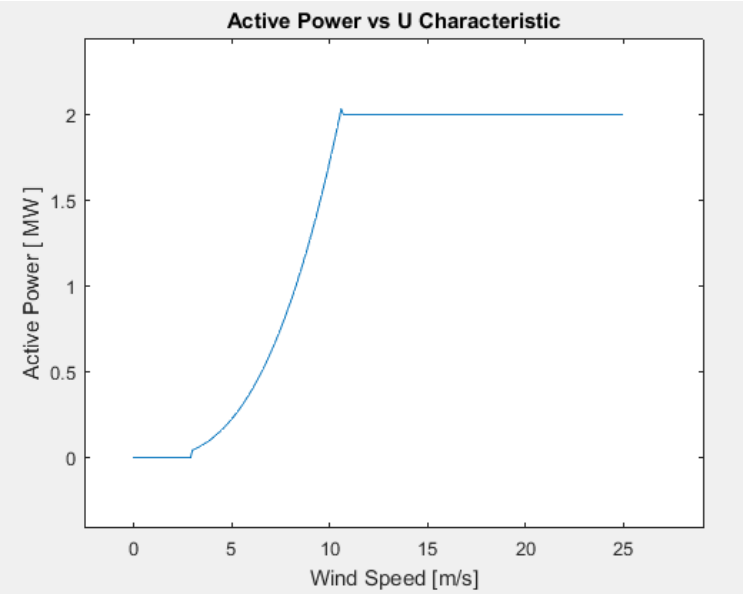

Figure 15. Active Power vs wind speed characteristic.

Figure 15 represents the evolution of the active power of the wind turbine, depending on the wind speed. From the graph, some important information can be obtained, as the cut-in and the cut-out wind speeds, the velocities at which the machine starts to operate and stops operating respectively. This indicates the range of air flow that is utilized by the wind turbine, being from 0 to 3 m/s the interval in which it is not profitable to produce energy and higher winds to 25 m/s too dangerous for the integrity of the structure. Then, it can be observed that from 3 m/s to 10.6 m/s the power experiences an increase in form of cubic function. This comes from (4. 7), where all variables can be assumed to be almost constant except the wind speed, as the catchment area is a fixed magnitude, air density will not vary too much and from 3 to 10.6 m/s the curve is in the region of maximum Cp, so the only value that is making the power to rise is the wind speed, elevated to the third power. From 10.6 m/s, the curve enters in the nominal power region, varying both the wind speed and the Cp, which starts being under optimal values thanks to the change in the pitch angle, making the aerodynamic force to decrease and obtaining as result a flat zone.

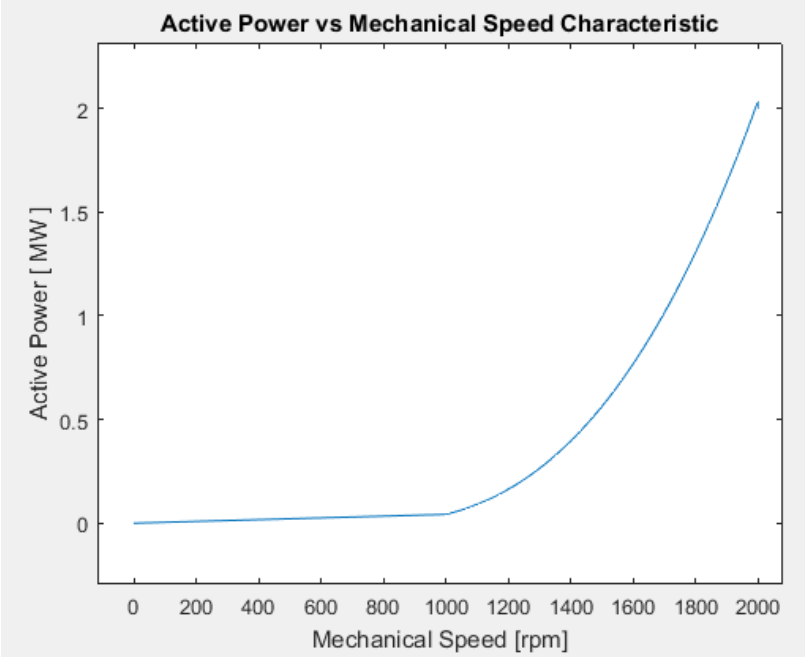

Figure 16. Active Power vs mechanical speed characteristic.

In this case, from Figure 16, we can deduce the range of mechanical speeds in which the turbine is producing power, which moves from 1 000 rpm to 2 000 rpm. These variations are given by the slip, which adopts values from 30% negative to 30% positive speeds, as we are considering the use of a type III machine with doubly fed induction generator and the synchronous speed is 1 500 rpm, provided by the grid. At first sight, the plot is very similar to Figure 15, as the cut-in speed coincides with 1 000 rpm and the maximum Cp region finishes at 10.6 m/s, at the maximum mechanical speed, which remains constant at 2 000 rpm for the nominal power of 2 MW until the 25 m/s threshold is surpassed, stopping the turbine, or the wind speed decreases again below 10.6 m/s.

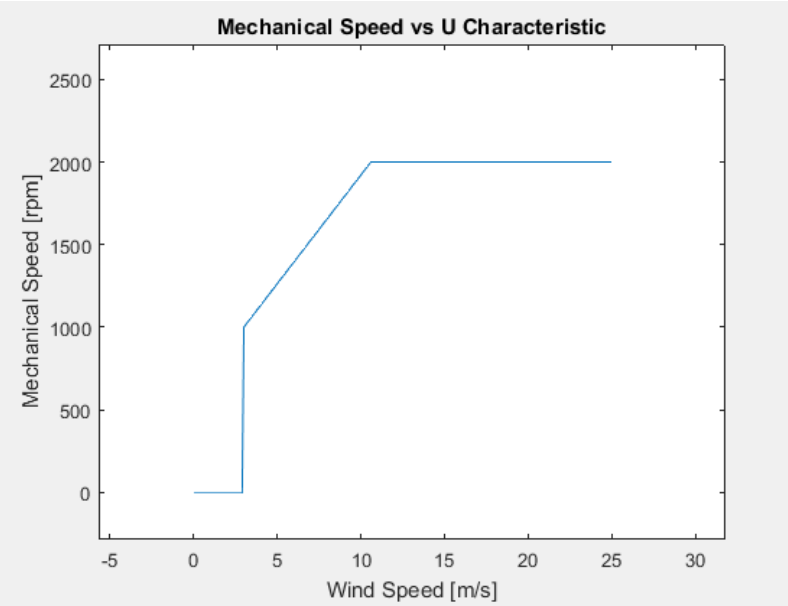

Figure 17. Mechanical speed vs wind speed characteristic.

Figure 17 represents better what it was described for the previous figure (Figure 16), as here the change from 0 to 1 000 rpm is more pronounced than in the active power vs mechanical speed characteristic. A linear proportion can be observed between the two variables in the maximum power point tracking region, as mechanical speed depends on the mechanical internal power entering the generator through the shaft, which at the same time is a function of the wind speed. Moreover, cut-in and cut-out can also be appreciated.

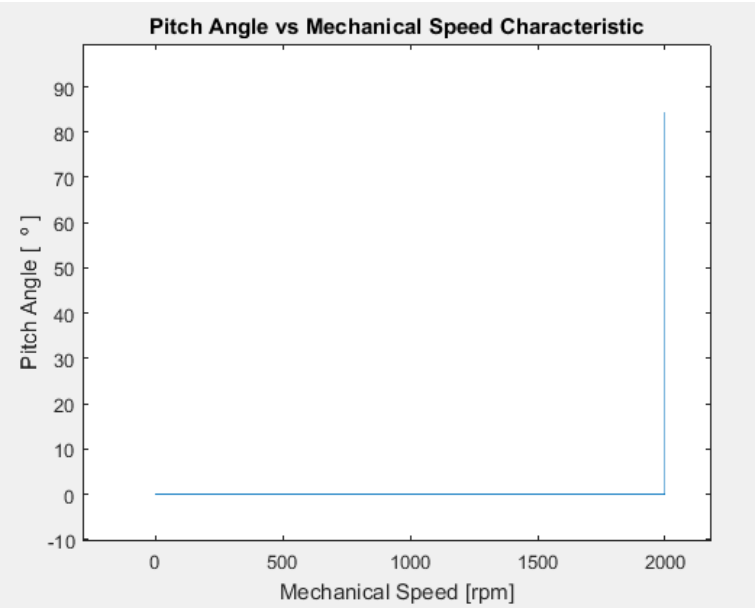

Figure 18. Pitch angle vs mechanical speed characteristic.

In the case of Figure 18, another characteristic curve is presented, in which pitch angle and mechanical speed summarizes the information from previous characteristic curves. As it can be seen, the pitch angle does not change from 0 to 2 000 rpm, which corresponds to the regions in which the wind speeds are too low for the turbine to be working (under

3 m/s) or the Cp is maximum. Then, above wind speeds of 10.6 m/s, the machine enters in the nominal power region and the Cp is no longer at maximum values. Is in that moment, that corresponds to the maximum mechanical speed with 2 000 rpm, when the pitch angle starts to vary from the initial 0 degrees to an angle that can reach 90 degrees at the cut-out speed of the wind turbine.

For this model, the wind energy convertion system is regulated through vector control with the reference set to the synchronous dq frame, which is defined by the stator voltage phasor.

4.3.1. Linear control techniques

Vector control appeared to amend the problems of previous control techniques as scalar control, whose dynamic response was very poor. Vector control, or field oriented control (FOC), was designed for induction generators and was introduced later on for doubly fed induction generators (DFIG) and consists on mathematic transformations to reduce the machine to a two-phase synchronous reference frame (dq). In the case of the doubly fed induction generator, the direct axis is oriented to the stator flux space vector or, if appropriate, the stator voltage, in order to accomplish a better control of the model by decoupling and linearizing the variables. Usually, the target variables to control are the stator reactive power and the electromagnetic torque.

To improve the control dynamics, the most common strategy is the implementation of the cascade regulation, in which each regulator controls one physic variable in an external control loop, that consigns the dq current to the internal control loop. In that way, the signal gives the reference to the pulse width modulators (PWM), producing the IGBTs activity.

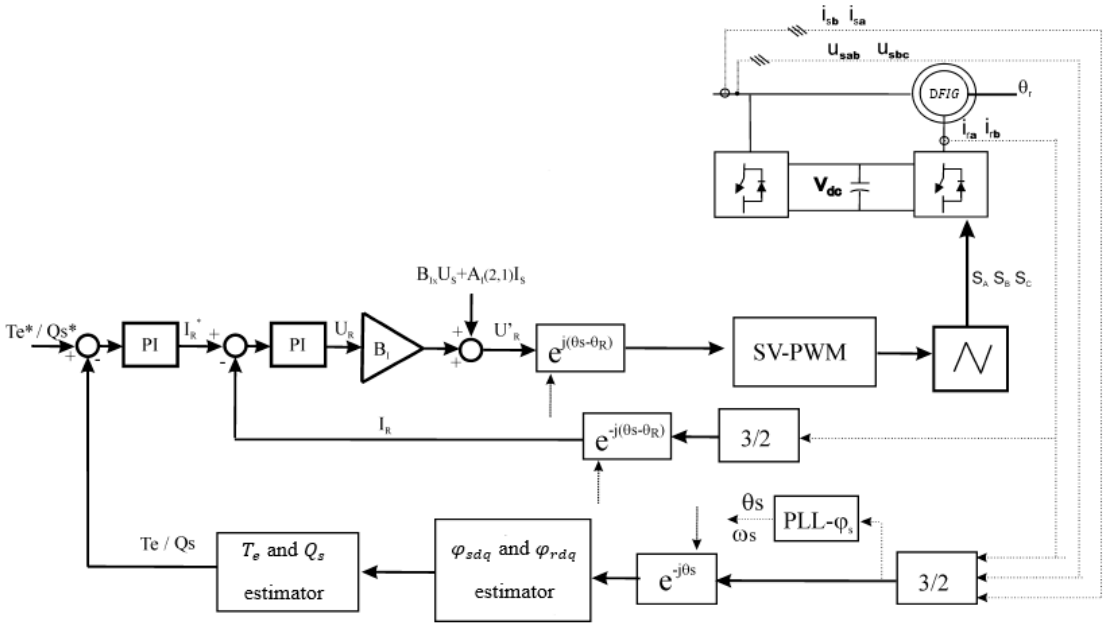

Figure 19. Vector control of a DFIG [21].

The grid side converter has as external control loop references the DC voltage in the DC link and the reactive power, even though this last variable is usually set to zero. In the case of the internal control loops, they receive current signals and apply voltage references to the modulation. In that modulation, the switching pulses are generated for the IGTBs from a space vector reference and a clock signal, that states the commutation frequency.

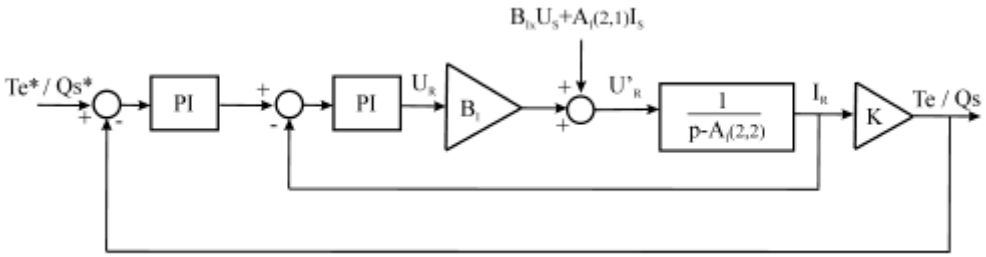

Figure 20. Vector control loop of electromagnetic torque and stator reactive power [21].

4.3.2. Non-linear control techniques

An alternative to the use of linear regulators and vector control is the average model control, by taking into account the nonlinear behavior of the inverter and the doubly fed induction generator along the time. The most important nonlinear approaches have been the direct torque control (DTC) and the direct power control (DPC).

Direct torque control is based in the instant regulation of electromagnetic torque and stator flux through the implementation of a voltage vector, allowing a correct positioning of the flux vector, achieving as consequence the torque and power control. Used mainly for induction generators, this technique does not use linear regulators or PWM modulators. This control is done by its amplitude, opposite to the PWM control, done in the pulse width.

To accomplish an adequate control of the induction generator, DTC compares the estimated electromagnetic toque and stator flux magnitude with the reference value of that variables by means of hysteresis regulators and sends the outputs of increasing or decreasing the torque and flux magnitude values, as appropriate. Then, the complex space is divided in six sectors and the sector in which the space vector of the flux is located. Depending on the sector, a voltage vector is selected from a predefined table to regulate the controlled variables.

For the doubly fed induction generator, DTC regulates the stator current through the rotor flux, instead of the rotor current control loops that appeared in vector control. In that way, voltage and flux in the stator can be considered to be constant vectors if losses are neglected. In a correct regulation of the DFIG, DTC evaluates the electromagnetic torque and reactive power errors and selects the rotor voltage space vector from a predefined table, so that the variables we want to control can evolve properly.

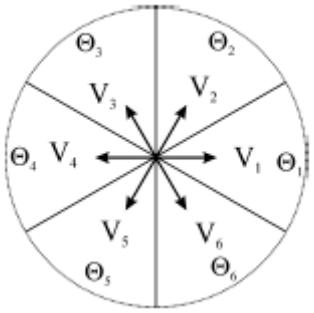

Figure 21. Sectors for the voltage space vector [21].

		Θ1	Θ2	Θ3	Θ4	Θ5	Θ6
Q_s	↑	6,1,2	1,2,3	2,3,4	3,4,5	4,5,6	5,6,1
	↓	3,4,5	4,5,6	5,6,1	6,1,2	1,2,3	2,3,4
T_e	↑	2,3	3,4	4,5	5,6	6,1	1,2
	↓	5,6	6,1	1,2	2,3	3,4	4,5

		Θ1	Θ2	Θ3	Θ4	Θ5	Θ6
Q_s ↑	T_e ↑	2	3	4	5	6	1
	T_e ↓	6	1	2	3	4	5
Q_s ↓	T_e ↑	3	4	5	6	1	2
	T_e ↓	5	6	1	2	3	4

Table 8. DTC decision table for DFIG [21].

Some advantages of this type of control are the possibility of regulating torque and stator reactive power or flux in a decoupled way or high robustness during the operating point or parameter changes. On the other hand, some drawbacks are the high losses from commutation, harmonics generation or less predictable temperatures and losses in the semiconductors due to unknown commutation frequencies.

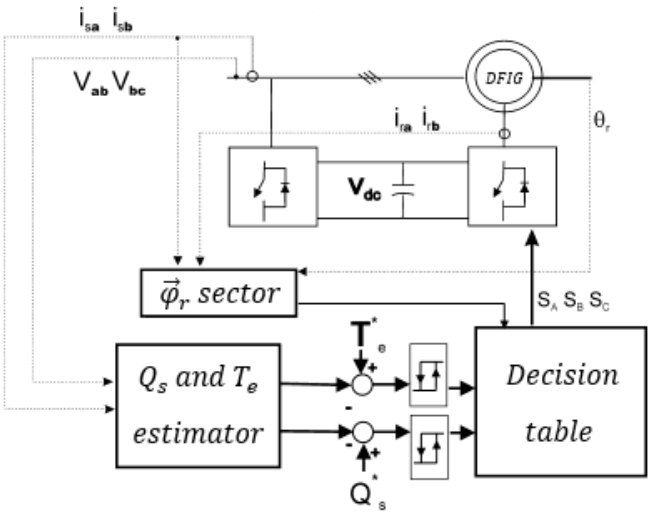

Figure 22. Direct Torque Control Scheme [21].

Direct power control is in the basics very similar to DTC, but in this case the variables to control are the active and reactive power from a power converter or the generator. As in the case of the DTC, no linear regulators or PWM modulations are needed.

This control strategy stated that in order to achieve a correct regulation of the variables, the necessary voltage vector must be selected, with the consequent change in position of the switches, depending on the decision of increasing or decreasing the controlled variables.

The application of DPC to doubly fed induction generators was presented by R. Datta [22]. In the case of this generator, the rotor side converter, when working as voltage source, can control both active and reactive power by applying the proper voltage vector and fixing in that way the rotor flux.

As well as for the DTC, DPC do have a predefined table that collects the effects of the rotor voltage on the active and reactive power. This table is used to state, for each 60 degrees sector, the most convenient vector to augment or diminish both components of the stator complex power. This can be appreciated in Figure 21, where the complex space is divided in six sectors, as in DTC. The decision table is influenced by the two hysteresis controllers, that calculate the error in active and reactive power.

Regarding DTC, R. Datta presents the idea of using null vectors in the table for the doubly fed induction generator control [22]. This consists on having six active vectors, from V_1 to V_6, with an evolution of $\vec{\varphi}_r$ being parallel to the applied voltage vector and another null vector, V_0 (0,0,0) or V_7 (1,1,1), making $\vec{\varphi}_r$ not to change neither in magnitude nor angle, depending its effect on the direction of rotation. During generator operation, $\vec{\varphi}_r$ will be leading $\vec{\varphi}_s$.

		Θ_1	Θ_2	Θ_3	Θ_4	Θ_5	Θ_6
$Q_s \downarrow$	$P_s \uparrow$	2	3	4	5	6	1
	$Q_s \downarrow$	6	1	2	3	4	5
		0.7	0.7	0.7	0.7	0.7	0.7
$Q_s \uparrow$	$P_s \uparrow$	3	4	5	6	1	2
	$Q_s \downarrow$	5	6	1	2	3	4
		0.7	0.7	0.7	0.7	0.7	0.7

Subsynchronous

		Θ_1	Θ_2	Θ_3	Θ_4	Θ_5	Θ_6
$Q_s \downarrow$	$P_s \uparrow$	2	3	4	5	6	1
		0.7	0.7	0.7	0.7	0.7	0.7
	$P_s \downarrow$	6	1	2	3	4	5
$Q_s \uparrow$	$P_s \uparrow$	3	4	5	6	1	2
		0.7	0.7	0.7	0.7	0.7	0.7
	$P_s \downarrow$	5	6	1	2	3	4

Supersynchronous

Table 9. DPC decision table for DFIG (with null vector) [21].

It is important to note that the only difference between tables Table 8 and Table 9 is the change of the electromagnetic torque in DTC by the active power in DPC.

The advantages and disadvantages of DPC are the same than the ones in DTC. The main difference between them is the fact that the variable that is not being controlled, this is, the active power in the case of DTC and the electromagnetic torque in the case of the DPC, experiences some coupling and oscillations.

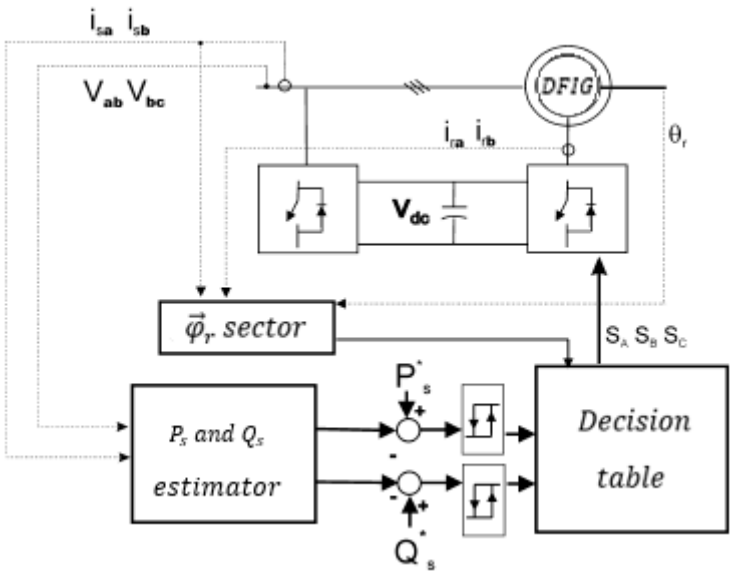

Figure 23. Direct Power Control Scheme [21].

4.3.3. Blades control system

In wind energy convertion systems with active control, in which the pitch angle can be regulated, the blades can be rotated by a pitch servo mechanism. This mechanism follows the reference angle indicated, tracking the optimum Cp point of operation or loosing part of the energy if wind speeds are too high.

Nonetheless, there are some limitations in rotation the servo can achieve, being these limits around -1º as lower limit and 90º as upper limit in the case of the pitch controlled turbines. For wind energy turbines with stall control, the limits change from -90º to 0º or even a few degrees positive. Anyway, the servo mechanism can also bound that limits, reducing them to a smaller range. Likewise, there is a certain speed that that the rotation cannot overpass. This speed is different in active stall wind turbines than in wind energy convertion systems with pitch control, being usually higher in the last ones. This speed can be observed to be between 5 and 10 degrees per second [1].

5. DOUBLY FED INDUCTION GENERATOR MODEL DESCRIPTION

The doubly fed induction machine belongs to the asynchronous machines classification along with the squirrel cage induction generator and is differentiated from this last one in the distinct way of connecting the rotor side. While in the squirrel cage induction generator the rotor is completely wound, doubly fed induction machines are connected to the grid through power converters.

This machine, the most used and sold worldwide due to its robust and simple construction, consists on an exterior case that covers a magnetic circuit which is composed by magnetic sheets isolated between them and arranges a three-phase winding along the internal surface. In the case of the rotor, it is built from magnetic sheets as well and adopts a cylindrical shape that arranges and hosts the winding in the external surface [23].

Therefore, as can be deduced from its structure, the correct working of the machine will depend on the interaction of magnetic fields from stator and rotor. These magnetic fields are created by the current flowing through the windings. In the case of the stator, the current and subsequently the magnetic field is produced by the grid, while in the rotor, power converters are in charge of setting the current, controlling also in that way other variables of the machine.

For a simpler development of the models, some assumptions have been taken into account [24]:

- Perfect symmetric machine.
- There exists a sinusoidal distribution in stator and rotor magnetic fields all along the air-gap.
- Variations in the inductance due to stator and rotor slots can be neglected.
- Hysteresis and magnetic saturation effects can be neglected.

Asynchronous machines work with different angular speeds in the rotor than the one set by the grid. This fact differentiates these machines from the synchronous ones and due to that characteristic, an electromagnetic torque is produced. So that the average magnetic torque is not null along the time, both stator and rotor magnetic fields must keep a constant angle between them [2], rotating at the same speed, this is the synchronous speed from the stator ω_s, as the electromagnetic torque is given by:

$$T_{em} = k \cdot |\psi_s| \cdot |\psi_r| \cdot \sin(\delta) \tag{5. 1}$$

being δ angle between stator and rotor magnetic fields. Therefore, if we want to keep that angle constant to obtain a uniform torque, the following angular speed relations must be accomplished:

$$\Omega_s[rpm] = \frac{60 \cdot f_s}{p} \tag{5. 2}$$

$$\omega_s[rad/s] = \omega_m + \omega_r \tag{5. 3}$$

$$s = \frac{\Omega_s - \Omega_m}{\Omega_s} \tag{5. 4}$$

$$\omega_r = s \cdot \omega_s \tag{5. 5}$$

$$f_r = s \cdot f_s \tag{5. 6}$$

where s is the slip or per unit (p.u.) angular speed difference between stator and rotor, p is the number of pair of poles the DFIG has and f_s is the frequency set by the grid.

Depending on the sign of the slip, we can differentiate 3 operation modes of the machine:

$$\omega_m < \omega_s \Rightarrow \omega_r > 0 \Rightarrow s > 0 \Rightarrow \text{Subsynchronous operation}$$

$$\omega_m > \omega_s \Rightarrow \omega_r < 0 \Rightarrow s < 0 \Rightarrow \text{Hypersynchronous operation}$$

$$\omega_m = \omega_s \Rightarrow \omega_r = 0 \Rightarrow s = 0 \Rightarrow \text{Synchronous operation}$$

5.1. Model Initialization

In this section, the initialization parameters and processes will be presented.

All calculus and simulations described in this chapter have been implemented with MATLAB and Simulink software in order to develop the doubly fed induction generator model.

For the purpose of initializing the simulation, several MATLAB files have been created with the calculations for the different variables needed in the process.

In the case of the Simulink simulation, only one file was created, calling all necessary values from the MATLAB files. This simulation utilizes physical units. Blocks and connections have been implemented from the Simulink library.

The wind energy convertion system chosen as model was a 2 MW turbine of 90 meters in diameter with 2 pairs of poles, connected to a European grid, this is, the frequency from the grid is 50 Hertz.

Parameter	Value
$P_{nominal}$	2 MW
f_s	50 Hz
P_p	2
V_s	690 V
R_s	$2.6 \cdot 10^{-3}\ \Omega$
R_r	$2.9 \cdot 10^{-3}\ \Omega$
R_0	$0\ \Omega$

L_m	$2.5 \cdot 10^{-3}$ H
l_s	$8.69 \cdot 10^{-5}$ H
l_r	$8.69 \cdot 10^{-5}$ H

Table 10. Parameters used during the initialization.

Then, applying the previously defined Equations (4. 7) and (5. 2), mechanical power (aerodynamic power has the same value than mechanical power if losses through the blades, gearbox and shafts are neglected) and synchronous speed can be calculated, from which we can get other variables such as the complex power in the stator, the mechanical and rotor speeds and the stator current, rotor current and rotor voltage during steady state, implementing all of them as initial values for the simulation.

Relating these variables, it can be obtained the doubly fed induction generator model, expressed with matrixes as:

$$[V] = [R][I] + 2\omega_m \cdot [G1][I] + \omega_s \cdot [G2][I] + \frac{d}{dt}[\psi] \tag{5. 7}$$

$$[V] = [R][I] + 2\omega_m \cdot [G1][I] + \omega_s \cdot [G2][I] + [L]\frac{d}{dt}[I] \tag{5. 8}$$

where the matrixes have been defined as:

$$[V]^T = [Re\{V_s\} \quad Im\{V_s\} \quad Re\{V_r\} \quad Im\{V_r\}]$$
$$[I]^T = [Re\{I_s\} \quad Im\{I_s\} \quad Re\{I_r\} \quad Im\{I_r\}]$$
$$[\psi]^T = [Re\{\psi_s\} \quad Im\{\psi_s\} \quad Re\{\psi_r\} \quad Im\{\psi_r\}]$$

indicating the subscript if the variable belongs to the stator or the rotor. The rest of the parameters are described by:

$$[R] = \begin{bmatrix} R_s & 0 & 0 & 0 \\ 0 & R_s & 0 & 0 \\ 0 & 0 & R_r & 0 \\ 0 & 0 & 0 & R_r \end{bmatrix} \qquad [L] = \begin{bmatrix} L_s & 0 & L_m & 0 \\ 0 & L_s & 0 & L_m \\ L_m & 0 & L_r & 0 \\ 0 & L_m & 0 & L_r \end{bmatrix}$$

$$[G1] = \begin{bmatrix} 0 & 0 & 0 & 0 \\ 0 & 0 & 0 & 0 \\ 0 & L_m & 0 & L_r \\ -L_m & 0 & -L_r & 0 \end{bmatrix} \qquad [G2] = \begin{bmatrix} 0 & -L_s & 0 & -L_m \\ L_s & 0 & L_m & 0 \\ 0 & -L_m & 0 & -L_r \\ L_m & 0 & L_r & 0 \end{bmatrix}$$

being

$$L_s = l_s + L_m \tag{5. 9}$$

$$L_r = l_r + L_m \tag{5. 10}$$

Likewise, the system can be finally defined by:

$$\frac{d}{dt}[I] = -[L]^{-1}([R] + 2\omega_m \cdot [G1] + \omega_s \cdot [G2])[I] + [L]^{-1}[V] \quad (5.\ 11)$$

with

$$[L]^{-1} = \frac{1}{\sigma L_s L_r}\begin{bmatrix} L_r & 0 & -L_m & 0 \\ 0 & L_r & 0 & -L_m \\ -L_m & 0 & L_s & 0 \\ 0 & -L_m & 0 & L_s \end{bmatrix} \quad (5.\ 12)$$

$$\sigma = 1 - \frac{{L_m}^2}{L_s L_r} \quad (5.\ 13)$$

In the simulations, rotor and stator voltage have been used together with the mechanical and stator rotational speeds as input vectors, while stator and rotor currents have been implemented as state variables.

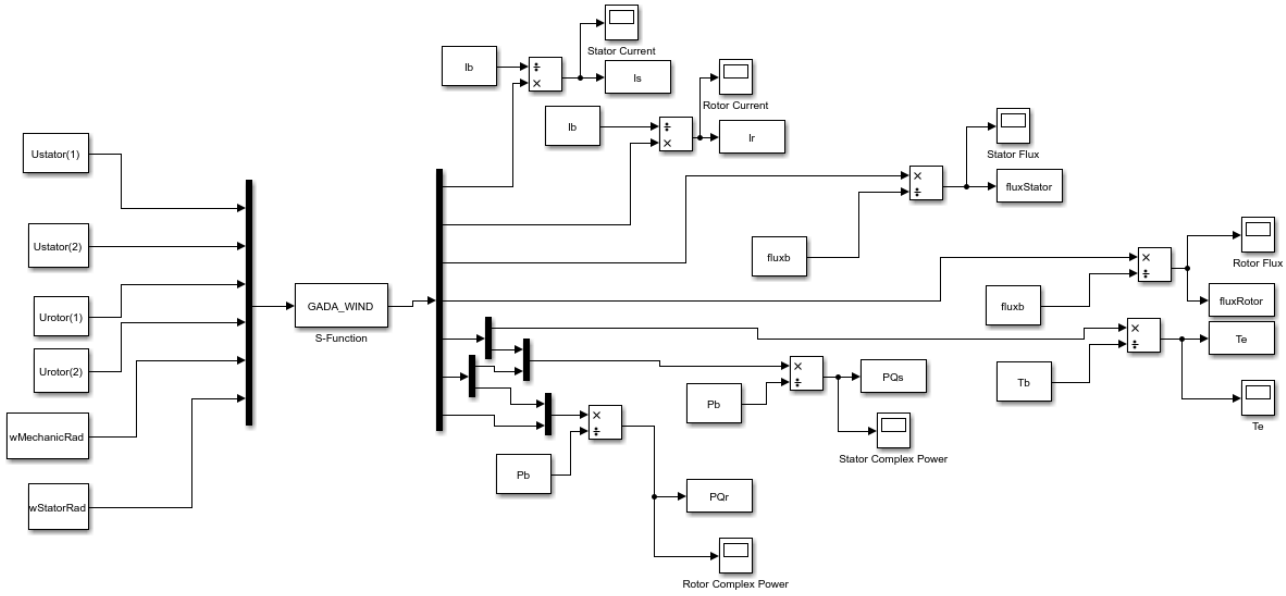

Figure 24. Simulation of the electric part of the DFIG.

5.2. Steady-State Model

An ideal and simplified representation of the DFIG consists a series of windings, three in the stator and another three in the rotor, as it can be seen in Figure 25.

Some assumptions have been made in order to make the model easier to understand:

- Only one of the three phases will be represented for both stator and rotor.
- Star configuration is assumed for both stator and rotor.
- The grid supplies a constant AC voltage in frequency and amplitude.
- The rotor will be fed as well by a constant frequency and amplitude AC voltage, from an independent source to the stator, as a power converter.

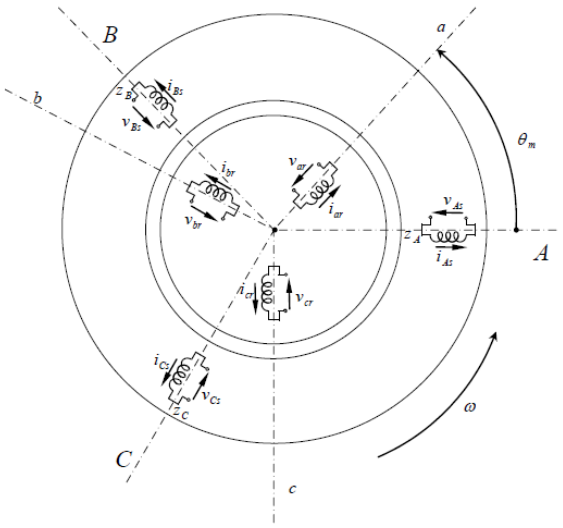

Figure 25. Ideal representation of the windings of a DFIG [2].

The implementation of the above simplifications leads to the following electric equivalent circuit:

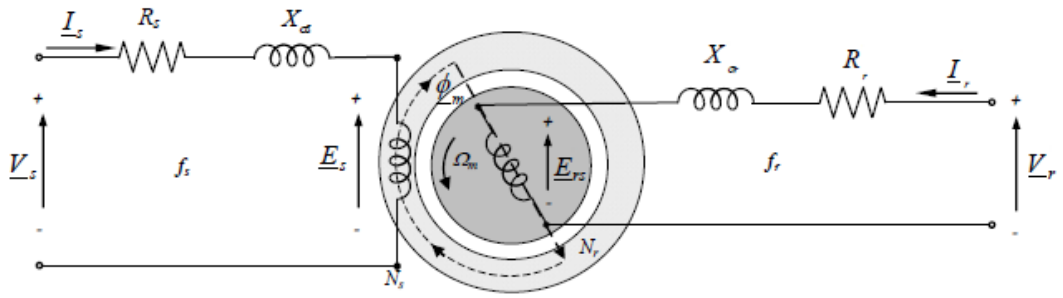

Figure 26. One phase of the DFIG steady-state equivalent circuit [2].

In the figure shown above, the stator frequency is constant as long as the stator is connected to the grid, while rotor frequency changes depending on the mechanical angular speed of the machine. Because of that, other variables in the rotor are also changing, as $X_{\sigma r} = j \cdot \omega_r \cdot L_{\sigma r}$.

The fact of having different frequencies in stator and rotor makes the development of the model tedious and confusing. The next step will be then to do a more practical approach by making all voltages and currents in stator and rotor operate under the same frequency. To reach so, a comparison between electromotive forces induced in stator and rotor must be done. From Lenz's law, we have that:

$$E = N\frac{d\Phi}{dt} \tag{5. 14}$$

being E the induced voltage, Φ the flux and N the number of turns. As consequence, the induced electromotive force in stator and rotor will be:

$$\underline{E_s} = \sqrt{2} \cdot \pi \cdot N_s \cdot f_s \cdot \underline{\Phi_m} \tag{5. 15}$$

$$\underline{E_r} = \sqrt{2} \cdot \pi \cdot N_r \cdot f_r \cdot \underline{\Phi_m} \tag{5. 16}$$

Dividing both of the equations above we get:

$$\frac{\underline{E_r}}{\underline{E_s}} = s \cdot \frac{N_r}{N_s} \tag{5. 17}$$

If we set the relation $\frac{E_s}{E_r}$ to be a factor called a that will allow to relate stator and rotor induced voltages at zero speeds, this is, when $s = 1$. Therefore:

$$\frac{\underline{E_r}}{\underline{E_s}} = \frac{1}{a} = \frac{N_r}{N_s} \Rightarrow a = \frac{N_s}{N_r} \tag{5. 18}$$

Now that the a factor is known and rotor variables can be related to the stator, some parameters must be reduced to the stator side:

$$R_r' = R_r \cdot a^2 \tag{5. 19}$$

$$L_{\sigma r}' = L_{\sigma r} \cdot a^2 \tag{5. 20}$$

where R_r' is the rotor resistance referred to the stator and $L_{\sigma r}'$ is the rotor inductance referred to the stator.

Following the same method, we also can obtain:

$$\underline{I_r'} = \frac{\underline{I_r}}{a} \tag{5. 21}$$

$$\underline{V_r'} = \underline{V_r} \cdot a \tag{5. 22}$$

$$\underline{E_r'} = \underline{E_r} \cdot a \tag{5. 23}$$

with $\underline{I_r'}$, $\underline{V_r'}$ and $\underline{E_r'}$ as the rotor current, rotor voltage and rotor induced voltage referred to the stator respectively.

Note that all variables with $'$ are reduced to the stator side, while variables without $'$ are the real magnitudes that can be checked in the machine. Obviously, this notation does not apply to the stator variables, as they are the real variables already located in the stator.

Then, from Figure 26 and the convertion of rotor variables referring them to the stator:

$$\frac{\underline{V_r'}}{s} - \underline{E_s} = (\frac{R_r'}{s} + j \cdot \omega_s \cdot L_{\sigma r}') \cdot \underline{I_r'} \tag{5. 24}$$

Which can also be combined to obtain the stator voltage:

$$\underline{V_s} = \frac{\underline{V_r'}}{s} - (R_s + j \cdot \omega_s \cdot L_{\sigma s}) \cdot \underline{I_s} + (\frac{R_r'}{s} + j \cdot \omega_s \cdot L_{\sigma r}') \cdot \underline{I_r'} \quad (5.\ 25)$$

The final equivalent circuit with rotor variables referred to stator would be:

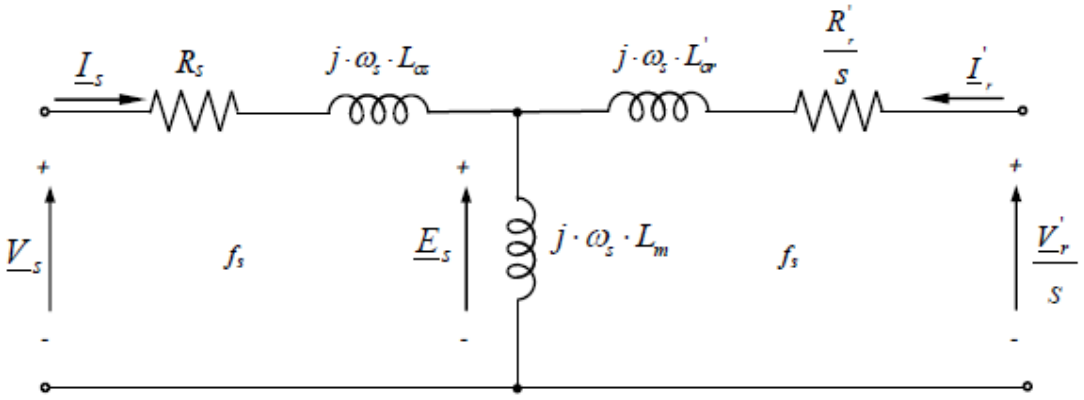

Figure 27. One phase of the DFIG steady-state equivalent circuit referred to the stator [2].

Now that we already have the equivalent circuit, other relevant variables for the generator can be calculated. For this purpose and in order to simplify the formulas, rotor voltage and resistance will be divided into two different terms, one depending on the slip and another without it:

$$\frac{\underline{V_r'}}{s} = \underline{V_r'} + \underline{V_r'}\left(\frac{1-s}{s}\right) \quad (5.\ 26)$$

$$\frac{R_r'}{s} = R_r' + R_r'\left(\frac{1-s}{s}\right) \quad (5.\ 27)$$

Due to this modification now it is much easier to get the power losses of the 3 phases that form the machine:

$$P_{cu\_s} = 3 \cdot R_s \cdot \left|\underline{I_s}\right|^2 \quad (5.\ 28)$$

$$P_{cu\_r} = 3 \cdot R_r' \cdot \left|\underline{I_r'}\right|^2 \quad (5.\ 29)$$

In the same way stator and rotor active power can be computed:

$$P_s = 3 \cdot Re\{\underline{V_s} \cdot \underline{I_s^*}\} \quad (5.\ 30)$$

$$P_r = 3 \cdot Re\{\underline{V_r'} \cdot \underline{I_r'^*}\} \quad (5.\ 31)$$

and can be related by the following equation:

$$P_r \cong -s \cdot P_s \quad (5.\ 32)$$

being the power positive if the machine is receiving power through stator or rotor and negative if the machine is delivering it.

Finally, the total flow of power could be expressed as:

$$P_s + P_r = P_{cu\_s} + P_{cu\_r} + P_{mec} \tag{5. 33}$$

where P_{mec} is positive when delivering power through the shaft working in motor mode and is negative when receiving power through the shaft working in generator mode:

$$P_{mec} = 3 \cdot R'_r \cdot \left(\frac{1-s}{s}\right) \cdot \left|\underline{I'_r}\right|^2 - 3 \cdot \left(\frac{1-s}{s}\right) \cdot Re\{\underline{V'_r} \cdot \underline{I'^*_r}\} \tag{5. 34}$$

From mechanical power, the next relation can be derived, the electromagnetic torque:

$$P_{mec} = T_{em} \cdot \Omega_m = T_{em} \cdot \frac{\omega_m}{p} \tag{5. 35}$$

$$T_{em} = \frac{3 \cdot p \cdot R'_r}{\omega_m} \cdot \left(\frac{1-s}{s}\right) \cdot \left|\underline{I'_r}\right|^2 - \frac{3 \cdot p}{\omega_m} \cdot \left(\frac{1-s}{s}\right) \cdot Re\{\underline{V'_r} \cdot \underline{I'^*_r}\} \tag{5. 36}$$

Finally, the reactive power can be also obtained:

$$Q_s = 3 \cdot Im\{\underline{V_s} \cdot \underline{I^*_s}\} = 3 \cdot \omega_s \cdot L_s \cdot \left|\underline{I_s}\right|^2 + 3 \cdot \omega_s \cdot L_m \cdot Re\{\underline{I'_r} \cdot \underline{I^*_s}\} \tag{5. 37}$$

$$Q_r = 3 \cdot Im\{\underline{V'_r} \cdot \underline{I'^*_r}\} = 3 \cdot s \cdot \omega_s \cdot L'_r \cdot \left|\underline{I'_r}\right|^2 + 3 \cdot s \cdot \omega_s \cdot L_m \cdot Re\{\underline{I_s} \cdot \underline{I'^*_r}\} \tag{5. 38}$$

Other important relation that must be taken into account is the one described by the magnetic fluxes, the inductances and the currents, both in stator and rotor, presented in its matrix form as:

$$[\psi] = [L][I] \tag{5. 39}$$

5.3. Dynamic Model

In order to get a better understanding of how this machine works, it is not enough to apply the steady-state model, as in reality we can observe transients and other kind of behaviors. Therefore, the use of dynamic models will help us not only to go one step further getting a deeper knowledge about its performance along the time but also to implement a better control on the DFIG avoiding high currents, dangerous transients or any other type of instability.

From the ideal and simplified representation of the DFIG shown in the steady-state model consisting in stator and rotor windings, the following electric equivalent circuit can be deduced:

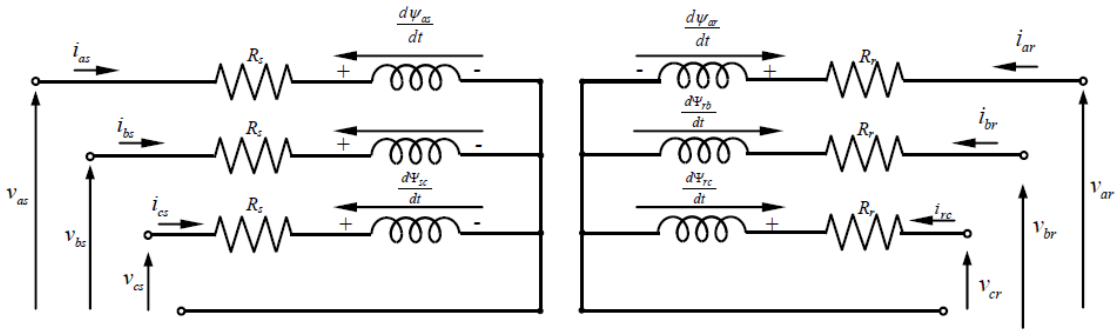

Figure 28. DFIG equivalent circuit [2].

From this model, we can relate the current, voltages and fluxes obtained instantaneously with the differential equations:

$$v_{as}(t) = R_s \cdot i_{as}(t) + \frac{d\psi_{as}(t)}{dt} \tag{5. 40}$$

$$v_{bs}(t) = R_s \cdot i_{bs}(t) + \frac{d\psi_{bs}(t)}{dt} \tag{5. 41}$$

$$v_{cs}(t) = R_s \cdot i_{cs}(t) + \frac{d\psi_{cs}(t)}{dt} \tag{5. 42}$$

where v_{as}, v_{bs} and v_{cs} are the stator voltages, R_s the resistance in the stator, i_{as}, i_{bs} and i_{cs} the stator currents and ψ_{as}, ψ_{bs} and ψ_{cs} are the stator fluxes. As we can observe, in the steady-state conditions the derivative with respect to time would be equal to cero and the variables described above would only vary with ω_s, whose value depends on the frequency of the grid.

Following the same method, we can also describe the equations in the rotor:

$$v_{ar}(t) = R_r \cdot i_{ar}(t) + \frac{d\psi_{ar}(t)}{dt} \tag{5. 43}$$

$$v_{br}(t) = R_r \cdot i_{br}(t) + \frac{d\psi_{br}(t)}{dt} \tag{5. 44}$$

$$v_{cr}(t) = R_r \cdot i_{cr}(t) + \frac{d\psi_{cr}(t)}{dt} \tag{5. 45}$$

belonging in this case all the voltages, currents, fluxes and resistance to rotor values referred to the stator. As the previous equations, rotor variables do also vary with the angular speed, in this case with ω_r.

5.3.1. αβ model

From the previous formulas, we can now obtain the space vector form of the voltages in the stator reference frame. To do so we must multiply $v_{as}(t)$ by $\frac{3}{2}$, $v_{bs}(t)$ by $\frac{3}{2}k$, $v_{cs}(t)$ by $\frac{3}{2}k^2$, adding them. This is the same result we obtain when using Clarke transformation:

$$\begin{bmatrix} x_a \\ x_b \\ x_c \end{bmatrix} = \frac{2}{3}\begin{bmatrix} 1 & 0 & \frac{1}{\sqrt{2}} \\ -\frac{1}{2} & \frac{\sqrt{3}}{2} & \frac{1}{\sqrt{2}} \\ -\frac{1}{2} & -\frac{\sqrt{3}}{2} & \frac{1}{\sqrt{2}} \end{bmatrix} \cdot \begin{bmatrix} x_\alpha \\ x_\beta \\ x_h \end{bmatrix} \tag{5. 46}$$

$$\begin{bmatrix} x_\alpha \\ x_\beta \\ x_h \end{bmatrix} = \frac{2}{3}\begin{bmatrix} 1 & -\frac{1}{2} & -\frac{1}{2} \\ 0 & \frac{\sqrt{3}}{2} & -\frac{\sqrt{3}}{2} \\ \frac{1}{\sqrt{2}} & \frac{1}{\sqrt{2}} & \frac{1}{\sqrt{2}} \end{bmatrix} \cdot \begin{bmatrix} x_a \\ x_b \\ x_c \end{bmatrix} \tag{5. 47}$$

After the transformation, we get the following equation for the stator voltage in space vector form:

$$\vec{v}_s^s = R_s \cdot \vec{i}_s^s + \frac{d\vec{\psi}_s^s}{dt} \tag{5. 48}$$

being $\vec{v}_s^s$, $\vec{i}_s^s$ and $\vec{\psi}_s^s$ the space vectors for stator voltage, stator current and stator flux respectively, represented in stator coordinates, this is, αβ reference frame. Applying the same procedure used in the stator, we can get the rotor voltage in space vector form:

$$\vec{v}_r^r = R_r \cdot \vec{i}_r^r + \frac{d\vec{\psi}_r^r}{dt} \tag{5. 49}$$

being $\vec{v}_r^r$, $\vec{i}_r^r$ and $\vec{\psi}_r^r$ the space vectors for rotor voltage, rotor current and rotor flux respectively, represented in rotor coordinates, this is, dq reference frame.

Fluxes can also be described in the space vector notation [2]:

$$\vec{\psi}_s^s = L_s \cdot \vec{i}_s^s + L_m \cdot \vec{i}_r^s \tag{5. 50}$$

$$\vec{\psi}_r^r = L_r \cdot \vec{i}_r^r + L_m \cdot \vec{i}_s^r \tag{5. 51}$$

where $\vec{i}_r^s$ and $\vec{i}_s^r$ are the rotor current referred to the stator and the stator current referred to the rotor respectively. In addition to this, we must take into account that L_s and L_r are self-inductances in stator and rotor and L_m is the mutual inductance.

Space vectors can be represented in different reference frames, such as stator (S), rotor (R) or synchronous (T):

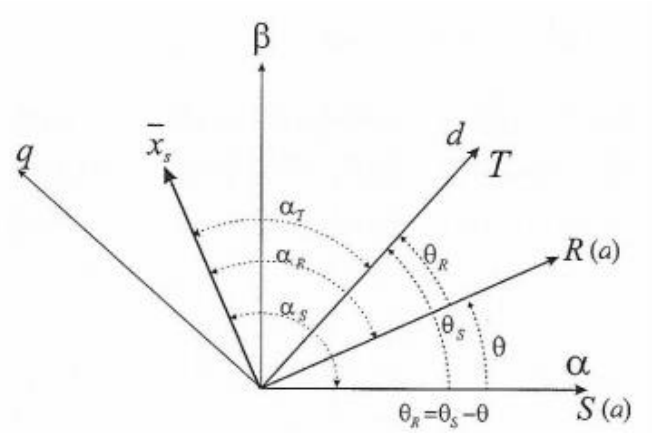

Figure 29. Space Vector Reference Frames [21].

where $\vec{x}_s$ can be described in any of the them:

$$\vec{x}_{(S)} = \vec{x}_s \cdot e^{j\alpha_S} \tag{5. 52}$$

$$\vec{x}_{(R)} = \vec{x}_s \cdot e^{j\alpha_R} \tag{5. 53}$$

$$\vec{x}_{(T)} = \vec{x}_s \cdot e^{j\alpha_T} \tag{5. 54}$$

As it can be observed from Figure 29, $\vec{x}_{(S)}$ belongs to the stator reference frame with axes α and β, $\vec{x}_{(R)}$ belongs to the rotor reference frame and $\vec{x}_{(T)}$ is set in a rotatory reference frame at synchronous speed.

In order to change from one reference frame to another, the following formulas must be applied:

$$\text{Change from S to T: } \vec{x}_{(T)} = \vec{x}_{(S)} \cdot e^{-j\theta_S} \tag{5. 55}$$

$$\text{Change from R to T: } \vec{x}_{(T)} = \vec{x}_{(R)} \cdot e^{-j\theta_R} \tag{5. 56}$$

$$\text{Change from R to S: } \vec{x}_{(S)} = \vec{x}_{(R)} \cdot e^{j\theta} \tag{5. 57}$$

being θ_S the d axis position of the synchronous reference frame, θ the position of the rotor and θ_R the subtraction of θ to θ_S.

Finally, the αβ model can be obtained by referring the space vectors to a stator reference frame, resulting in the following equations:

$$\vec{v}_s^s = R_s \cdot \vec{i}_s^s + \frac{d\vec{\psi}_s^s}{dt} \tag{5. 58}$$

$$\vec{v}_r^s = R_r \cdot \vec{i}_r^s + \frac{d\vec{\psi}_r^s}{dt} - j \cdot \omega_m \cdot \psi_r^s \tag{5. 59}$$

$$\vec{\psi}_s^s = L_s \cdot \vec{i}_s^s + L_m \cdot \vec{i}_r^s \tag{5. 60}$$

$$\vec{\psi}_r^s = L_r \cdot \vec{i}_r^s + L_m \cdot \vec{i}_s^s \tag{5. 61}$$

being ω_m the mechanical angular speed.

In the same way, stator and rotor power or electromagnetic torque can be calculated:

$$P_s = \frac{3}{2} Re\{\vec{v}_s \cdot \vec{i}_s^*\} = \frac{3}{2}(v_{\alpha s} \cdot i_{\alpha s} + v_{\beta s} \cdot i_{\beta s}) \tag{5. 62}$$

$$P_r = \frac{3}{2} Re\{\vec{v}_r \cdot \vec{i}_r^*\} = \frac{3}{2}(v_{\alpha r} \cdot i_{\alpha r} + v_{\beta r} \cdot i_{\beta r}) \tag{5. 63}$$

$$Q_s = \frac{3}{2} Im\{\vec{v}_s \cdot \vec{i}_s^*\} = \frac{3}{2}(v_{\beta s} \cdot i_{\alpha s} - v_{\alpha s} \cdot i_{\beta s}) \tag{5. 64}$$

$$Q_r = \frac{3}{2} Im\{\vec{v}_r \cdot \vec{i}_r^*\} = \frac{3}{2}(v_{\beta r} \cdot i_{\alpha r} - v_{\alpha r} \cdot i_{\beta r}) \tag{5. 65}$$

$$T_{em} = \frac{3}{2} \cdot p \cdot Im\{\vec{\psi}_r^* \cdot \vec{i}_r\} = \frac{3}{2} \cdot p \cdot (\psi_{\alpha r} \cdot i_{\beta r} - \psi_{\beta r} \cdot i_{\alpha r}) \tag{5. 66}$$

where * is representing the conjugate of the space vector it comes with and all the variables are referred to the stator.

By using Q_r, $\vec{\psi}_s^s$ and $\vec{\psi}_r^s$ equations, a simpler expression for T_{em} can be obtained:

$$\begin{aligned} T_{em} = \frac{3}{2} \cdot p \cdot Im\{\vec{\psi}_s \cdot \vec{i}_r^*\} &= \frac{3}{2} \cdot p \cdot Im\{\vec{\psi}_s^* \cdot \vec{i}_s\} = \\ &= \frac{3}{2} \cdot \frac{L_m}{L_r} \cdot p \cdot Im\{\vec{\psi}_r \cdot \vec{i}_s^*\} = \\ &= \frac{3}{2} \cdot \frac{L_m}{\sigma \cdot L_s \cdot L_r} \cdot p \cdot Im\{\vec{\psi}_r^* \cdot \vec{\psi}_s\} = \\ &= \frac{3}{2} \cdot L_m \cdot p \cdot Im\{\vec{i}_s \cdot \vec{i}_r^*\} \end{aligned} \tag{5. 67}$$

being σ the leakage coefficient, as described in (5. 13).

5.3.2. dq model

The next differential equations will follow the vector space notation in a synchronous reference frame with respect to the reference they are expressed in, being “s” from the stator and “r” from the rotor. In order to implement the dq model, the Park transformation must be introduced:

$$\begin{bmatrix} x_a \\ x_b \\ x_c \end{bmatrix} = \frac{2}{3} \begin{bmatrix} \cos(\alpha) & -\sin(\alpha) \\ \cos\left(\alpha - \frac{2\pi}{3}\right) & \sin\left(\alpha - \frac{2\pi}{3}\right) \\ \cos\left(\alpha + \frac{2\pi}{3}\right) & \sin\left(\alpha + \frac{2\pi}{3}\right) \end{bmatrix} \cdot \begin{bmatrix} x_d \\ x_q \end{bmatrix} \tag{5. 68}$$

$$\begin{bmatrix} x_d \\ x_q \end{bmatrix} = \frac{2}{3}\begin{bmatrix} \cos(\alpha) & \cos(\alpha - \frac{2\pi}{3}) & \cos(\alpha + \frac{2\pi}{3}) \\ \sin(\alpha) & \sin(\alpha - \frac{2\pi}{3}) & sin(\alpha + \frac{2\pi}{3}) \end{bmatrix} \cdot \begin{bmatrix} x_a \\ x_b \\ x_c \end{bmatrix} \quad (5.\ 69)$$

By using the stator and rotor voltages in space vector form ($\vec{v}_s^{\,s}$ and $\vec{v}_r^{\,r}$) along with the Park transformation, the following formulas can be deduced:

$$\vec{v}_s = R_s \cdot \vec{i}_s + \frac{d\vec{\psi}_s}{dt} + j \cdot \omega_s \cdot \vec{\psi}_s \quad (5.\ 70)$$

$$\vec{v}_r = R_r \cdot \vec{i}_r + \frac{d\vec{\psi}_r}{dt} + j \cdot (\omega_s - \omega_m) \cdot \vec{\psi}_r \quad (5.\ 71)$$

And from the fluxes calculated in the αβ model we can also get:

$$\vec{\psi}_s = L_s \cdot \vec{i}_s + L_m \cdot \vec{i}_r \quad (5.\ 72)$$

$$\vec{\psi}_r = L_r \cdot \vec{i}_r + L_m \cdot \vec{i}_s \quad (5.\ 73)$$

In that way, the resulting dq model of the DFIG in synchronous coordinates would be as it is shown in the following figure:

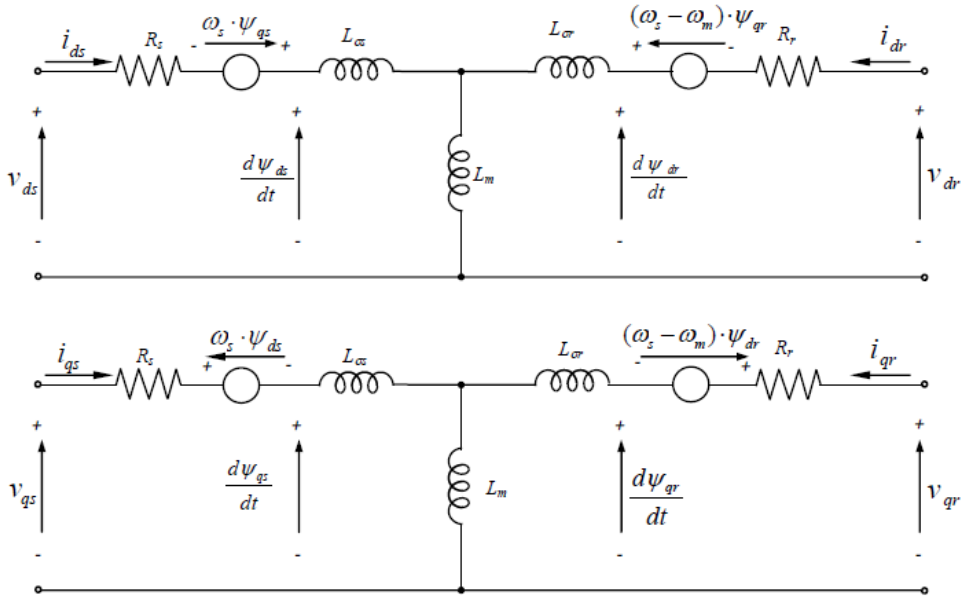

Figure 30. dq model of the DFIG in synchronous coordinates [2].

The stator and rotor power as well as the electromagnetic torque follow in the dq model the same expression as in the αβ model:

$$P_s = \frac{3}{2} Re\{\vec{v}_s \cdot \vec{i}_s^{\,*}\} = \frac{3}{2}(v_{ds} \cdot i_{ds} + v_{qs} \cdot i_{qs}) \quad (5.\ 74)$$

$$P_r = \frac{3}{2} Re\{\vec{v}_r \cdot \vec{i}_r^*\} = \frac{3}{2}(v_{dr} \cdot i_{dr} + v_{qr} \cdot i_{qr}) \tag{5. 75}$$

$$Q_s = \frac{3}{2} Im\{\vec{v}_s \cdot \vec{i}_s^*\} = \frac{3}{2}(v_{qs} \cdot i_{ds} - v_{ds} \cdot i_{qs}) \tag{5. 76}$$

$$Q_r = \frac{3}{2} Im\{\vec{v}_r \cdot \vec{i}_r^*\} = \frac{3}{2}(v_{qr} \cdot i_{dr} - v_{dr} \cdot i_{qr}) \tag{5. 77}$$

$$T_{em} = \frac{3}{2} \cdot p \cdot Im\{\vec{\psi}_r^* \cdot \vec{i}_r\} = \frac{3}{2} \cdot p \cdot (\psi_{dr} \cdot i_{qr} - \psi_{qr} \cdot i_{dr}) \tag{5. 78}$$

where all the variables are referred to the stator.

5.3.3. State-space representation of the αβ model

Taking and rearranging the equations for $\vec{v}_s^s$, $\vec{v}_r^s$, $\vec{\psi}_s^s$ and $\vec{\psi}_r^s$, we obtain a new model described by a following formula, taking fluxes as state-space magnitudes:

$$\frac{d}{dt}\begin{bmatrix}\vec{\psi}_s^s \\ \vec{\psi}_r^s\end{bmatrix} = \begin{bmatrix} \dfrac{-R_s}{\sigma \cdot L_s} & \dfrac{R_s \cdot L_m}{\sigma \cdot L_s \cdot L_r} \\ \dfrac{R_r \cdot L_m}{\sigma \cdot L_s \cdot L_r} & \dfrac{-R_r}{\sigma \cdot L_r} - j \cdot \omega_m \end{bmatrix} \cdot \begin{bmatrix}\vec{\psi}_s^s \\ \vec{\psi}_r^s\end{bmatrix} + \begin{bmatrix}\vec{v}_s^s \\ \vec{v}_r^s\end{bmatrix} \tag{5. 79}$$

which can be developed with the αβ components:

$$\frac{d}{dt}\begin{bmatrix}\psi_{\alpha s} \\ \psi_{\beta s} \\ \psi_{\alpha r} \\ \psi_{\beta r}\end{bmatrix} = \begin{bmatrix} \dfrac{-R_s}{\sigma \cdot L_s} & 0 & \dfrac{R_s \cdot L_m}{\sigma \cdot L_s \cdot L_r} & 0 \\ 0 & \dfrac{-R_s}{\sigma \cdot L_s} & 0 & \dfrac{R_s \cdot L_m}{\sigma \cdot L_s \cdot L_r} \\ \dfrac{R_r \cdot L_m}{\sigma \cdot L_s \cdot L_r} & 0 & \dfrac{-R_r}{\sigma \cdot L_r} & -\omega_m \\ 0 & \dfrac{R_r \cdot L_m}{\sigma \cdot L_s \cdot L_r} & \omega_m & \dfrac{-R_r}{\sigma \cdot L_r} \end{bmatrix} \cdot \begin{bmatrix}\psi_{\alpha s} \\ \psi_{\beta s} \\ \psi_{\alpha r} \\ \psi_{\beta r}\end{bmatrix} + \begin{bmatrix}v_{\alpha s} \\ v_{\beta s} \\ v_{\alpha r} \\ v_{\beta r}\end{bmatrix} \tag{5. 80}$$

If we change the state-space magnitude taking the currents instead of fluxes, we get:

$$\frac{d}{dt}\begin{bmatrix}\vec{i}_s^s \\ \vec{i}_r^s\end{bmatrix} = \frac{1}{\sigma \cdot L_s \cdot L_r}\begin{bmatrix} -R_s \cdot L_r - j \cdot \omega_m \cdot {L_m}^2 & R_r \cdot L_m - j \cdot \omega_m \cdot L_m \cdot L_r \\ R_s \cdot L_m + j \cdot \omega_m \cdot L_m \cdot L_s & -R_r \cdot L_s + j \cdot \omega_m \cdot L_r \cdot L_s \end{bmatrix} \cdot \begin{bmatrix}\vec{i}_s^s \\ \vec{i}_r^s\end{bmatrix} + \\ + \frac{1}{\sigma \cdot L_s \cdot L_r}\begin{bmatrix} L_r & -L_m \\ -L_m & L_s \end{bmatrix} \cdot \begin{bmatrix}\vec{v}_s^s \\ \vec{v}_r^s\end{bmatrix} \tag{5. 81}$$

which can also be developed in the αβ components:

$$\frac{d}{dt}\begin{bmatrix} i_{\alpha s} \\ i_{\beta s} \\ i_{\alpha r} \\ i_{\beta r} \end{bmatrix} = \frac{1}{\sigma \cdot L_s \cdot L_r}\begin{bmatrix} -R_s \cdot L_r & \omega_m \cdot {L_m}^2 & R_r \cdot L_m & \omega_m \cdot L_m \cdot L_r \\ -\omega_m \cdot {L_m}^2 & -R_s \cdot L_r & -\omega_m \cdot L_m \cdot L_r & R_r \cdot L_m \\ R_s \cdot L_m & -\omega_m \cdot L_s \cdot L_m & -R_r \cdot L_s & -\omega_m \cdot L_r \cdot L_s \\ \omega_m \cdot L_s \cdot L_m & R_s \cdot L_m & \omega_m \cdot L_r \cdot L_s & -R_r \cdot L_s \end{bmatrix} \cdot \begin{bmatrix} i_{\alpha s} \\ i_{\beta s} \\ i_{\alpha r} \\ i_{\beta r} \end{bmatrix} + \\ + \frac{1}{\sigma \cdot L_s \cdot L_r}\begin{bmatrix} L_r & 0 & -L_m & 0 \\ 0 & L_r & 0 & -L_m \\ -L_m & 0 & L_s & 0 \\ 0 & -L_m & 0 & L_s \end{bmatrix} \cdot \begin{bmatrix} v_{\alpha s} \\ v_{\beta s} \\ v_{\alpha r} \\ v_{\beta r} \end{bmatrix} \quad (5.82)$$

Therefore, as can be seen, by changing the state-space magnitudes we can obtain different models.

6. CASE STUDY AND SIMULATIONS

In this chapter, different cases will be described and an analysis of the results given by the doubly fed induction generator simulation will be presented.

In the initial state, it is considered to be operating under steady state operation, with the parameters appointed in Table 10. Moreover, it will be considered an initial constant wind speed of 6 m/s.

After applying the calculations presented in section 5.1., we will get the results for the first operation point. As the assumption is the wind to blow at constant speed, the outputs are meant to be constant too. The variables that will be studied are the stator and rotor currents, stator and rotor fluxes, stator and rotor complex power and the electromagnetic torque:

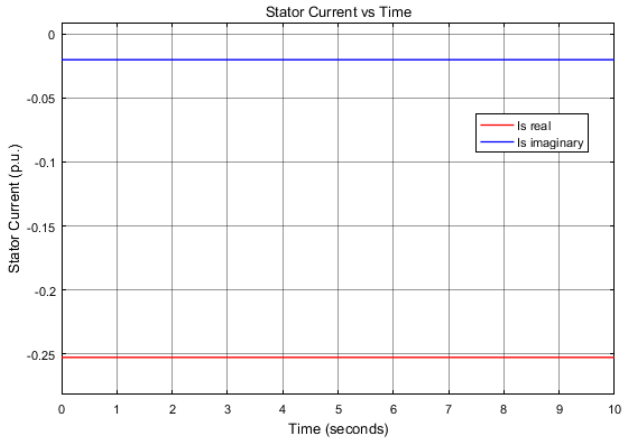

Figure 31. Stator Current During Initialization.

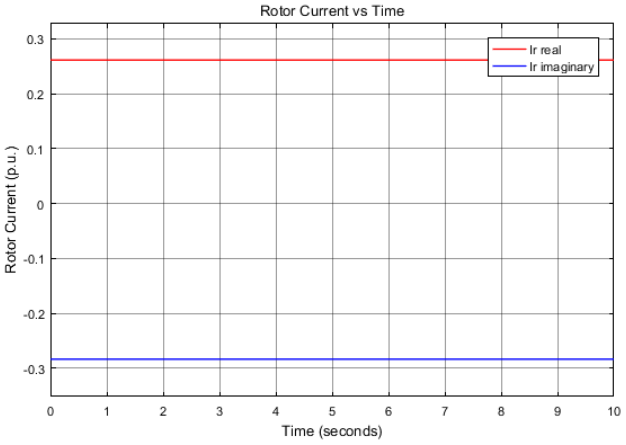

Figure 32. Rotor Current During Initialization.

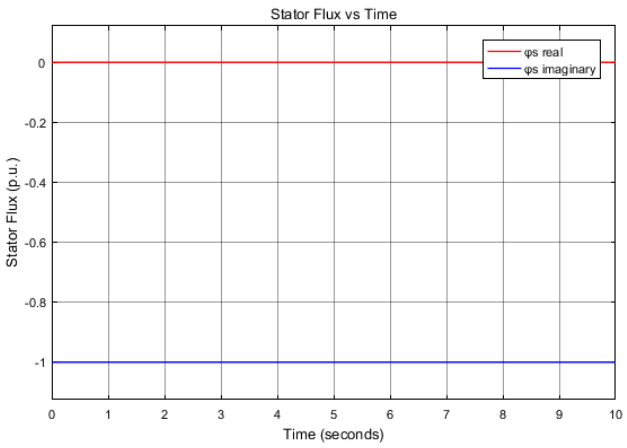

Figure 33. Stator Flux During Initialization.

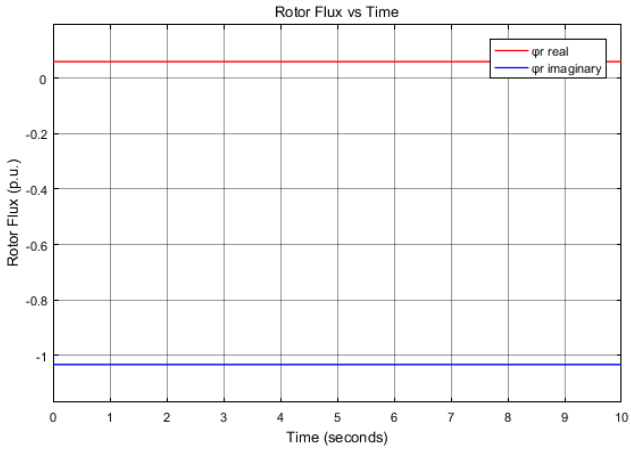

Figure 34. Rotor Flux During Initialization.

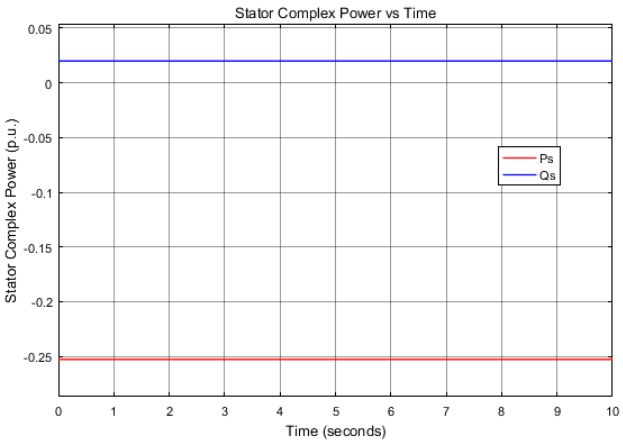

Figure 35. Stator Complex Power During Initialization.

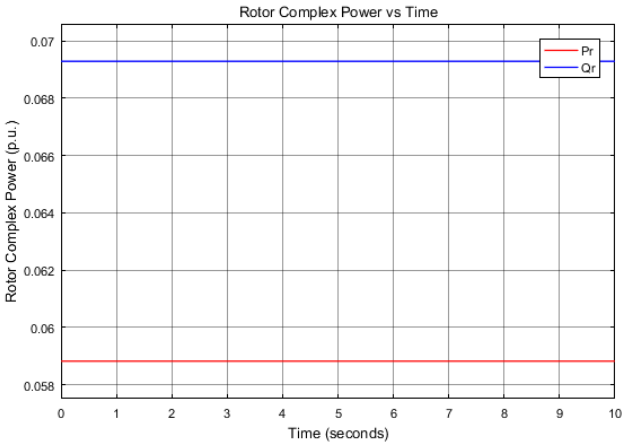

Figure 36. Rotor Complex Power During Initialization.

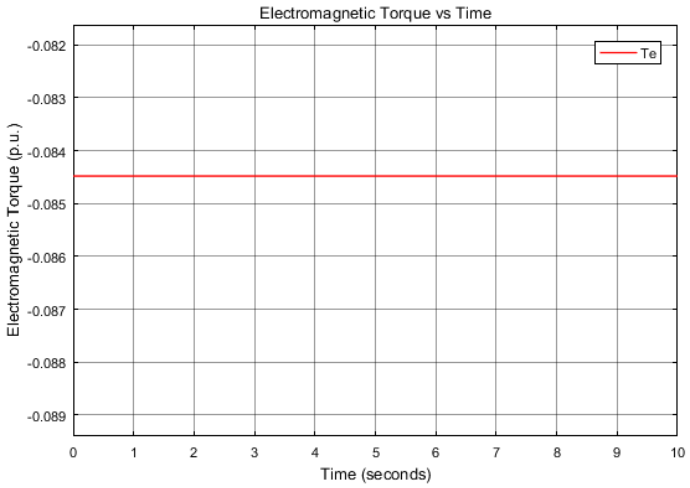

Figure 37. Electromagnetic Torque During Initialization.

Note that the red lines represent the real part of each variable, while the blue part are the imaginary part. In the previous graphs, the vertical axes are presented in p.u., this is, its corresponding value respect to a base figure, while the horizontal axes represent time in seconds.

In the case that the variables were not well correlated, the output of the simulation would not be constant, showing oscillations since the beginning of the simulation. Later on, after a time that depends on how decompensated were the variables, the machine could stabilize, as it always tries to find an equilibrium point of operation. Nonetheless, there is also the possibility that the variables were so decompensated that the equilibrium point is never reached. An example of a wrong initialization can be observed in Figure 38.

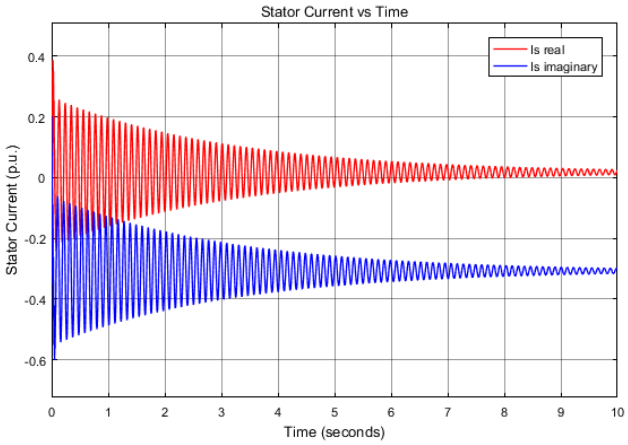

Figure 38. Wrong initialization of the stator current.

The following cases will be subjected to study are:

- Change in the operation point.
- Voltage drop during operation.

6.1. Change in the Operation Point

In this first case, the most common situation as it is a change in the operation point, will be studied. This situation is given when the system is subjected to an unbalance between the aerodynamic and the electromagnetic torque, related by the expression:

$$T_{aero} - T_e = J\frac{d\omega_m}{dt} \tag{6. 1}$$

where J is the inertia of the system.

Under steady-state operation, both the aerodynamic and electromagnetic torque have the same value, reaching an equilibrium. Therefore, according to equation (6. 1), the derivative of the mechanical speed should be zero, this is, the mechanical speed is constant, maintaining all variables constant as well, as seen along the first part of this chapter.

However, an unbalance can come as result of a change in wind speed, making the rotational speed of the turbine to vary, causing at the same time a change in the aerodynamic torque, as it is stated by (4. 9). According to equation (6. 1), the subtraction of the electromagnetic torque to the aerodynamic torque produces a non-zero result for the mechanical speed derivative. This means that the mechanical speed is no longer a constant, making also the rotor wind speed to change, according to equation (5. 3). Because of this change, the doubly fed induction generator will react, trying to find again the equilibrium. In that process, different systems take part, as the stator and rotor currents or the rotor voltage will adopt new values. After some time, that lasts more or less depending on the magnitude of the unbalance and the control systems, but usually takes a fraction of second, the relation of currents, voltages and rest of variables are set in a point in which the electromagnetic torque from the generator and the aerodynamic torque

produced as result of the wind speed, have again the same magnitude, rearranging the whole system in a new operational equilibrium.

For this case of study, two different situations will be subjected to analysis.

In the first situation, the wind energy convertion system will be subjected to a sudden change in wind speed from 6 m/s to 10 m/s. In order to simulate this change, the new mechanical speed corresponding to the new wind velocity has been calculated and through a clock signal, the new value will be introduced at a determined time set in this case from second 2.

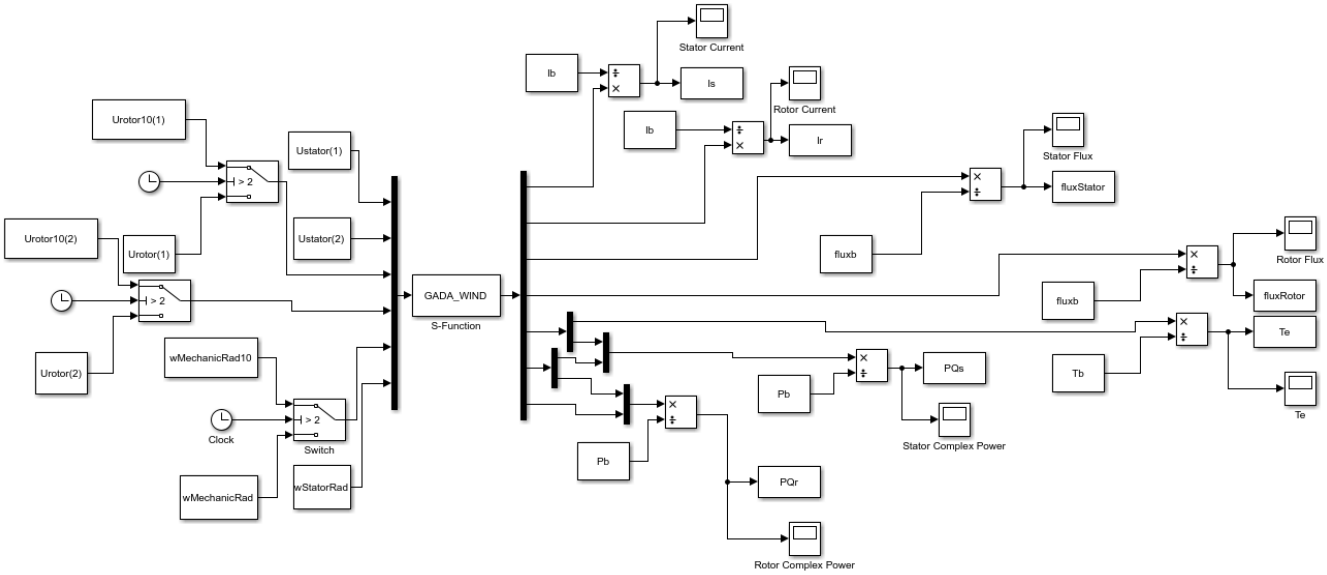

Figure 39. Simulation of the DFIG during a sudden change in the operating point.

The most relevant results from the simulation are:

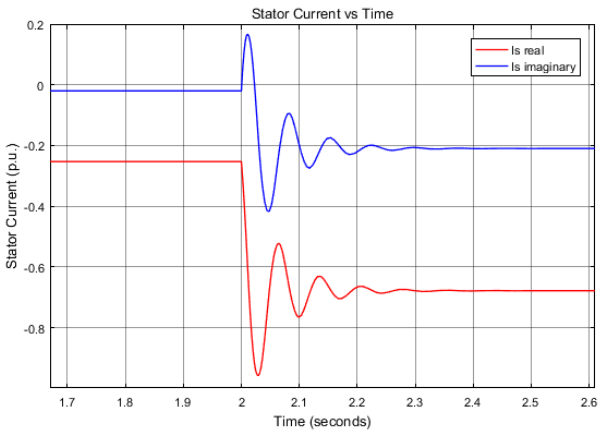

Figure 40. Stator current during a sudden change in the operation point.

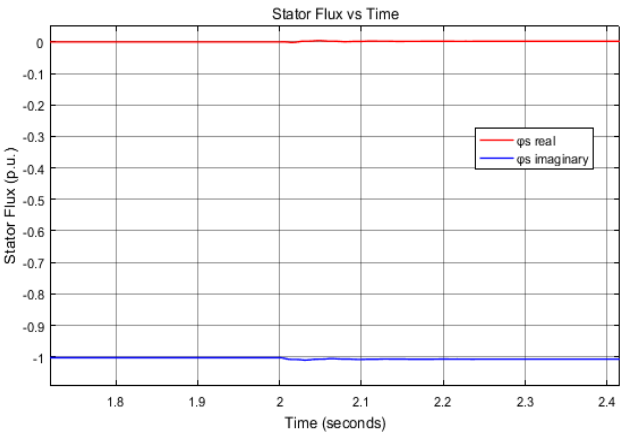

Figure 41. Stator flux during a sudden change in the operation point.

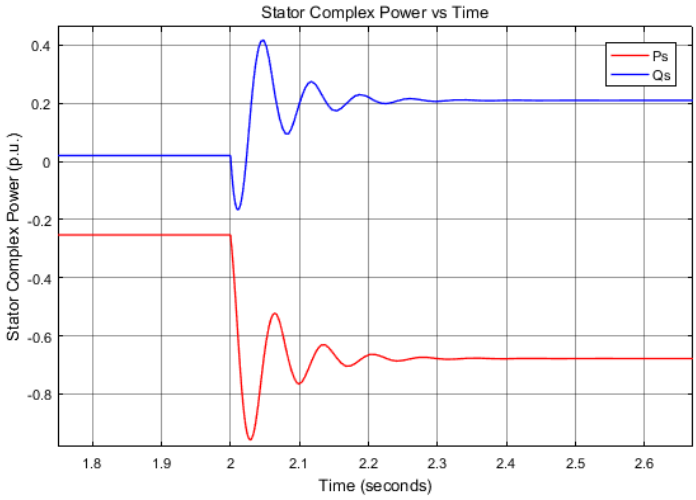

Figure 42. Stator Complex Power during a sudden change in the operation point.

As it can be observed, in the moment in which the wind speed changes, a spike is produced in all variables, as consequence of the unbalance. It takes around 0.3 to 0.35 seconds to reach again the equilibrium to all variables, where the only factor that do not change is the stator voltages. This happens as result of the protections of the wind energy convertion system, which are made in order not to modify the stator voltage in frequency or magnitude, as the instability of the machine could be transmitted to the grid. Actually, due to the inertia of the national or regional power systems, the effect of only one wind turbine would be not noticed, remaining magnitude and frequency almost at the same levels. Nevertheless, if all power generation technologies were connected to the grid without any protection, there would not be any constant magnitude or frequency and as consequence, the inertia would not try to force the systems to be set at 690 peak voltage and 50 Hz of frequency for European grids.

From Figure 40, it can be shown how the stator current in the real part is -0.25 at the beginning of the simulation and evolves to a minimum value in the spike of -0.95 p.u., never overpassing its initial magnitude, while the spike in the imaginary part goes from 0.15 to -0.4 p.u. with an initial value of -0.02 p.u. This makes the spike to reach maximum amplitudes of 0.7 and 0.55 p.u. for real and imaginary parts respectively. These spikes are a considerable change in current regarding the values at time zero. However, after six spikes, each of them reducing its amplitude as the model finds its new equilibrium point, the variable is stabilized at -0.68 p.u. for the real part and -0.21 for the imaginary part of the stator current.

The case of the stator flux in Figure 41 is curious because at first sight, it seems to be constant all along the simulation. However, this is a result of the fact that the stator voltage does remain constant. Therefore, from equation (5. 48), it can be deduced that if the voltage does not vary, the stator flux would only depend on the current that flows through the stator resistance. As it has been seen before, the spike in stator current, although noticeable, it is not too large in comparison with other situations that will be studied later. All this makes the stator flux not to vary, preserving its initial value of $-j$ p.u. and having spikes that do not even reach 0.1 p.u.

An important graph is Figure 42, where it can be observed the evolution of the stator complex power, this is, the power that is being injected to the grid. Its response to the sudden change in the operation point goes from an initial value of $-0.25 + 0.02j$ p.u. to a final value of -0.68 p.u. of active power and 0.21 p.u. of reactive power. Then, more power is being injected to the grid after the increase in wind speed. The fact that active power has a negative sign is because of the generator convention, in which the power leaving the stator of the machine is considered to be negative. It is also interesting to note the initial spikes of both active and reactive power, around the 0.7 p.u. of amplitude. In the case of the stator reactive power, it even reaches negative values during that initial spike.

As the second situation, a usual behavior of the wind will be analyzed. The wind energy convertion system will be subjected to increasing and decreasing changes in wind speed making a ramp. Again, this change will be translated in the simulation as a change in the mechanical speed corresponding to the new wind velocities.

The mechanical speed values introduced in the simulation, imitating the wind speed changes, result in the following plot:

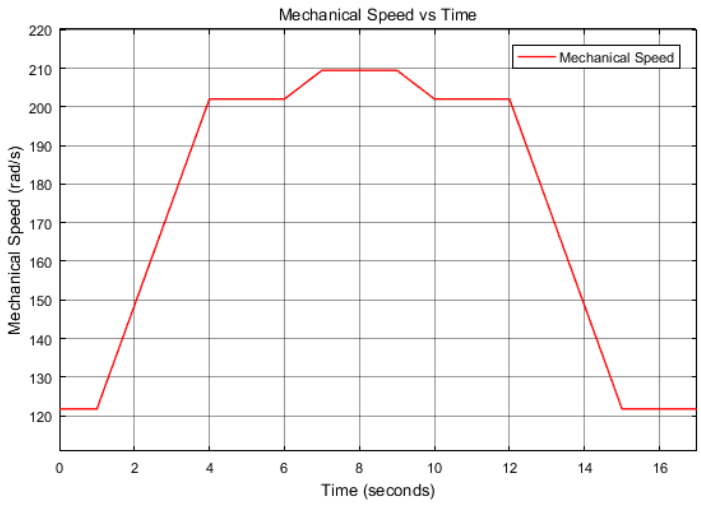

Figure 43. Evolution of the mechanical speed during smooth changes in wind speed.

For this case, it has been considered to have an initial wind speed of 6 m/s, which starts to vary from second one, increasing with constant slope until it reaches 10 m/s at second four. Then, the wind maintains its magnitude for two seconds, to increase again until it reaches 14 m/s. This is not completely translated to the mechanical speed, as the machine enters the nominal power region at 10.6 m/s and as consequence, at this very same velocity, the mechanical speed also reaches its maximum value, 2 000 rpm or 209.44 rad/s. Then, the wind starts decreasing its speed from 14 m/s and at second 10, the wind speed returns to 10 m/s. After two seconds of stabilization, it continues lowering its magnitude in a uniform way until it reaches 6 m/s or 121.75 rad/s.

According to this behavior of the wind, the following results have been obtained:

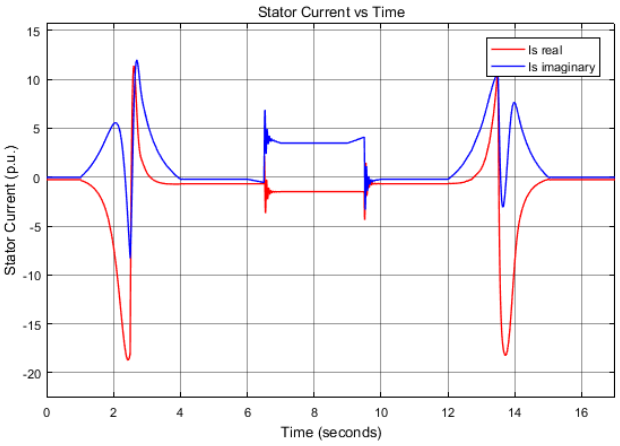

Figure 44. Stator current during smooth changes in wind speed.

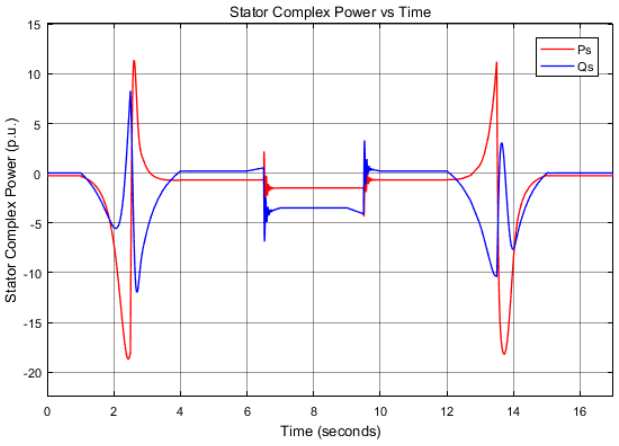

Figure 45. Stator complex power during smooth changes in wind speed.

As it can be observed in Figure 44, stator current starts operating at its initialization value and since second one, when the wind starts increasing, it varies its value until it arrives at second four in a new operation point. This evolution is done in a smoother way than in the previous case, in which a sudden variation of wind speed caused spikes in current, flux and power variables. The wind rises again its magnitude from second six to eight, but as previously explained, the mechanic speed cannot overpass its maximum limit of 2 000 rpm and as consequence, once this level is reached, it is maintained in a uniform value. It is before arriving at that limit, between seconds six and seven, when several spikes can be appreciated before the stabilization of the machine. Since second eight, the simulation becomes symmetric to the previous behavior, as the wind follows the same sequence, but this time decreasing its magnitude. After fifteen seconds, the wind speed is again 6 m/s and the stator current reaches its initial value.

In Figure 45, stator complex power evolves in a similar way to stator current. At the initial time, with 6 m/s, the machine is generating around $-0.25 + 0.02j$. With the increase in wind speed, a smooth transition can be appreciated until the intermediate value of 10 m/s is reached and the power stabilizes. Between seconds six to eight the wind increases, but due to the reasons previously explained, since second seven, the machine enters the nominal power area, stabilizing around 1 p.u. of active power. In the same way than for the stator current, the evolution of stator current follows a symmetric behavior to the one that it was describing, reaching again $-0.25 + 0.02j$ at the end of the simulation. It can be appreciated that each time the wind speed becomes constant, the active power is increased when the wind is rising and is decreased when the wind speed is diminishing.

It is noticeable in both stator current and stator complex power variables, that the variations during wind speed ramps reach very high magnitudes, being greater than 10 p.u. in the case of the imaginary part in the stator current, -15 p.u. for the real part, or -15 p.u. and 10 p.u. for the active and reactive power respectively.

6.2. Voltage Drop During Operation

In this case of study, another situation as a voltage drop during operation, will be studied. This situation is given due to some problems in the transmission system, that can be

caused by sudden changes in close loads or the faults in power systems, as short-circuits, fallen trees on transmission lines or atmospheric discharges. These problems consist on a severe and sudden decrease in voltage, whose magnitude can vary a lot depending on the harshness of the drop cause.

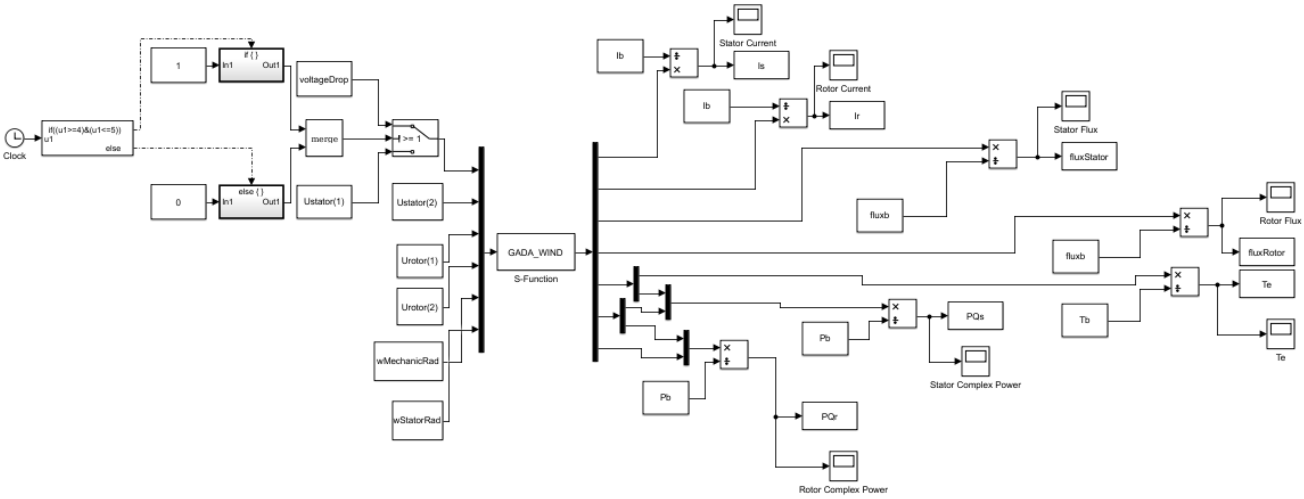

Figure 46. Simulation of the DFIG during a voltage drop.

For this case of study, two different situations will be analyzed. One during a voltage drop to half of the nominal voltage and a second situation in which a total voltage drop occurs. In both situations, the total time elapsed since the voltage drop to the recovery of the nominal voltage will be one second:

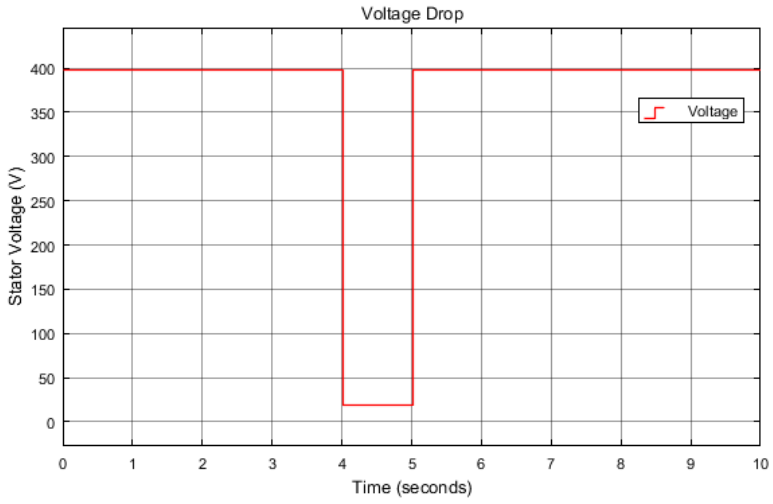

Figure 47. Example of a voltage drop to 5% of its nominal value.

For the case of the voltage drop, the change of rotor voltage depends on the technology used by the wind turbine, not as in the previous study case in which a change of wind speed does imply that the rotor voltage will try to adapt to the new situation given from the mechanical speed. Under voltage drops, the anomaly comes from the stator, connected to the grid. Therefore, the variation of rotor voltage will only depend on advanced technologies able to react fast enough to voltage drops. These innovations are described by David Santos [21]. For the purpose of this case of study, it will be considered that the

machine does not have the technology that would enable to change the rotor voltage during the voltage drop.

In the first situation, the wind energy convertion system will be subjected to a voltage drop of half of the nominal voltage, to observe the reaction of the doubly fed induction generator.

These are the most relevant results obtained from the simulation:

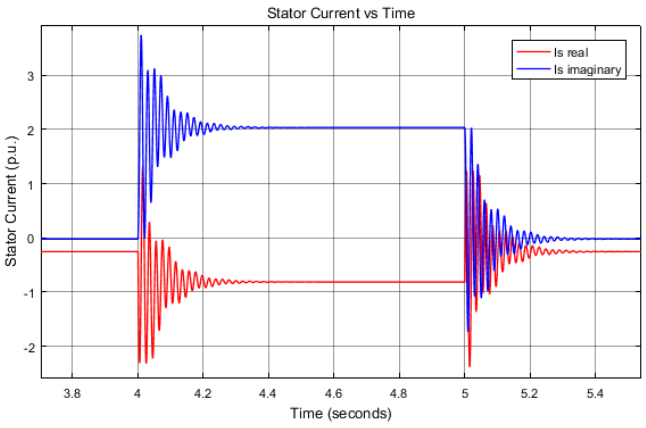

Figure 48. Stator current during a voltage drop to half the nominal voltage.

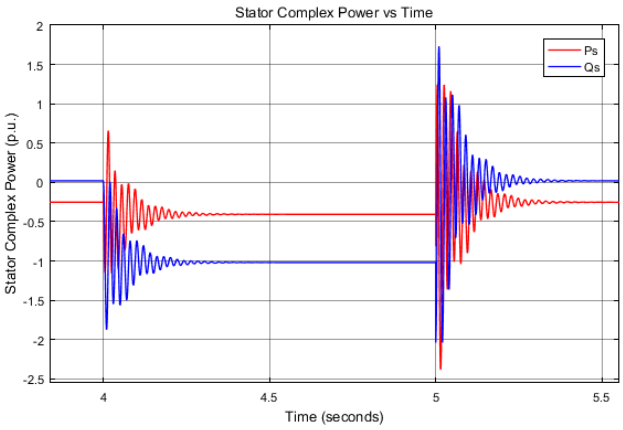

Figure 49. Stator complex power during a voltage drop to half the nominal voltage.

In Figure 48, we can observe how at second four, the voltage drop makes the stator current to suffer a high transient, in which there are spikes of almost 4 p.u. in the imaginary part. This transient lasts approximately 0.5 seconds to reach again the stabilization at the new voltage, but one second after the sudden fall starts, the nominal voltage is restored with another transient that makes the stator current to be at its initial values. This variable starts at $-0.02 - 0.25j$, the same value than at the end of the simulation, once the voltage is restored and during the voltage drop it reaches a stable value of $-0.81 + 2.04j$, being relevant the change in the imaginary part of the stator current, that increases by 2 p.u.

In Figure 49, a similar behavior to the stator current can be seen for the evolution of the stator complex power. The same transients can be observed at seconds four and five, at which the voltage drop starts and finishes respectively. As in the previous variable, stator complex power does also take around half a second to stabilize the doubly fed induction generator after the spikes, that reach a maximum amplitude of 1.8 p.u. during the voltage drop in the active power and more than 3.5 p.u. in the reactive power during the restoration of the nominal voltage. Before and after the voltage drop, the complex power is $-0.25 + 0.02j$ and during the voltage drop, once the power is stabilized, a value of $-0.4 - 1.02j$, being remarkable the change in reactive power, that changes 1 p.u.

It is noticeable that looking at the transients of the stator complex power in Figure 49, the first one, when the voltage drop occurs, is smaller than the second one, when the nominal voltage is restored. This happens as a consequence of the low voltage observed during second four, which makes the doubly fed induction generator to increase the module of the current in order to be close to the power previously supplied. As consequence, once the voltage is restored, since the current has increased, the power notices an extreme

increment, although the transient is quickly solved again by the doubly fed induction generator, recovering its initial values.

As second situation, the voltage drop that the wind turbine will experience will be a total drop. So that the simulation can be performed, the stator voltage will be reduced to a 5% of its initial value.

The most relevant results obtained from the simulation are:

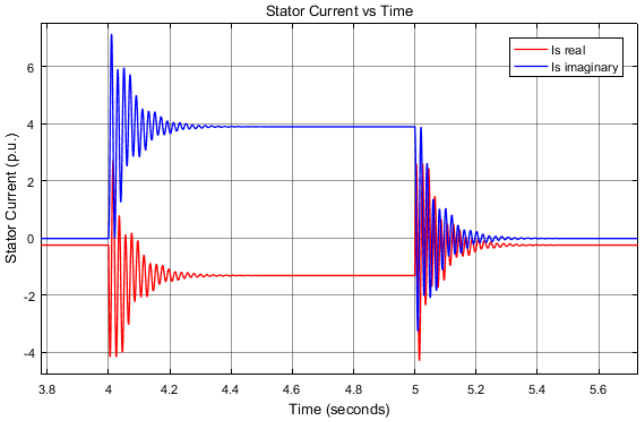

Figure 50. Stator current during a voltage drop to 5% of the nominal voltage.

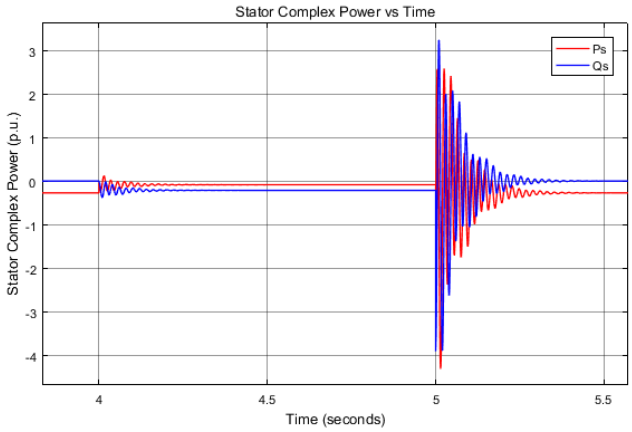

Figure 51. Stator complex power during a voltage drop to 5% of the nominal voltage.

In Figure 50, we can observe how the voltage drop, much more drastic in this situation than before, causes larger transients and larger variations in the stator current. Again, the initial and final values are $-0.02 - 0.25j$ p.u., while the variable reaches a stable value of $-1.3 + 3.9j$ p.u. during the voltage drop. The larger amplitudes for the spikes are 7 p.u. in both fourth and fifth seconds.

Different is the case of Figure 51, in which it is shown the impressive evolution of the stator active and reactive power. As well as before, the initial and final value is $-0.25 + 0.02j$, but during the voltage drop, the power is reduced to $-0.06 - 0.2j$. As explained before, the negative sign of the active power corresponds to the generator convention of power leaving the generator through the stator. When the voltage drop is finished, that active power experiences a remarkable spike that almost reaches -4.5 p.u. While the amplitude of the largest spike in the first transient is of 0.5 p.u., small due to the almost non-existent voltage, the same magnitude measured at the largest spike of the second transient is of 7 p.u.

As in the previous situation, transients are big in comparison to the magnitudes of the stabilized stator current and power, but it is noticeable that due to the larger drop in voltage in the second case, transients are much more radical. This leads to the problem explained before of experiencing really high currents so that the power delivered to the grid can be maintained around the value that was being delivered before the voltage drop. In that way, once the drop is finished and the nominal voltage is restored, increasing the power in a new transient. As it has been considered an extreme decrease of 5%, the initial spike of the complex power in the stator is also extreme, reaching an amplitude of 7 p.u.

7. CONCLUSION

7.1. Results Discussion

The general conclusions obtained for each part of the doubly fed induction generator simulation will be presented.

In first place, the initialization of the model was presented, showing accurate and robust results, comparing them also with an example of a wrong performance during the initialization. In addition, the working process of the initialization and the model were explained.

In the case of the change in the operation point, the results were satisfactory, as an adequate behavior of the machine was obtained as output, according to the expected values extracted from the bibliography and theory reflected in equations and formulas. In the first situation, during a sudden change in wind speed, the simulation reflects a sudden jump in stator current and power variables, representing the wind blowing at 6 m/s first and a gust of 10 m/s later on. Afterwards, a more complex simulation of the reaction of the doubly fed induction generator under the effect of increasing and decreasing ramps of wind speed was done, showing big changes in the variables, although much smoother than in the previous case without ramp.

In the situation of voltage drop during one second, the simulation results were very satisfactory, as again, according to the expected results obtained from the theory, the attained outputs showed expected behavior. Due to the relations described along the thesis between complex power, current and voltages, the amplitude of the spikes as well as the changes in power could be explained, noticing that the larger the voltage drop is, the larger the spike will be when the nominal voltage is restored and the lower the power injected to the grid will be during the voltage drop.

As final affirmations, it can be stated that according to what it has been shown along the thesis:

- The model of the doubly fed induction generator simulates the behavior of the machine in a robust and accurate way. This affirmation is extended to both the steady state and the dynamic development.
- The model of the doubly fed induction generator has been validated with examples presented in the bibliography, obtaining successful results. Moreover, the rest of the models that compose the wind turbine have also been achieved, even though not in a complete stage and without validation.

7.2. Conclusion

Along this thesis, the main topics that surround a wind energy convertion system with doubly fed induction generator have been presented. It has been developed a theoretical base of the evolution of the technology since the first uses of wind to propel devices to the last innovations and models available in the market, the different models of the wind turbine, as the physical, electric and control ones have been discussed, focusing on the

description of the generator implemented in the wind energy convertion system and several cases of its behavior have been presented as well, analyzing its evolution under different situations as changes in the point of operation and voltage drops, by implementing simulations with Simulink and MATLAB software.

I would like to remark the great utility of this thesis, as it has not only improved the way of focusing and approaching to deeper knowledge works, but it has also helped to understand a complex system as it is the one presented here, the interaction between its elements and the relation of the models with the equations and formulas that describe them.

Most of the simulation techniques used along this work were, at the very beginning, partially unknown for the author. Because of that, the development of the simulation also implies a parallel learning of both the software and simulation building process, understanding the correlations of real wind energy convertion systems with the models, trying to improve the number of similarities among them, besides the theoretical approach to the models that have been performed through an adequate bibliography. Therefore, it can be deduced that this thesis has been useful for learning purposes as well as a future basis for coming works.

The main part of this thesis has been the development of the doubly fed induction generator simulation, based in the wind energy convertion systems of type III, that are based on the use of this type of electric generator. In order to develop that part of the thesis, the following working strategies have been followed:

- Identification of the different parameters that can be found in the machine.
- Understanding of the description of the theory from the bibliography in which the doubly fed induction generator models are based.
- Programming of the main relation of variables inside the electrical generator in MATLAB, as well as some essential functions to describe several models, as the wind sequence model or the control of the coefficient of performance, that depends on the tip speed ratio and the pitch angle.
- Construction of the simulation of different models of the wind energy convertion system in Simulink, as the doubly fed induction generator, the mechanical coupling or the control loops.
- Implementation of the simulation of the doubly fed induction generator model in different situations as change in the operating point or behavior under a voltage drop of one second.

In order to accomplish this thesis, a great deal of important information have been obtained from relevant bibliography, related with the implementation of the different models that compose the wind turbine. As result, most of the models have been simulated, but because of the lack of time that implies the development of such an advanced matter, it has been presented only the simulation of the doubly fed induction generator, previously validated. Some additional details of the rest of models implemented in the simulation will be presented in the next chapter, future works.

8. FUTURE WORKS

This thesis has been the first contact with the simulation of a wind energy convertion system. Continuing the work presented here, a further development of the models can be achieved, reaching a better understanding of the functioning of the wind turbine and how to stabilize the doubly fed induction generator under unbalanced situations.

Therefore, some of the working lines that can be developed in the future to complete the present thesis are:

- Validate the models. Some of the models must be validated with specialized bibliography in order to obtain full reliability from them.

- Finalizing the wind energy convertion system simulation. Although most of the components have been described and implemented in Simulink, not all of them are consistent or have parameters similar enough to the ones that can be found in real wind turbines.

- Expanding the simulation scope, scaling it up to a wind farm. Once the models have been validated and the simulation is completed, the application of several wind power systems in a wind farm is a project that goes a step further, is interesting and less time-consuming having the base work done.

- Getting deeper in some of the control models. They can be improved and new techniques can be implemented to accomplish a better performance in the control of the wind energy convertion system.

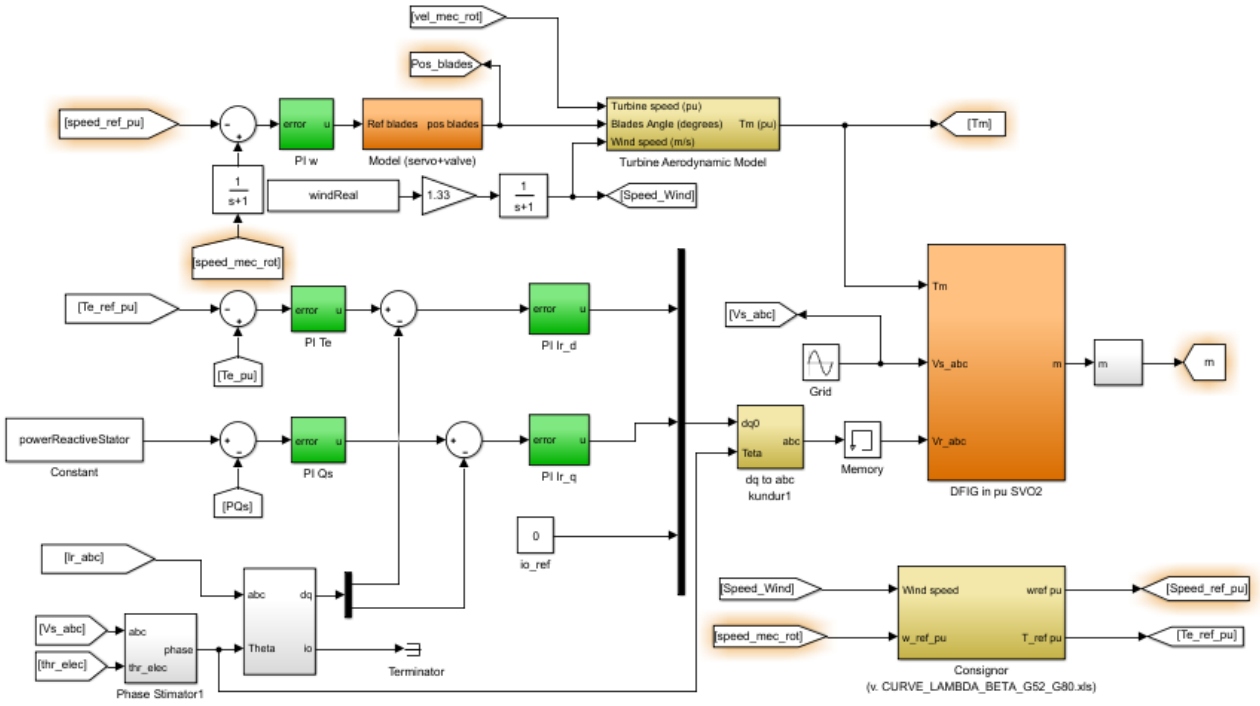

Figure 52. Model of the whole wind turbine simulation in Simulink.

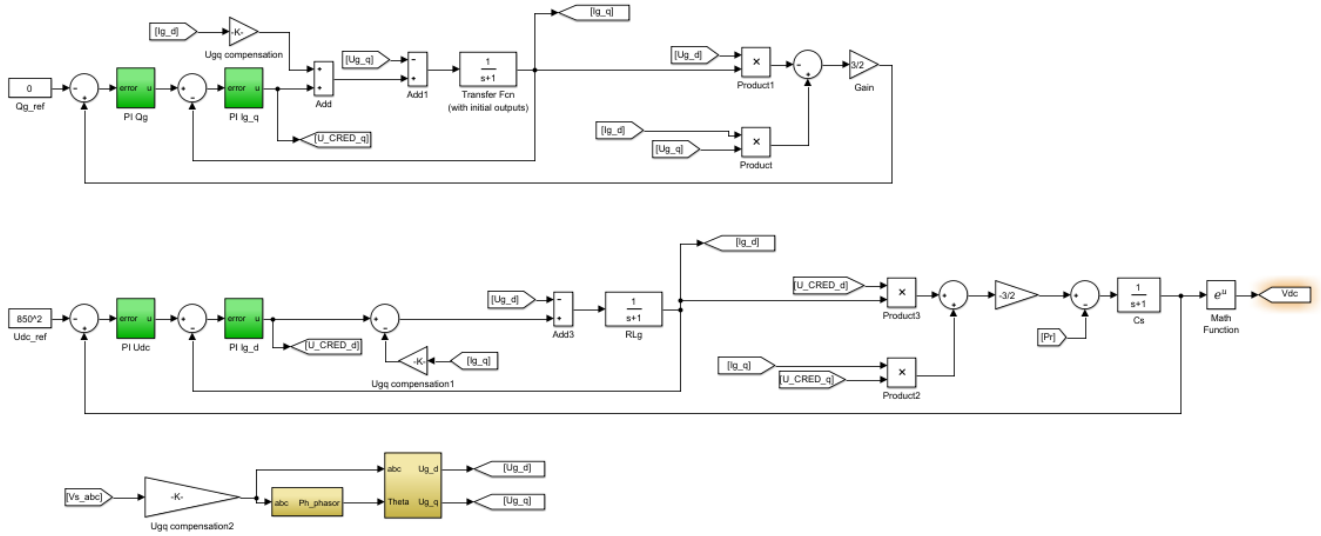

Figure 53. Control Loops of the wind turbine Model in Simulink.

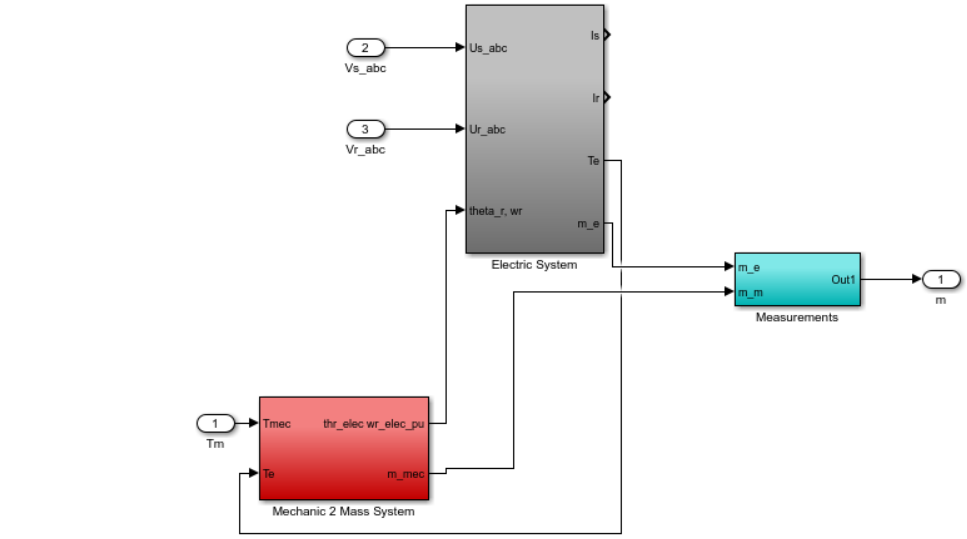

Figure 54. Complete Doubly Fed Induction Generator Model in Simulink.

9. BIBLIOGRAPHY

1. T. Ackermann. “Wind power in power systems”, Wiley, 2012.
2. G. Abad, J. López, M.A. Rodríguez, L. Marroyo, G. Iwanski. “Doubly Fed Induction Machine: Modeling and Control for Wind Energy Generation Applications”, Wiley, 2011.
3. R. E. Lucas. “Lectures on Economic Growth”, Harvard University Press, 2002.
4. IEA, NEA, OECD. “Projected Costs of Generating Electricity”, 2015.
5. http://www.ammonit.com/en. Ammonit.
6. L. Xi, M. B. McElroy, J. Kiviluoma. “Global Potential for Wind-Generated Electricity”, Wind Energy Engineering, 2017.
7. S. Heier. “Grid Integration of Wind Energy: Onshore and Offshore Conversion Systems”, Wiley, 2014.
8. A. Lecuona. “Energía Eólica: Principios Básicos y Tecnología”, Universidad Carlos III de Madrid, 2004.
9. https://energy.gov. U.S. Department of Energy.
10. http://www.windpower.org. Danish Wind Industry Association.
11. T. Burton, D. Sharpe, N. Jenkins, E. Bossanyi. “Wind Energy Handbook”, Wiley, 2001.
12. M. Borg, M. Collu. “Offshore floating vertical axis wind turbines, dynamics modelling state of the art. Part III: Hydrodynamics and coupled modelling approaches”, “Renewable and Sustainable Energy Reviews”, 46, 296-310, 2015.
13. http://www.ren21.net. REN21.
14. https://www.navigantresearch.com. Navigant Research.
15. J. L. Rodríguez Amenedo. “Análisis Dinámico y Diseño del Sistema de Control de Aeroturbinas de Velocidad Variable con Generador Asíncrono de Doble Alimentación”, Universidad Carlos III de Madrid, 2000.
16. H. Stiesdal, C. Nybroe, J. Furze, H. Piggott. “Bonus Info: The Wind Turbine Components and Operation”, Bonus Energy, 1999.
17. Heier, S. “Grid integration of wind energy conversion systems”, Wiley, 2009.
18. P. M. Anderson, A. Bose. “Stability simulation of wind turbine systems”, IEEE, 1983.
19. P. S. Veers. “Modeling stochastic wind loads on vertical axis wind turbines”, Sandia National Laboratories, 1984.
20. A. Schuster. “A matrix converter without reactive clamp elements for an induction motor drive system”, IEEE PESC’s, Volume 1, IEEE, New York, pp. 714–720, 1998.

21. D. Santos Martín. “Control de Potencia con Programación Dinámica de Generadores Asíncronos de Doble Alimentación”, Universidad Carlos III de Madrid, 2008.

22. R.Datta, V.T.Ranganathan. “Direct power control of grid-connected wound rotor induction machine without rotor position sensors”, IEEE Trans. Ind. Appl. Power Electron., vol. 16, no.3, 2001.

23. J. Fraile Mora. “Máquinas Eléctricas”, McGraw Hill, 2004.

24. P. Kundur. “Power System Stability and Control”, McGraw Hill, 1994.